Universidad
Pública de Navarra
Nafarroako
Unibertsitate Publikoa

Departamento de Ingeniería Eléctrica y Electrónica
Ingeniaritza Elektriko eta Elektroniko Saila

SYNTHESIS AND DESIGN OF NOVEL METAMATERIAL RADIATION STRUCTURES

Tesis Doctoral realizada por / Doctoral Thesis by

Noelia Ortiz Pérez de Eulate

Dirigida por / Supervised by

Dr. Francisco Falcone Lanas

Dr. Mario Sorolla Ayza

Pamplona, 2017

This thesis has been typeset using the MiKTEX2.5 distribution of LaTeX 2_ε.

I, Francisco Falcone, as PhD supervisor, authorizes the publication of this thesis in the format of Journal Paper compendium, in accordance with ruling A3/2015 of the Universidad Pblica de Navarra.

Pamplona, 31 May, 2017

La memoria de esta tesis se articula como un compendio de trabajos. Dichos trabajos, han sido publicados en revistas científicas internacionales cuyos contenidos estan sometidos a la revisión por parte de pares especialistas en el dominio de la física y de la ingeniería de antennas (peer reviewed journal).

1. N. Ortiz, J. D. Baena, M. Beruete, F. Falcone, M. A. G. Laso, T. Lopetegi, R. Marqus, F. Martn, J. Garca-Garca, and M. Sorolla, "Complementary split-ring resonator for compact waveguide filter design," *Microwave and Optical Technology Letters*, vol. 46, no. 1, pp. 88–92, 2005.

2. N. Ortiz, F. Falcone, and M. Sorolla, "Enhanced gain dual band patch antenna based on complementary rectangular split-ring resonators," *Microwave and Optical Technology Letters*, vol. 53, no. 3, pp. 590–594, 2011.

3. ——, "Gain improvement of dual band antenna based on complementary rectangular split-ring resonator," *ISRN Communications and Networking*, vol. 2012, no. 17, 2012.

4. N. Ortiz, J. C. Iriarte, G. Crespo, and F. Falcone, "Design and implementation of dual-band antennas based on a complementary split ring resonators," *Waves in Random and Complex Media*, vol. 25, no. 3, pp. 309–322, 2015.

5. N. Ortiz, G. Crespo, J. C. Iriarte, and F. Falcone, "Generation of circularly polarized waves based on electro inductive-wave (eiw) coupling to chains of complementary split ring resonators," *Journal of Applied Physics*, vol. 120, no. 17, p. 174905, 2016.

To my parents, Joaquín and Mari Carmen
To my husband, Roberto
In memory of Mario Sorolla Ayza

Abstract

The present thesis deals with the design and practical implementation of novel netamaterial planar antenna structures based on Complementary Split Ring Resonator (CSRR) particles.

As CSRR particles display a very attractive electrical performance when used as unit cell for metasurfaces, the authors of this thesis have proposed to implement such particles in waveguide filters. In this case, the possibility to design waveguide filters with lengths equal to the thickness of a metallic sheet is confirmed. Consequently, the proposed structure constitutes a significant reduction of the dimensions of the well-known resonant cavity waveguide filters coupled by irises.

The behavior of CSRR particles within compact waveguide filter suggested the authors to use them as stand alone radiating elements. As expected, due to the reduced electrical volume of CSRRs, such particles exhibited low radiation efficiency. In order to improve the radiation efficiency, the idea to implement CSRRs inside a larger structure came to us. Measurement results confirm this hypothesis and raise the question to design multi-band antennas. In order to implement multi-band antennas, several CSRRs are inserted at different positions in the patch. It is then observed that the grouping of CSRRs can provide either multi-band operation or polarization rotation capabilities, when Electro-Inductive Waves (EIW) are supported.

Finally, thanks to EIW propagation, the idea to use longer CSRR chains as radiating structures came to us. As an intermediate step, and in order to validate simulated results, a finite array composed of nine CSRRs is manufactured and partially tested. Though partial, this test results are very encouraging and motivate a more in deep measurement campaign. This campaign is expected to result into new publications on this topic. These results support the use of the proposed CSRR chains for the design of leaky wave antennas.

Keywords

Complementary Split Ring Resonator, Metamaterial Planar antenna, Circular Polarization, Multi-band Band antenna, Electro-Inductive Wave propagation.

Acknowledgements

First and foremost, to my thesis supervisor, Francisco Falcone. This work has been possible thanks to his support and encouragement over these years. I also feel in great debt to Mario Sorolla Ayza for having proposed me the possibility to work on this research work under his supervision and under the supervision from Francisco Falcone.

I would like to thank Gonzalo Crespo and Juan Carlos Iriarte for their continuous collaboration and support in the manufacturing and measurement of the prototypes designed for this thesis.

I would like to express my gratitude to my colleagues at Rymsa Space S.A. in Madrid, at TTI Norte S.L. in Santander, at ViaSat Antenna Systems S.A. in Lausanne and at Amodus S.A. in Le Mont-sur-Lausanne; who with their daily work give me an example of professionalism and friendship.

I would like to dedicate this last paragraph to those people who are always by my side, to those who support me and those that make my life so beautiful as it is. Specially, my gratefulness to my husband, Roberto: thank you for filling my life with love every day and thank you for your support in the elaboration of this memoir.

Finally I would like to thank God and life just for being alive and send an enormous hug to my parents, they are my guidance in life.

In memory of Mario Sorolla: Mario, this thesis is my tribute to you. Thank you !

Contents

List of Acronyms

CRLH	Composite Right/Left handed
CSRR	Complementary Split Ring Resonator
CPW	Coplanar Waveguide
EM	Electromagnetic
EMSIW	Eight Mode Substrate Integrated Waveguides
EPFL	Ecole Polytechnique Fédérale de Lausanne
LHM	Left Handed Material
MIMO	Multiple-Input-Multiple-Output
NRI	Negative Refraction Index
SIW	Substrate Integrated Waveguides
SRR	Split Ring Resonator
UWB	Ultra WideBand

1. Introduction

Tout ce qui n'est pas donné, est perdu.

Proberbe Indien

This thesis reports the research work I performed within the doctorate program "'Programa de Doctorado en Comunicaciones"', for the degree of Philosophy Doctor (PhD) in Telecommunications Engineering of the Universidad Pblica de Navarra (UPNA).

In April 2005 I proposed Professor Mario Sorolla Ayza to perform a thesis under his supervision. At that time I had already left UPNA few months ago and had started working full time as Electrical Engineer, at RYMSA S.L in Madrid. He happily accepted my proposal in spite of the disadvantages of having a part-time PhD student. He proposed me to do research on antennas using Complementary Split Ring Resonators (CSRRs) under the guidance and supervision of Professor Francisco Falcone Lanas and himself. From that moment I started under their direction the challenging work which has provided the results presented in this thesis.

This thesis has been developed on my free time, without official financial support from 2005 and its results are not related to the activities I have performed as Antenna Engineer at the different companies I have worked in Spain and Switzerland over the last ten years [see CV]. The manufacturing and testing of all the prototypes developed in the frame of this thesis have been possible thanks to the support of Departamento de Ingeniera Elctrica y Electrnica at UPNA and the inestimable personal engagement of the Professors Francisco Falcone, Juan Carlos Iriarte and Gonzalo Crespo.

The aim of this chapter is to center the topic of the thesis within its context, to explain the objectives and to present the personal contributions that have been achieved under the research work.

To whom is reading this memory, I wish you enjoy.

1.1 Field of Study and Objectives of the Thesis

The field of study of this thesis falls within the framework of the synthesis and design of novel antenna structures based on Metamaterials in the microwave frequency range.

The *objective of this thesis* is to contribute to the development of Planar Metamaterial antennas. The structures used for the development of the Metamaterial antennas presented in this work are the Complementary Split Ring Resonators (CSRRs).

The initial goal of this thesis was to take profit of the intrinsic benefits of CSRR particles at their sub-lambda operation in order to design miniaturized Metamaterial antennas. However, the first achievements of this thesis drove the research apart from the miniaturized Metamaterial antennas towards designs using arrays of CSRR particles within conventional rectangular patch antennas as well as leaky wave antennas based on CSRR array structures.

The *objective of the present memoir* is, finally, to provide a reasoned outline of the design of Metamaterial antennas based on CSRR and its results, with the vocation that also the reader could derive some benefit from the resulting document.

1.2 Thesis Outline and Original Contributions

This section summarizes the contents of the chapters of the thesis memoir.

In *Fig. 1.1* the logic of the thesis is shown.

Chapter 1 presents the field of study and the objectives of this thesis. This chapter also includes the context and the historical review of guided structures and planar antennas based on CSRRs.

Chapter 2 is centered in a discrete waveguide filter design. This type of filter is composed of a CSRR etched in the center of a metallic sheet. This original layout reduces the dimensions of the well-known resonant-cavity waveguide filters coupled by irises. The contribution of the author on this topic is included in *Section 2.2.3*. In addition, in this chapter from a more general point of view a sample development by the author of a distributed waveguide filter is presented. This work has resulted into a patent which is presented and described as a

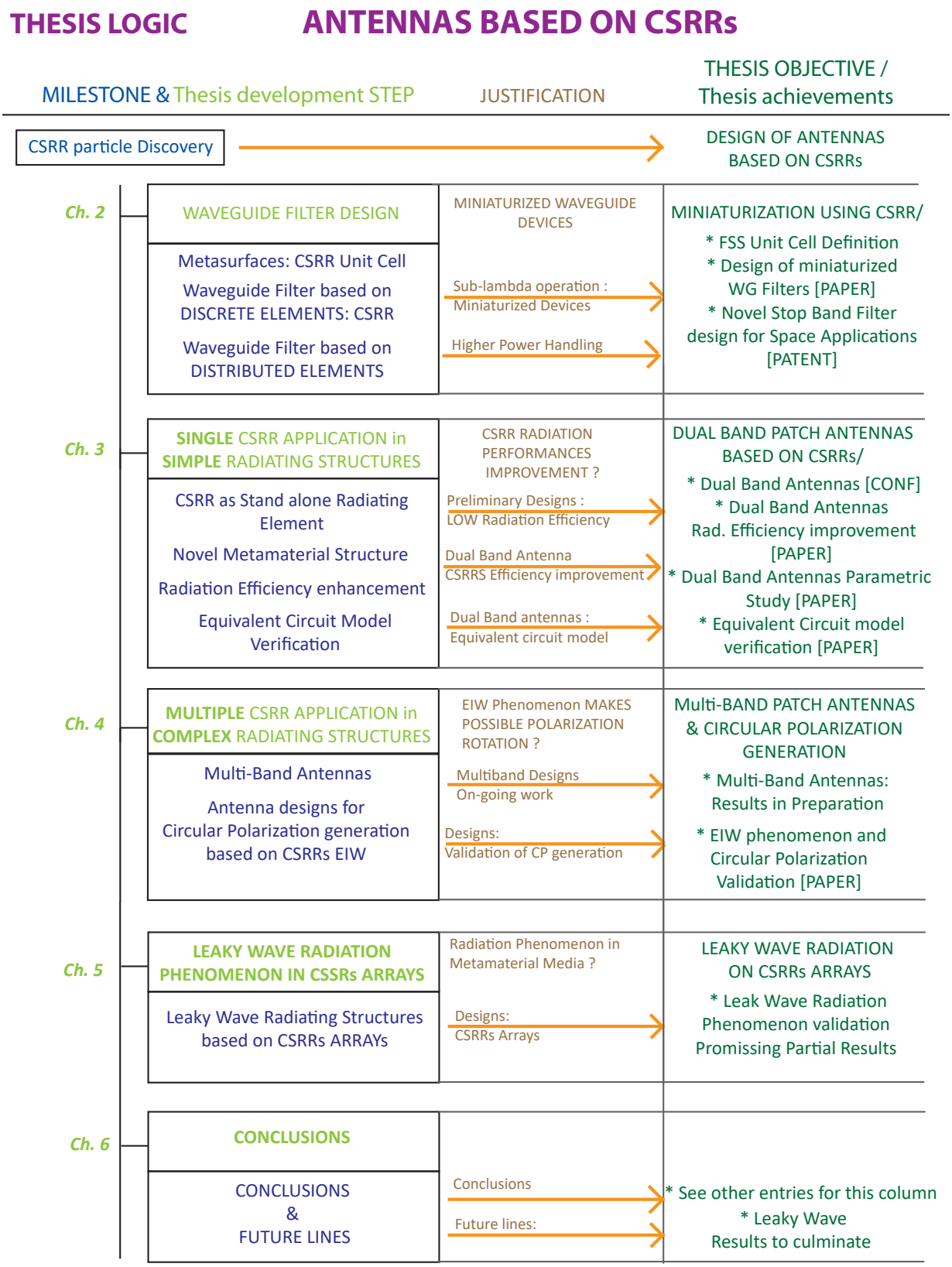

Figure 1.1. Thesis Justification Objectives

counterpart of the discrete filter element that is the CSRR itself. The aforementioned patent is described in *Section 2.1.1*.

Chapter 3 focuses in the study of the radiation performances of a CSRR inside a rectangular patch antenna. Within this novel Metamaterial structure, the radiation efficiency of the CSRR is improved compared to the radiation efficiency of the CSRR as an stand along radiating element. Three original contributions are published by the author on the work presented in this chapter. These contributions are explained in *Section 3.2.4*, *Section 3.2.5* and *Section 3.2.6*.

Chapter 4 focuses in different CSRR array configurations which allow polarization rotation in a rectangular patch antenna. The polarization rotation is mastered by Electro Inductive Wave (EIW) phenomenon originated by the electric coupling among the CSRRs; which are specifically located inside the rectangular patch. The contribution of the author on this topic is included in *Section 4.2*.

Chapter 5 presents the possibility to use CSRR arrays for the design of leaky wave antennas. Partial measurement results of this work shows promising results in this field. These results are foreseen to be published in the incoming months.

Chapter 6 summarizes the concluding remarks and outlines the possible future research directions inspired by the work presented in this memoir.

Every chapter contains an independent list of references.

1.3 Historical Overview

This section is an overview of the main research results based on Complementary Split Ring Resonators (CSRRs). The overview starts within a description of the context of this thesis and it follows with the presentation of the main achievements fulfilled in guided and in planar antennas structures based on CSRRs including the results presented in this thesis.

1.3.1 Context

The conception of this thesis is placed somewhere between the end of 2004 and the beginning of 2005. At that time the topic of Metamaterials was at its peak and the *Microwave and Millimeter Wave* research group of the UPNA, conducted by Professor Mario Sorolla Ayza, has an international lead together with other two research groups in Spain: the research group conducted by Ricardo Marqus and the research group conducted by Professor Ferran Martin, at University the Sevilla and

at University Autonoma de Barcelone; respectively. Those three research groups were focusing their research activities in the design of microwave planar structures based on Split Ring Resonators. The invention of the CSRR particle was a result of the cooperation among these three research groups and it was firstly announced in the work [1]. From that moment the motivation of designing Metamaterial antennas based on CSRR isolated particles and arrays came up and it consequently this idea became the main subject of this thesis.

In order to center the discovery of the CSRR particle in time based on the theoretical background, follows the pioneers theoretical and experimental works on Metamaterials which conducted to the concept of the CSRR.

1879 - 1944: Professor L. I. Mandel'shtam from Moscow Universitity [2] states in his lecture notes that, since the phase velocitiy does not have to have the same direction as the power flow vector, "negative refraction" is thus possible.

1945: The paper "Group velocity in a crystal lattice" [3] by L. I. Mandel'shtam proposes the existence of a frequency range in which EM waves propagate through certain crystal lattices with negative group velocity (i.e. : the group velocity is directed oppositely to the phase velocity).). In this work physical examples of structures supporting waves with negative velocity were also presented.

1951: Malyuzhinets in his work [4] based on the Sommerfeld radiation condition in backward-wave media, he used as an example of "negative refraction" one-dimension artificial transmission line.

1957: D. V. Sivukhin states that media with negative parameters are backward-wave media but raises the question of the existence of such media [5]. The artificial synthesis of such substances, now known as Left Handed Materials (LHM), is not yet available.

1959: R.A. Silin discusses the negative refraction phenomenon in periodical media [6].

1967: V. G. Veselago studies the electrodynamics of substances with simultaneously negative values of dielectric permittivity and magnetic permeability [7]. Althought these substances are not supposed to be present in nature, interesting properties are theoretically predicted for them, such as the reversal of the Snell Law, Doppler effect and Cherenkov radiation. These properties are derived from the fact that negative values of dielectric permittivity and magnetic permeability give rise to a negative refraction index (NRI) and backward wave propagation. Such substancies, now termed left handed materials (LHM), were not artificially fabricated by that moment.

1999: J. D. Pendry, presents the Split Ring Resonator (SRR) in his work [8]. The SRR particle consists on a pair of concentric rings, with slits etched in opposite sides. Those particles exhibit a negative effective permeability in the vicinity of its resonant frequency.

2000: Along this year two main achievements are fulfilled.

On the one hand the first experimentally observable LHM operating in the microwave region is reported by D. Smith *et al.* in [9]. The structure was fabricated by combining a periodic array of metal posts with an array of non.magnetics SRRs. The meatallic posts behave like a two dimensional (2D) plasma with negative permittivity up to the plasma frequency, while the SRRs exhibit a negative effective permeability in the vicinity of its resonant frequency. This first prototype exhibits a left-handed behaviour for one direction of propagation (1D LHM) and for one polarization of the fields. An improved 2D isotropic version of this structure will be proposed in [10].

On the other hand, J. D. Pendry proposes the term superlens in [11]. He predicts that such LHM-lenses will enable a perfect image reconstruction thanks to their capability to magnify and refocus the near-Field evanescent components.

2002: During this year two main contributions were achieved.

In the first half of this year the results of an experiment envisaging the integration of the SRR within Coplanar Waveguides and Microstrip lines are published in [12]. This experiment consists in loading a conventional metallic rectangular waveguide with a dielectric sheet hosting a set of SRR particles. The SRR particles were designed in order to have the quasi-static resonance frequency below the cut-off frequency of the waveguide.This result was another experimental validation of LHM phenomena.

In the second half of 2002, the research group leaded by C. Caloz and T. Itoh presents in [13] a circuit approach to the synthesis of metamaterials. These Metamaterials are obtained by periodically loading a transmission line with lumped L-C elements.

From 2002 the design of Metamaterial devices in planar technology such as guided devices (i.e. filters, couplers, etc.) and antennas are boosted. From this year two main research lines are defined. The first research line is based on Metamaterial structures based on the periodically transmission lines loaded with lumpled elements, using the Metamaterial solution presented in [13]), while the second research line is based on Split Ring Resonators printed in different planar technologies, i.e. Coplanar Waveguide or in Microstrip line technologies.

2004: The Complementary Split Ring Resonator (CSRR) is first presented in [1] as the complementary particle of the Split Resonator. In this work a new approach, based on the complementary particle of the Split Ring Resonator for designinig Metamaterial and LHMs is presented.

The contributions reported in this section and the advantages of the electrical performances of the CSRR, are indeed the starting points of the study of this thesis. Thanks to those contributions the possibility of designing planar Metamaterial antennas based on CSRRs is envisaged.

As a synthesis, in *Fig. 1.2* the context of the thesis is explained, including the main chronological milestones listed in this section.

1.3.2 CSRR Based developments for planar guided structures

In this section a review of the state of the art of CSRR particles based developments for planar guided structures is presented. As the CSRR is the complementary particle of the SRR particle see [1], this section starts with the research works based on SRRs until the moment that the CSRR particle is presented in [1]. From the moment that the CSRR is published, this section follows by CSRR based developments on planar Metamaterial and LHM medias.

In [14, §5.1.5] the experiment results obtained in [12] and in [15] are summarized. Those experiments results, which are conducted in 2002, envisage the application of SRR particles in conventional transmission line technology. From that moment the research activity of applying SRR particles in Coplanar Waveguides in order to design planar Metamaterial devices; such as filters in microwave range, is started.

In 2003 and 2004, the first works based on SRR particles applied to Coplanar Waveguides starts to be published. In order to excite the SRR particles in the Coplanar Waveguides, those particles are etched in the back-side of the substrate and are aligned with the slots of the Coplanar Waveguides. Then, a high inductive coupling between lines and rings is achieved, with the result of a sharp and narrow rejection in the vicinity of the resonant frequency of the rings. This performance introduces the possibility to design compact Metamaterial stop band filters, as the design that is presented in [16], [17] and [18].

In November of 2004 the CSRR particle is firstly presented in [1]. Complementary to SRR particles, CSRR particles can be easily excited in Planar Microstrip Lines. The CSRR particles are excited by etching them on the ground plane of the Microstrip Line and by aligning them to its conductive line, with the result of a pass band behavior close of the resonant frequency of the rings. Thus, within this new configuration it is able to design miniaturized band-pass filters in Microstrip Technology, see the following works, which are published during 2005: [19], [20] and [21]. In addition, the analytical equivalent-circuit models is proposed for the isolated and coupled SRR/CSRR particles in [22]. In that work, the stopband/passband characteristics of the analyzed SRR/CSRR loaded transmission lines are derived. It is also shown that in the long wavelength limit, these stopbands/passbands can be interpreted as due to the presence of negative/positive values for the effective /spl epsiv/ and /spl mu/ of the line.

Between 2004 and 2007 the design of Metamaterial and Left-Handed stop-band, pass-band filters and couplers based on the implementation of CSRR particles in Coplanar Waveguide and

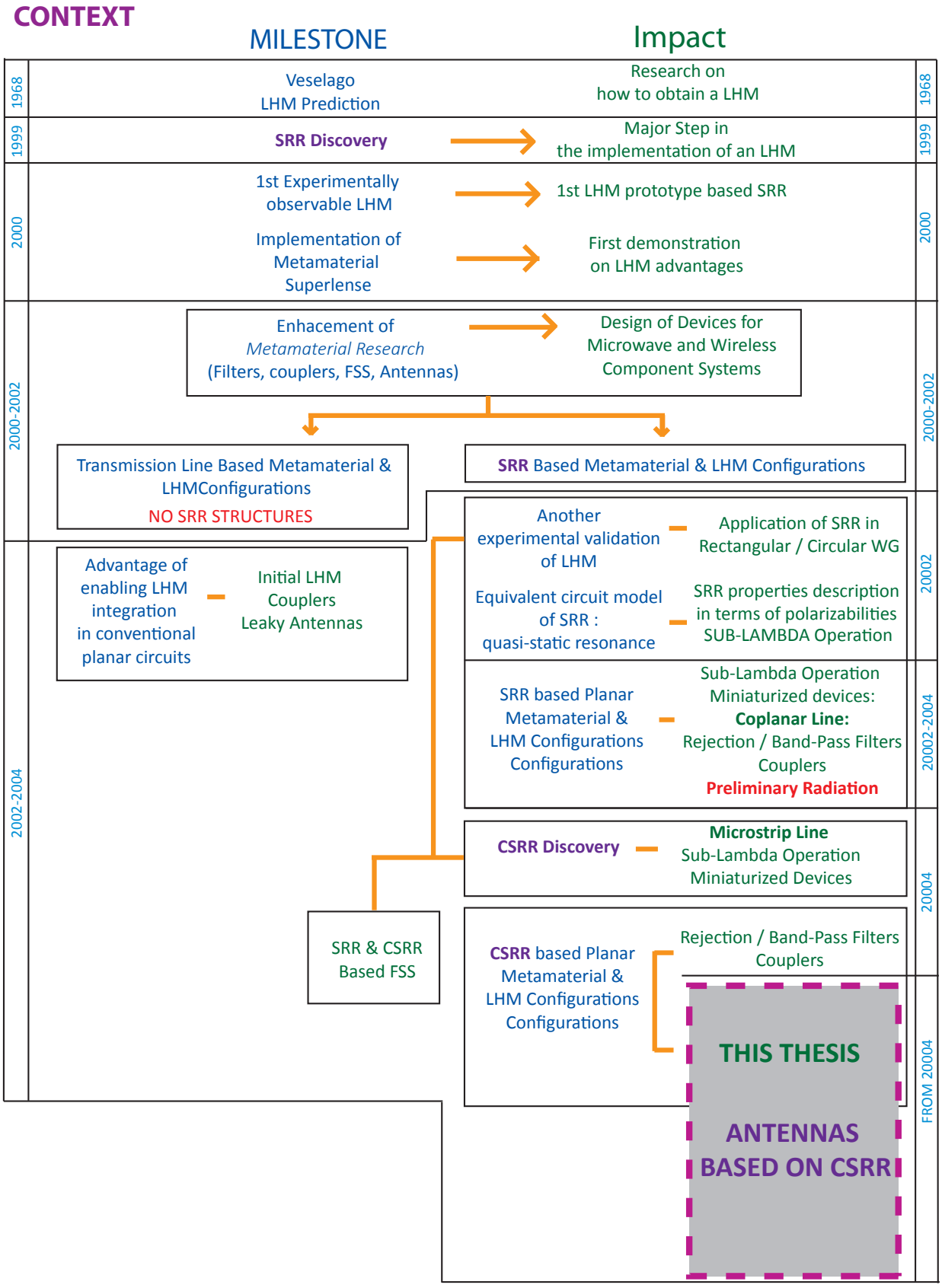

Figure 1.2. Context of the thesis

Microstrip Line Technology is at its peak [23], [24], [25], [26], [27] and [28]. Specifically, in 2007 wider bandwidth filter responses compared to the ones presented so far are achieved based in Composite Right/Left-Handed Metamaterial Transmission Lines loaded with CSRRs [29].

On the one hand, from 2007 to the present, more sophisticated Metamaterial and LHM devices based on CSRRs are developed. For example in 2008 a new type of left handed microstrip lines implemented by means of CSRRs are firstly proposed in [30]. In these new type left handed microstrip lines, the CSRRs are etched on the signal strip, which alternating with series gaps. Additionally, shunt connected stubs are also introduced. Within this new type of left handed microstrip lines the design flexibility is enhanced. In the work [30] two compact devices, a narrow band power divider and a band pass filter are implemented in this new type of left handed microstrip line. The resulting power divider is 50% smaller than the previous power dividers implemented by means of CSRRs. In addition to these results, this new type of left handed microstrip line approach is opened to those systems where the ground plane cannot be etched. In the last years, the electrical performances of dual and single band pass filters based on CSRRs are improved in [31], [32], [33], [34], [35] and [36], with the result of selectivity and/or bandwidth improvement. In the same way, low pass filters based on CSRRs are developed exhibiting higher electrical performances in [37], [38] and [39]. In relation to rejection filters based CSRRs the most relevant research works are presented in [40], [28] and [41].

On the other hand, from the year 2007 to the present, CSRRs are applied to Substrate Integrated Waveguides (SIW) to design band-pass filters in [42], [43], [44], [45], [46], [47], [48] and [49]. In addition to these designs, based on Substrate Integrated Waveguides more complex devices, such as miniaturized diplexers and couplers are designed in [50] and [51], respectively.

In *Fig. 1.3* a summary of the main developments and their motivation based on CSRR planar guided structures is presented. The developments on Waveguide structures is left for its presentation in *Chapter 2*.

1.3.3 CSRR Based developments for planar antennas

In this section a review of the state of the art of CSRR particles based developments for planar antennas is presented. Leaky wave antennas are out of the scope of this section, as their state of the art will be covered in *Chapter 5*.

In the case of planar antennas based on SRR and CSRR particles, the research results appear lately in time compared to the guided structures. Indeed, comparatively less attention is directed towards the application of SRR and CSRR particles to antennas and antenna systems. It is only after the presentation of the CSRR particle in [1] that the initial works on the radiation phenomena based on SRRs in planar LHM devices are presented in the thesis [14, §5.3.5] in 2005. Going further, the complete work related to this phenomena is presented in [52] in February of 2007. The

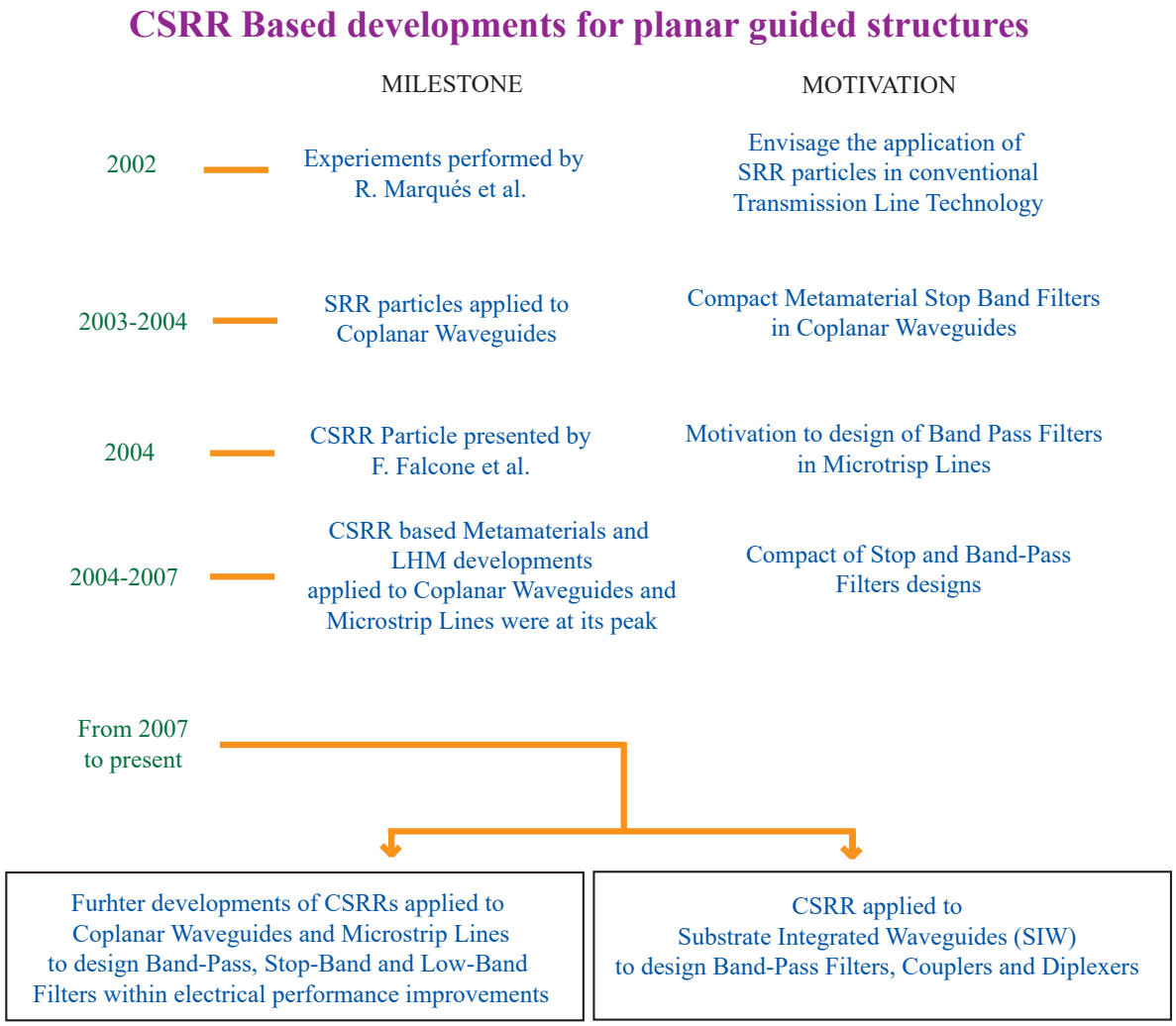

Figure 1.3. Development Summary on CSRR based guided structures

initial results presented in [14, §5.3.5] open the possibility to use SRRs as miniaturized and flexible radiating elements for antennas and arrays in wireless communication applications. Equally, this possibility can also be extended to CSRRs.

In overall, the application of the CSRR particles in antennas is divided in four categories. The first category handles with the scope of using the CSRR particle in existing antennas (such as ultra-wide-band monopole antennas) in order to achieve notched behavior. The second category deals with the implementation of the CSRR particles in the patch or in the ground plane of existing patch antennas in order to obtain dual or multiband antennas. The third category is devoted to the design of miniaturized antennas by using CSRR particles. Finally, in the fourth category the CSRR particles are inserted in existing antennas in order to improve the antenna performances, such as efficiency, gain or bandwidth.

In this section the state of the art of Metamaterial and LHM Planar antennas based on CSRRs is addressed by introducing the main relevant works of each category.

- Category 1: Notched behavior performance using CSRRs.

From 2008 compact printed ultra-wideband (UWB) monopole antennas with dual-band notched characteristics are presented in the literature, see [53], [54] and [55]. This applicability is to prevent the interference problem due to existing nearby communication system with the operating frequency of the UWB antenna. The dual band behavior is achieved by etching the CSRR particle in the patch of the monopole antenna.

- Category 2: Dual Band or Multiband Antennas using CSRRs.

In 2009 the first works resulting in dual band antennas using CSRRs in conventional antennas came out, see [56] and [42]. In those first works, the CSRR particle is etched in the patch of a conventional patch antenna. Specifically in [56] the lowest resonant frequency is driven by the CSRR particle itself, while the second resonant frequency is originated by the conventional patch itself. In lately designs the CSRR particle is etched in the ground plane of the conventional patch antenna, see [57], [58] and [59]. Recently in 2016 a dual-band multiple-input-multiple-output (MIMO) antenna with pattern diversity is designed in [60], targeting at the 2.4 GHz wireless local area network and 1.8 GHz global system of mobile communication application bands. The proposed scheme in the work [60] uses arrays of printed dipoles fed with signals of equal amplitude but different input-phase values to achieve diverse radiation patterns in the operating frequency bands. The printed dipoles are loaded with complementary split-ring resonators to obtain one additional lower-frequency resonance, ensuring simultaneous miniaturisation and dual-band characteristics.

- Category 3: Miniaturized antennas using CSRRs.

With the rapid growth of the wireless communication, there has been an increasing demand for the low-profile and efficient electrically small antennas. Metamaterials, including EM bandgap structures, double negative materials, and left-handed materials, have been well investigated over the years. These artificial materials are introduced into the current antenna systems to enhance the performance, especially in the size reduction of the conventional antennas. Consequently, the CSRR particle is a key structure in order to become real this motivation thanks to the subwavelength behavior of those particles. In 2007 the initial works start to be published, see [61], which it focuses on using left-handed materials for size reduction of microstrip antennas, etching the CSRR particle in the ground plane.

In 2011 more complex structures come out based on miniaturized patch antennas loaded with complementary split-ring resonators and reactive impedance surface (RIS), see [45] and [50]. In those structures the CSRR is incorporated on the patch to excite the antenna at a low CSRR resonance frequency, while the RIS is inserted below the patch to miniaturize the antenna size and improve the antenna radiation performance. In 2013 an electrically small substrate integrated waveguide (SIW) antenna is proposed in [62]. Its electrical size is reduced by loading a complementary split-ring resonator on the eighth-mode SIW (EMSIW).

- Category 4: Antennas properties improvement using CSRRs. By inserting a single or various CSRR particles in a conventional antenna different properties of such antennas can be improved.

  - Works [42] in 2009 and [50] in 2012 show the capability of modifying the polarization of a conventional patch by etching a CSRR particle in the antenna patch. In 2013 in [63] a coplanar waveguide (CPW)-fed dual band antenna operating at linear and circular polarization is presented. In this design the radiation element is a composite right/left-handed (CRLH) unit cell. This radiation element exhibits two resonant frequencies. Thanks to a rectangular complementary split ring resonator a TM01 mode orthogonal to +1st-Order is excited and a circularly polarized patch-like radiation characteristic at the upper frequency is achieved. In 2016 in [64] circularly polarized waves based on Electro Inductive-Wave (EIW) coupling to chains of complementary split ring resonators is achieved etching a CSRR array in the patch of a rectangular patch antenna.
  - Several works show radiation efficiency improvement of planar antennas inserting complementary split ring resonators. In 2010 [65] a dual-band dual-mode patch antenna based on the resonant-type metamaterial transmission line is proposed. The resonant-type metamaterial transmission line can provide zeroth-mode resonance at the lower frequency and positive-mode resonance at the upper frequency. For improvement of radiation efficiency, a complementary single split ring resonator is introduced to realise the resonant-type metamaterial transmission line. In 2011 in [66] the radiation efficiency of the resonant driven by the complementary split ring resonator is improved, by optimising the position of the resonant particle in the patch of a conventional patch antenna.

In 2015 in [67, Table 3] a state of the art study of dual band patch antennas based on CSRRs is provided. The design presented in [67] exhibits highest radiation efficiencies compared to other antennas designs presented in the state of the art of that work.

– In 2011 in [68] thanks to a complementary split ring resonator loaded ground structure, the capability of beam steering in a compact path antenna is enabled. This result could reduce the cost of a phased-array system to meet the requirement of the wireless communications. The double CSRR-loaded antenna presented in this work exhibits a scan possibility from -51 to 48 by changing the parameters of CSRR structure.

In *Fig. 1.4* a summary of the main developments and their motivation based on CSRR planar antennas is presented. The developments on Leaky Wave antennas will be presented in Chapter 6.

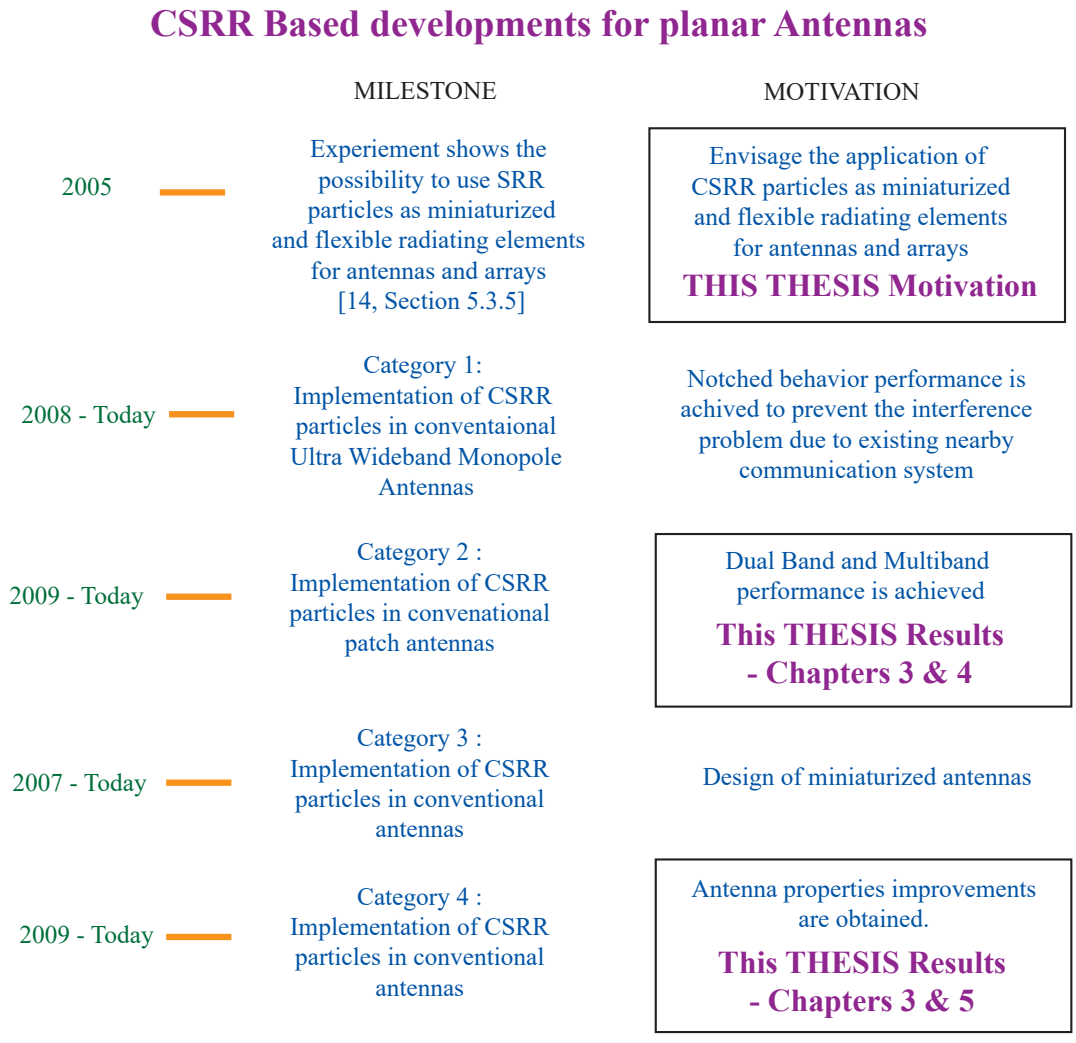

Figure 1.4. Development Summary on CSRR based planar Antennas

References

[1] F. Falcone, T. Lopetegi, M. Laso, J. Baena, J. Bonache, M. Berurete, R. Marqus, F. Martin, and M. Sorolla, "Babinet principle applied to metasurface and metamaterial design," *Phys. Rev. Lett.*, vol. 93, no. 12, pp. 197 491–1197 491–4, 2004.

[2] L. Mandelshtam, "Lectures on some problems of the theory of oscillations (1944), in complete collection of works," *Moscow: Academy of Sciences*, vol. 5, pp. 428–467 (in Russian), 1950.

[3] ——, "Group velocity in a crystal lattice," *Zhurnal Eksperimentalnoi i Teoreticheskoi Fiziki*, vol. 15, no. 9, pp. 476–478 (in Russian. English translation in Sov. Phys. ZETF), 1945.

[4] G. Malyuzhinets, "A note on the radiation principle," *Zhurnal Technicheskoi Fiziki*, vol. 21, pp. 940–942 (in Russian), 1951.

[5] D. Sivukhin, "The energy of electromagnetic waves in dispersive media," *Opt. Spektrosk.*, vol. 3, pp. 308–312, 1957.

[6] R. Silin, "Waveguiding properties of two-dimensional periodical slow-wave systems," *Voprosy Radioelektroniki, Elektronika*, vol. 4, pp. 11–33 (in Russian), 1959.

[7] V. Veselago, "The electrodynamics of substances with simultaneously negative values of permeability and permittivity," *Soviet Phys Uspekhi*, 1968.

[8] J. Pendry, A. Holden, D. Robbins, and W. Stewart, "Magnetism from conductors and enhanced nonlinear phenomena," *IEEE Trans. Microwave Theory Techn.*, vol. 47, pp. 2075–2084, 1999.

[9] D. Smith, W. Padilla, D. Vier, S. Nemat-Nasser, and S. Schultz, "Composite medium with simultaneously negative permeability and permittivity," *Physical Review Letters*, vol. 84, no. 18, pp. 4184–4187, May 2000.

[10] A. Shelby, D. Smith, S. Nemat-Nasser, and S. Schultz, "Microwave transmission through a two-dimensional, isotropic, left-handed metamaterial," *Applied Physics Letters*, vol. 78, no. 4, pp. 489–491, 2001.

[11] J. Pendry, "Negative refraction makes a perfect lens," *Physical Review Letters*, vol. 85, no. 18, pp. 3966–3969, 2000.

[12] R. Marques, F. Medina, and R. El-Idrissi, "Role of bianisotropy in negative permeabilitty and left-handed metamaterials," *Physical Review B*, vol. 65, pp. 144 440–1 144 440–6, 2002.

[13] C. Caloz and T. Itoh, "Application of the transmission line theory of left-handed (lh) materials to the realization of a microstrip lh line," in *in IEEE Antennas and Propagation Int. Symp. (AP-S) and USNC/URSI Meeting*, San Antonio, Jun. 2002, p. 412415.

[14] F. Falcone, "Synthesis and applications of microwave metamaterials in planar circuit technology: From electromagnetic bandgaps to left handed materials," Ph.D. dissertation, Departamento de Ingeniería Eléctrica y Electrónica, Universidad Pública de Navarra, Pamplona, Spain, 2005.

[15] R. Marques, J. Martel, F. Mesa, and F. Medina, "Left-handed media simulation and transmission of em waves in subwavelength split-ring resonator-loaded metallic waveguides," *Physical Review Letters*, 2002.

[16] F. Martín, F. Falcone, J. Bonache, R. Marqués, and M. Sorolla, "Miniaturized coplanar waveguide stop band filters based on multiple tuned split ring resonators," *IEEE Microwave and Wireless Components Letters*, vol. 13, no. 12, pp. 511–513, Dec 2003.

[17] F. Falcone, F. Martín, J. Bonache, R. Marqués, and M. Sorolla, "Coplanar waveguide structures loaded with split-ring resonators," *Microwave and Optical Technology Letters*, vol. 40, no. 1, pp. 3–6, 2004.

[18] J. García-García, F. Martin, F. Falcone, J. Bonache, I. Gil, T. Lopetegi, M. A. G. Laso, M. Sorolla, and R. Marques, "Spurious passband suppression in microstrip coupled line band pass filters by means of split ring resonators," *IEEE Microwave and Wireless Components Letters*, vol. 14, no. 9, pp. 416–418, Sept 2004.

[19] J. Bonache, I. Gil, J. Garcéia-García, and F. Martin, "Complementary split ring resonators for microstrip diplexer design," *Electronics Letters*, vol. 41, no. 14, pp. 810–811, July 2005.

[20] J. Bonache, F. Martín, J. Garía-García, I. Gil, R. Marqués, and M. Sorolla, "Ultra wide band pass filters (uwbpf) based on complementary split rings resonators," *Microwave and Optical Technology Letters*, vol. 46, no. 3, pp. 283–286, 2005.

[21] J. Bonache, F. Martín, F. Falcone, J. D. Baena, T. Lopetegi, J. García-García, M. A. Laso, I. Gil, A. Marcotegui, R. Marqués, and M. Sorolla, "Application of complementary split-ring resonators to the design of compact narrow band-pass structures in microstrip technology," *Microwave and Optical Technology Letters*, vol. 46, no. 5, pp. 508–512, 2005.

[22] J. D. Baena, J. Bonache, F. Martín, R. M. Sillero, F. Falcone, T. Lopetegi, M. A. G. Laso, J. García-García, I. Gil, M. F. Portillo, and M. Sorolla, "Equivalent-circuit models for split-ring resonators and complementary split-ring resonators coupled to planar transmission lines," *IEEE Transactions on Microwave Theory and Techniques*, vol. 53, no. 4, pp. 1451–1461, April 2005.

[23] J. Bonache, I. Gil, J. Garcia-Garcia, and F. Martín, "Novel microstrip bandpass filters based on complementary split-ring resonators," *IEEE Transactions on Microwave Theory and Techniques*, vol. 54, no. 1, pp. 265–271, Jan 2006.

[24] E. Jarauta, M. A. G. Laso, T. Lopetegi, F. Falcone, M. Beruete, J. D. Baena, A. Marcotegui, J. Bonache, J. García, R. Marqués, and F. Martín, "Novel microstrip backward coupler with metamaterial cells for fully planar fabrication techniques," *Microwave and Optical Technology Letters*, vol. 48, no. 6, pp. 1205–1209, 2006.

[25] J. Bonache, M. Gil, I. Gil, J. García-García, and F. Martín, "On the electrical characteristics of complementary metamaterial resonators," *IEEE Microwave and Wireless Components Letters*, vol. 16, no. 10, pp. 543–545, Oct 2006.

[26] P. Mondal, M. K. Mandal, A. Chaktabarty, and S. Sanyal, "Compact bandpass filters with wide controllable fractional bandwidth," *IEEE Microwave and Wireless Components Letters*, vol. 16, no. 10, pp. 540–542, Oct 2006.

[27] J. García-García, J. Bonache, I. Gil, F. Martin, M. C. Velázquez-Ahumada, and J. Martel, "Miniaturized microstrip and cpw filters using coupled metamaterial resonators," *IEEE Transactions on Microwave Theory and Techniques*, vol. 54, no. 6, pp. 2628–2635, June 2006.

[28] C. Li, K. y. Liu, and F. Li, "Design of microstrip highpass filters with complementary split ring resonators," *Electronics Letters*, vol. 43, no. 1, pp. 35–36, Jan 2007.

[29] M. Gil, J. Bonache, J. García-García, J. Martel, and F. Martín, "Composite right/left-handed metamaterial transmission lines based on complementary split-rings resonators and their applications to very wideband and compact filter design," *IEEE Transactions on Microwave Theory and Techniques*, vol. 55, no. 6, pp. 1296–1304, June 2007.

[30] M. Gil, "Synthesis and applications of new left handed microstrip lines with complementary split-ring resonators etched on the signal strip," *IET Microwaves, Antennas & Propagation*, vol. 2, pp. 324–330(6), June 2008.

[31] G.-L. Wu, "Design of novel dual-band bandpass filter with microstrip meander-loop resonator and csrr dgs," *Electronics Letters*, vol. 78, pp. 17–24, 2008.

[32] A. Vélez, F. Aznar, J. Bonache, M. C. Velázquez-Ahumada, J. Martel, and F. Martín, "Open complementary split ring resonators (ocsrrs) and their application to wideband cpw band pass filters," *IEEE Microwave and Wireless Components Letters*, vol. 19, no. 4, pp. 197–199, April 2009.

[33] X. Luo, "Wideband bandpass filter with excellent selectivity using new csrr-based resonator," *Electronics Letters*, vol. 46, pp. 1390–1391(1), September 2010.

[34] A. Ebrahimi, W. Withayachumnankul, S. F. Al-Sarawi, and D. Abbott, "Compact dual-mode wideband filter based on complementary split-ring resonator," *IEEE Microwave and Wireless Components Letters*, vol. 24, no. 3, pp. 152–154, March 2014.

[35] A. K. Horestani, M. Durn-Sindreu, J. Naqui, C. Fumeaux, and F. Martín, "S-shaped complementary split ring resonators and their application to compact differential bandpass filters with common-mode suppression," *IEEE Microwave and Wireless Components Letters*, vol. 24, no. 3, pp. 149–151, March 2014.

[36] A. Naghar, A. Alejos, F. Falcone, O. Aghzout, and M. Sánchez, "Selectivity improvement in dual-band band pass filter by coupled complementary split ring resonators," in *2015 USNC-URSI Radio Science Meeting (Joint with AP-S Symposium)*, July 2015, pp. 190–190.

[37] A. Casanueva, A. León, O. González, A. Mediavilla, M. Arias, and N. Amar, "Improved compact microstrip low pass filter with novel distributions of complementary split ring resonators (csrrs)," in *2009 Asia Pacific Microwave Conference*, Dec 2009, pp. 1450–1453.

[38] H.-Y. Zeng, G.-M. Wang, C.-X. Zhang, and L. Zhu, "Compact microstrip low-pass filter using complementary split ring resonators with ultra-wide stopband and high selectivity," *Microwave and Optical Technology Letters*, vol. 52, no. 2, pp. 430–433, 2010.

[39] H. Taher, "High-performance low-pass filter using complementary square split ring resonators defected ground structure," *IET Microwaves, Antennas Propagation*, vol. 5, no. 7, pp. 771–775, May 2011.

[40] J. Naqui, A. Fernández-Prieto, M. Duran-Sindreu, F. Mesa, J. Martel, F. Medina, and F. Martín, "Common-mode suppression in microstrip differential lines by means of complementary split ring resonators: Theory and applications," *IEEE Transactions on Microwave Theory and Techniques*, vol. 60, no. 10, pp. 3023–3034, Oct 2012.

[41] A. Ebrahimi, W. Withayachumnankul, S. F. Al-Sarawi, and D. Abbott, "Compact second-order bandstop filter based on dual-mode complementary split-ring resonator," *IEEE Microwave and Wireless Components Letters*, vol. 26, no. 8, pp. 571–573, Aug 2016.

[42] X.-C. Zhang, Z.-Y. Yu, and J. Xu, "Novel band-pass substrate integrated waveguide (siw) filter based on complementary split ring resonators (csrrs)," *Progress In Electromagnetics Research*, vol. 72, pp. 39–46, 2007.

[43] Che, Wenquan, Li, Chao, Deng, Kuan, Yang, and Lisheng, "A novel bandpass filter based on complementary split rings resonators and substrate integrated waveguide," *Microwave and Optical Technology Letters*, vol. 50, no. 3, pp. 699–701, 2008.

[44] L. S. Wu, X. L. Zhou, Q. F. Wei, and W. Y. Yin, "An extended doublet substrate integrated waveguide (siw) bandpass filter with a complementary split ring resonator (csrr)," *IEEE Microwave and Wireless Components Letters*, vol. 19, no. 12, pp. 777–779, Dec 2009.

[45] Y. D. Dong, T. Yang, and T. Itoh, "Substrate integrated waveguide loaded by complementary split-ring resonators and its applications to miniaturized waveguide filters," *IEEE Transactions on Microwave Theory and Techniques*, vol. 57, no. 9, pp. 2211–2223, Sept 2009.

[46] Q. L. Zhang, W. Y. Yin, S. He, and L. S. Wu, "Compact substrate integrated waveguide (siw) bandpass filter with complementary split-ring resonators (csrrs)," *IEEE Microwave and Wireless Components Letters*, vol. 20, no. 8, pp. 426–428, Aug 2010.

[47] Y. Dong, C. T. M. Wu, and T. Itoh, "Miniaturised multi-band substrate integrated waveguide filters using complementary split-ring resonators," *IET Microwaves, Antennas Propagation*, vol. 6, no. 6, pp. 611–620, April 2012.

[48] J. d. Jin and D. h. Yu, "Substrate integrated waveguide band-pass filter with coupled complementary split ring resonators," in *2014 XXXIth URSI General Assembly and Scientific Symposium (URSI GASS)*, Aug 2014, pp. 1–4.

[49] A. R. Azad and A. Mohan, "Sixteenth-mode substrate integrated waveguide bandpass filter loaded with complementary split-ring resonator," *Electronics Letters*, vol. 53, no. 8, pp. 546–547, 2017.

[50] Y. Dong and T. Itoh, "Substrate integrated waveguide loaded by complementary split-ring resonators for miniaturized diplexer design," *IEEE Microwave and Wireless Components Letters*, vol. 21, no. 1, pp. 10–12, Jan 2011.

[51] M. Danaeian, A. R. Moznebi, K. Afrooz, and H. Hakimi, "Miniaturised equal/unequal siw power divider with bandpass response loaded by csrrs," *Electronics Letters*, vol. 52, no. 22, pp. 1864–1866, 2016.

[52] I. Arnedo, J. Illescas, M. Flores, T. Lopetegi, M. A. G. Laso, F. Falcone, J. Bonache, J. García-García, F. Martín, J. A. Marcotegui, R. Marqués, and M. Sorolla, "Forward and backward leaky wave radiation in split-ring-resonator-based metamaterials," *IET Microwaves, Antennas Propagation*, vol. 1, no. 1, pp. 65–68, February 2007.

[53] J. Liu, S. Gong, Y. Xu, X. Zhang, C. Feng, and N. Qi, "Compact printed ultra-wideband monopole antenna with dual band-notched characteristics," *Electronics Letters*, vol. 44, no. 12, pp. 710–711, June 2008.

[54] D. Jiang, Y. Xu, R. Xu, and W. Lin, "Compact dual-band-notched uwb planar monopole antenna with modified csrr," *Electronics Letters*, vol. 48, no. 20, pp. 1250–1252, September 2012.

[55] W. T. Li, Y. Q. Hei, W. Feng, and X. W. Shi, "Planar antenna for 3g/bluetooth/wimax and uwb applications with dual band-notched characteristics," *IEEE Antennas and Wireless Propagation Letters*, vol. 11, pp. 61–64, 2012.

[56] N. Ortiz, F. Falcone, and M. Sorolla, "Dual band patch antenna based on complementary rectangular split-ring resonators," in *2009 Asia Pacific Microwave Conference*, Dec 2009, pp. 2762–2765.

[57] Y. Xie, L. Li, C. Zhu, and C. Liang, "A novel dual band patch antenna with complementary split ring resonators embedded in the ground plane," *Progress In Electromagnetics Research Letters*, vol. 25, pp. 117–126, 2011.

[58] Y. Sidana, R. K. Chaudhary, and K. V. Srivastava, "A novel dual-band hexagonal patch antenna coupled with complementary split ring resonator," in *2012 Asia Pacific Microwave Conference Proceedings*, Dec 2012, pp. 1343–1345.

[59] T. Agrawal, S. Srivastava, and M. Dadel, "Dual and triple band rectangular patch antenna using complementary split ring resonator (csrr)," in *2015 IEEE Applied Electromagnetics Conference (AEMC)*, Dec 2015, pp. 1–2.

[60] D. Sarkar, K. Saurav, and K. V. Srivastava, "Dual band complementary split-ring resonator-loaded printed dipole antenna arrays for pattern diversity multiple-input multiple-output applications," *IET Microwaves, Antennas Propagation*, vol. 10, no. 10, pp. 1113–1123, 2016.

[61] A. U. Limaye and J. Venkataraman, "Size reduction in microstrip antennas using left-handed materials realized by complementary split-ring resonators in ground plane," in *2007 IEEE Antennas and Propagation Society International Symposium*, June 2007, pp. 1869–1872.

[62] S. Sam and S. Lim, "Electrically small complementary split-ring resonator antenna on eighth-mode substrate integrated waveguide," *Electronics Letters*, vol. 49, no. 8, pp. 519–521, April 2013.

[63] C. Zhou, G. Wang, Y. Wang, B. Zong, and J. Ma, "Cpw-fed dual-band linearly and circularly polarized antenna employing novel composite right/left-handed transmission-line," *IEEE Antennas and Wireless Propagation Letters*, vol. 12, pp. 1073–1076, 2013.

[64] N. Ortiz, G. Crespo, J. C. Iriarte, and F. Falcone, "Generation of circularly polarized waves based on electro inductive-wave (eiw) coupling to chains of complementary split ring resonators," *Journal of Applied Physics*, vol. 120, no. 17, p. 174905, 2016.

[65] J. X. Niu, "Dual-band dual-mode patch antenna based on resonant-type metamaterial transmission line," *Electronics Letters*, vol. 46, no. 4, pp. 266–268, February 2010.

[66] N. Ortiz, F. Falcone, and M. Sorolla, "Radiation efficiency improvement of dual band patch antenna based on a complementary rectangular split ring resonator," in *Proceedings of the 5th European Conference on Antennas and Propagation (EUCAP)*, April 2011, pp. 830–834.

[67] N. Ortiz, J. C. Iriarte, G. Crespo, and F. Falcone, "Design and implementation of dual-band antennas based on a complementary split ring resonators," *Waves in Random and Complex Media*, vol. 25, no. 3, pp. 309–322, 2015.

[68] W. Cao, Y. Xiang, B. Zhang, A. Liu, T. Yu, and D. Guo, "A low-cost compact patch antenna with beam steering based on csrr-loaded ground," *IEEE Antennas and Wireless Propagation Letters*, vol. 10, pp. 1520–1523, 2011.

2. Waveguide Filter Design

Il faut faire de la vie un rêve et faire d'un rêve une réalité.

Pierre Curie

Based on the results made in metasurfaces by using the Complementary Split Ring Resonators as a unit cell, the idea of using such particle for the design of compact Waveguide filters came up to our minds at the end of 2004. In 2005, the first author's contribution on this topic is published. To the best of the author's knowledge, the author's contributions on this topic do precede to other works.

There is a wide array of different types of waveguide filters. In general, the design of Waveguide filters can be tackled by using discrete or distributed elements along the waveguide. Examples of the discrete elements are the chain of coupled resonators that can be modeled as a ladder network of LC circuits. One of the most common types consists of a number of coupled resonant cavities based on different means of coupling; such us apertures, irises and posts. On the other hand, among distributed elements corrugated filters and dielectric resonator filters are considered. Each canonical solution has advantages and disadvantages. In that sense, waveguide filters based on distributed elements allow power handling capability over wide bandwidths within the constraint of resulting in large filter dimensions. On the contrary, waveguide filters based on discrete elements exhibit compact dimensions within the disadvantages of narrow bandwidths and low power handling capabilities.

In this thesis both type of waveguide designs have been addressed and in this chapter author's contributions in both directions are presented. In relation to the contribution on distributed filters, the first section of this chapter presents the results of a project between European Space Agency and Public University of Navarra. Those results are presented in the resulted patent annexed to this chapter. On the other hand, the Complementary Split Ring Resonator particle is envisaged to be used in the design of compact Waveguide filters. The outcomes of this research are comprised in the author's paper presented in the last section of this chapter.

2.1 Waveguide Filter based on Distributed Elements

The waveguide filter based on distributed elements presented in this thesis is designed in the frame of a research project between European Space Agency and Public University of Navarra. The goal of the project is to design a Band-Stop filter for output Multiplexers. This filter must consequently withstand kiloWatt or higher order power levels. In order to fulfill such specification a solution based on distributed elements is chosen.

The novelty of the Band-Stop filter developed in the frame of this project is that the distributed sinusoidal perturbations along the waveguide relies on the principle of Bragg rejection. So far, Bragg structures have been devoted in the field of microwaves for producing converters and filters for low power applications [1], [2] and [3]. It is remarkable that it is the first time that such perturbations are used as in this project circumstances for the design of high power and broadband multimode filters.

2.1.1 Patent: Band-Stop Filter for an Output Multiplexer

The designed filter consists of a classical high-power E-plane corrugated low-pass filter that is cascaded with a periodically longitudinal sinusoidal perturbation. The period of the longitudinal sinusoidal variation is the Bragg period for the fundamental guided mode at a center frequency of the band to be stopped.

In the frame of aforementioned project (*Section 2.1*) a filter prototype has been designed, manufactured and tested. The results of the mentioned project resulted into a patent, which is included below in this section. This patent has been done in collaboration with Javier Gil and Mario Sorolla Ayza from Public University of Navarra. The contribution of this filter in the field of satellite communications is summarized as follows:

- The longitudinal perturbation allows the minimum gap of the corrugated filter to be kept wide which, along with the smoothness and the wide gap of the periodic-structure itself, enables high-power TE10 mode operation in the whole structure as the spurious pass bands are suppressed. Thus, the presented filter presents higher power handling capabilities compared to the one presented by conventional E-plane corrugated filters.
- The resulting prototype presents several kilowatts handling capability and the spurious pass-bands will be suppressed up to the third harmonic (around 40 GHz). The presented profile increases the Multipaction phenomenon threshold, which is essential to allow kiloWatt or higher order power levels power handling capabilities.

US007468641B2

(12) **United States Patent**
Sorolla et al.

(10) **Patent No.: US 7,468,641 B2**
(45) **Date of Patent: Dec. 23, 2008**

(54) **MICROWAVE BANDSTOP FILTER FOR AN OUTPUT MULTIPLEXER**

(75) Inventors: **Mario Sorolla**, Castello (ES); **Dietmar Schmitt**, Wassenaar (NL); **Marco Guglielmi**, Wassenaar (NL); **Javier Gil**, Pamplona (ES); **Noelia Ortiz Perez De Eulate**, Alsasua (ES)

(73) Assignee: **Agence Spatiale Europeenne**, Paris (FR)

(*) Notice: Subject to any disclaimer, the term of this patent is extended or adjusted under 35 U.S.C. 154(b) by 230 days.

(21) Appl. No.: **11/492,883**

(22) Filed: **Jul. 26, 2006**

(65) **Prior Publication Data**

US 2007/0024394 A1 Feb. 1, 2007

(30) **Foreign Application Priority Data**

Jul. 27, 2005 (FR) 05 08005

(51) **Int. Cl.**
H01P 1/00 (2006.01)
H01P 5/12 (2006.01)
H01P 9/00 (2006.01)

(52) **U.S. Cl.** **333/135**; 333/122; 333/157; 333/208; 333/248

(58) **Field of Classification Search** 333/122, 333/134–136, 157, 208–212, 248; 385/37
See application file for complete search history.

(56) **References Cited**

U.S. PATENT DOCUMENTS

2,912,695 A 11/1959 Cutler
3,046,503 A * 7/1962 Cohn 333/210
3,082,384 A * 3/1963 Crane et al. 333/209
3,263,116 A * 7/1966 Azam et al. 315/3.6
3,597,710 A * 8/1971 Levy 333/210

(Continued)

FOREIGN PATENT DOCUMENTS

DE 42 18 815 A1 12/1993

(Continued)

OTHER PUBLICATIONS

O.R. Asfar et al., "Microwave filter response of nonuniformly corrugated circular waveguide", Journal of Electromagnetic Waves and Applications, vol. 9, No. 1/2, 1995, pp. 127-143.

(Continued)

Primary Examiner—Benny Lee
Assistant Examiner—Kimberly E Glenn
(74) *Attorney, Agent, or Firm*—Clark & Brody

(57) **ABSTRACT**

A microwave bandstop filter comprises a waveguide segment of cross-section that presents longitudinal variation of sinusoidal type modulated by an amplitude function that is continuous, the period of said longitudinal variation of sinusoidal type being the Bragg period for the fundamental guided mode at a center frequency of the band to be stopped. A filter assembly comprises a microwave lowpass filter presenting a cutoff frequency and at least one interfering passband at frequencies higher than said cutoff frequency, and at least one bandstop filter as defined above, connected to the output of said lowpass filter, in which the amplitude and the period of said longitudinal variation, and also the length over which it extends are such that they stop said interfering passband of said lowpass filter. An output multiplexer for a multichannel microwave transmitter includes such a filter assembly.

16 Claims, 5 Drawing Sheets

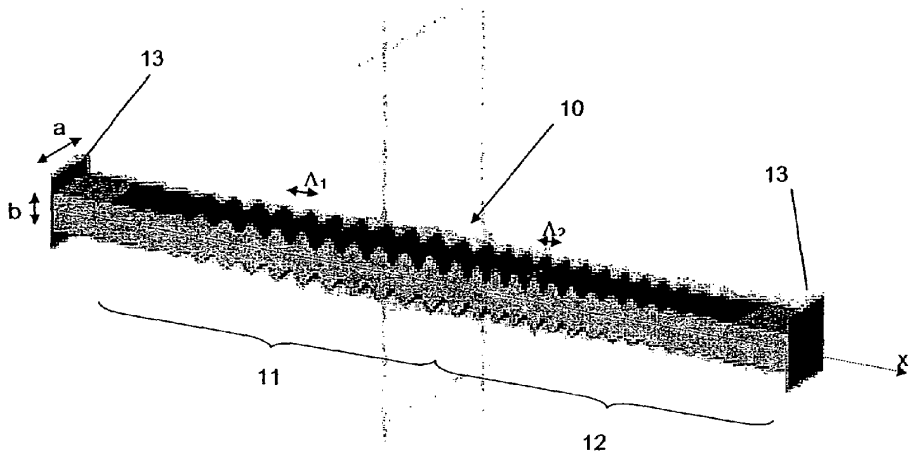

U.S. PATENT DOCUMENTS

4,745,617	A	5/1988	Harvey	
4,847,574	A *	7/1989	Gauthier et al.	333/21 A
5,600,740	A	2/1997	Asfar	
5,942,956	A *	8/1999	Haq et al.	333/21 R
6,118,978	A *	9/2000	Ihmels	455/12.1
6,191,670	B1	2/2001	Nguyen	
6,285,267	B1 *	9/2001	Hauth et al.	333/210

FOREIGN PATENT DOCUMENTS

DE	4218815	A1 *	12/1993
EP	1492194	A1 *	12/2004

OTHER PUBLICATIONS

M. Ludovico et al., "Multipaction Analysis and Power Handling Evaluation in Waveguide Components for Satellite Antenna Applications", exp, vol. 1, No. 1, Dec. 2001, pp. 20-23.

N.F. Kovalev et al., "Wave Transformation in a Multimode Waveguide with Corrugated Walls", Radiophysics and Quantum Electronics, vol. 11, No. 5, 1968, pp. 449-450.

B.Z. Katsenelenbaum et al., "Theory of Nonuniform Waveguides, the cross-section method", IEEE Electromagnetic Wave Series, vol. 44, London, 1998.

* cited by examiner

U.S. Patent Dec. 23, 2008 Sheet 1 of 5 US 7,468,641 B2

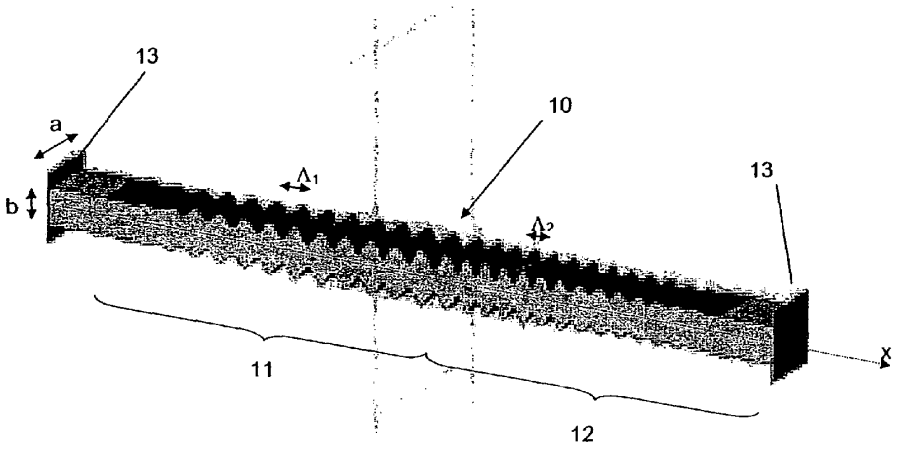

FIG. 1A

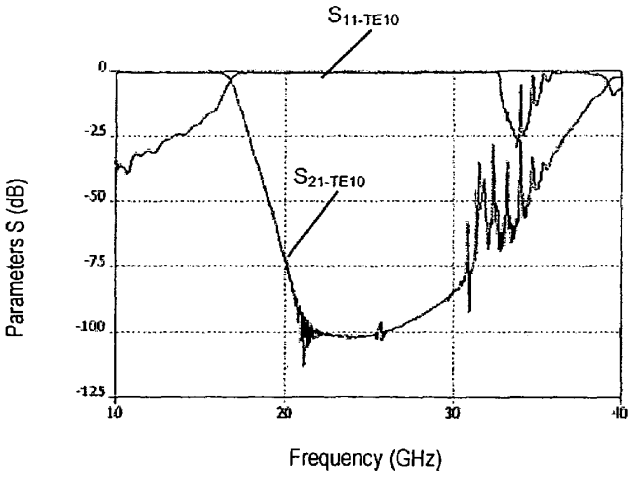

FIG. 1B

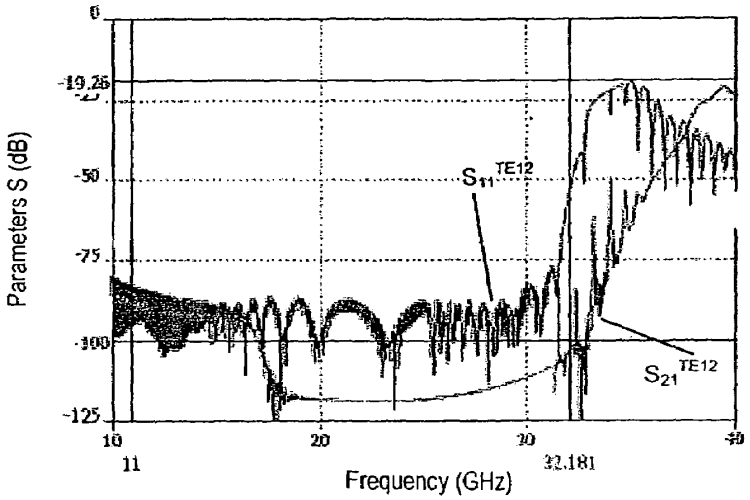

FIG. 1C

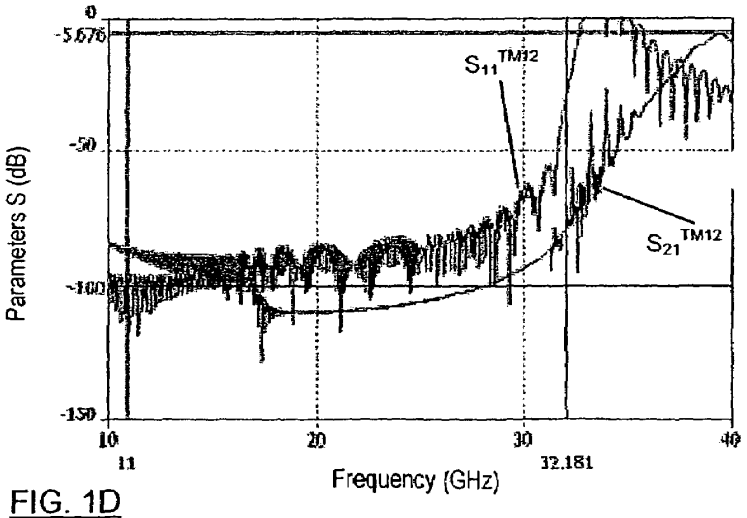

FIG. 1D

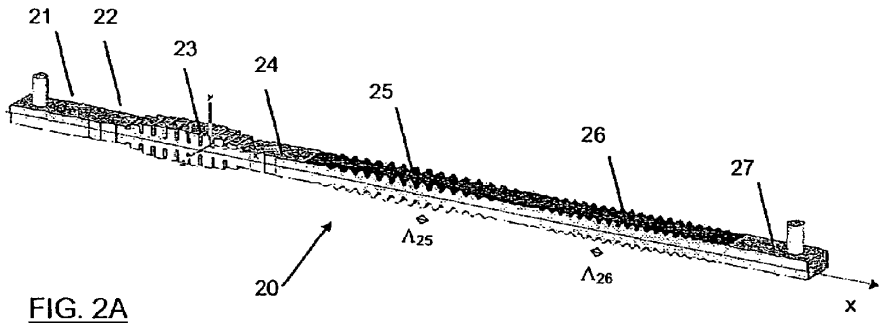

FIG. 2A

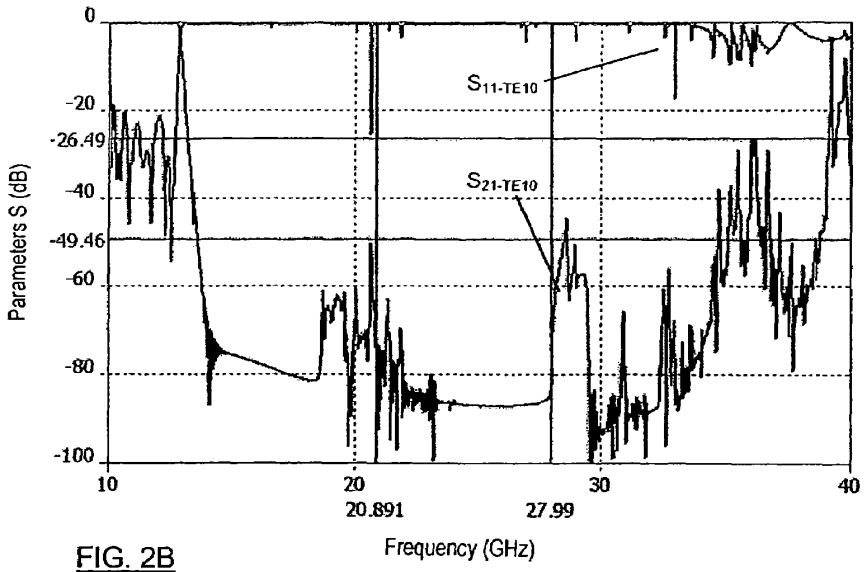

FIG. 2B

U.S. Patent Dec. 23, 2008 Sheet 4 of 5 US 7,468,641 B2

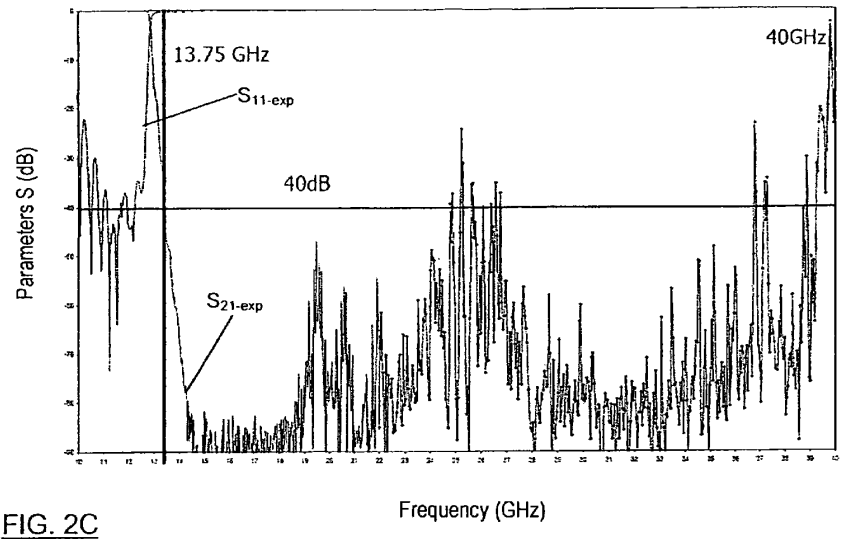

FIG. 2C

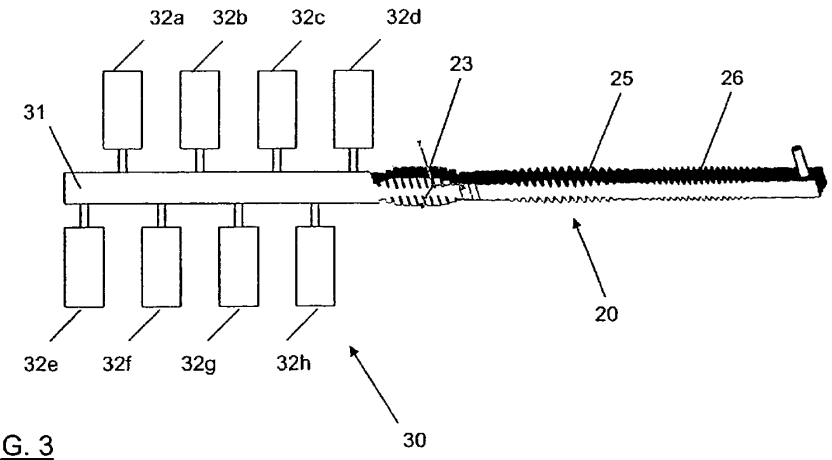

FIG. 3

FIG. 4A

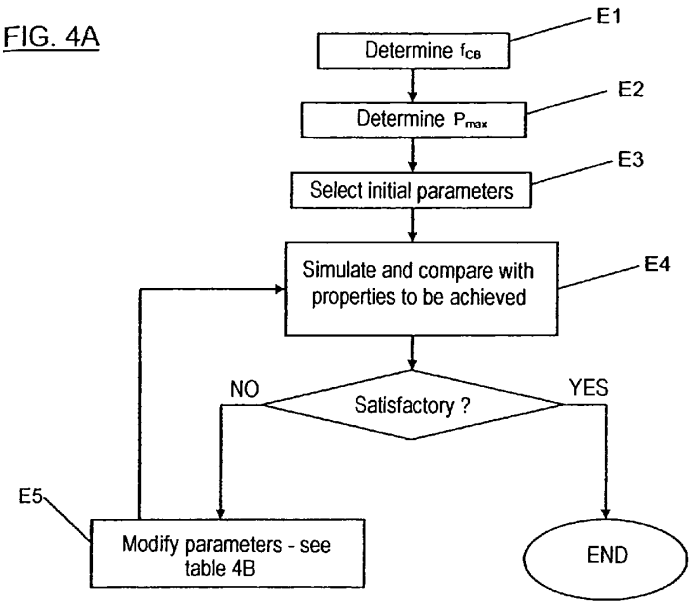

	$A(f_{CB})>A'(f_{CB})$	$A(f_{CB})\cong A'(f_{CB})$	$A(f_{CB})<A'(f_{CB})$
LB>LB'	–	–	Increase scale factor of P(x)
LB≅LB'	–	–	Increase amplitude without exceeding Pmax Increase scale factor of P(x) Introduce Φ(x)
LB<LB'	Decrease scale factor of P(x)	Decrease scale factor of P(x) Increase amplitude without exceeding Pmax Introduce Φ(x)	Increase amplitude without exceeding Pmax Increase scale factor of P(x) Introduce Φ(x)

FIG. 4B

US 7,468,641 B2

MICROWAVE BANDSTOP FILTER FOR AN OUTPUT MULTIPLEXER

The invention relates to a bandstop filter for operating in the microwave region of the spectrum, and more particularly in bands X to K or Ka, and enabling signals to be transmitted at high power, of kilowatt or higher order.

Such a filter is intended particularly, but not exclusively, for application to output multiplexers of transmitters in telecommunications satellites.

The invention also relates to a filter assembly including such a bandstop filter, and to an output multiplexer of a microwave multichannel transmitter including such a filter assembly.

BACKGROUND OF THE INVENTION

Microwave transmitters for telecommunications satellites use an output multiplexer (OMUX) for combining the various transmission channels. In modern systems, it can be necessary to combine as many as 18 or more channels, and since the power of each channel in the Ku band (12 gigahertz (GHz) to 18 GHz) generally lies in the range 150 watts (W) to 250 W, the output multiplexer must be capable of accommodating total power levels of several kilowatts. In general, such a multiplexer uses a common manifold structure for combining the various channels. At the common output from the manifold, non-linear effects, e.g. due to connection flanges, lead to the appearance of interference signals due to intermodulation and known as parasitic intermodulation products (PIMP) which can occur in the passband of the receiver. The traditional approach for reducing the magnitude of intermodulation products consists in providing, upstream from the common manifold, a lowpass filter for each channel, so as to eliminate the harmonics of the payload signal; in particular, it has been found necessary to eliminate interference signals at least up to the third harmonic.

In order to reduce the weight and size of the multiplexer, it would be preferable to use a common lowpass filter instead of individual filters for each channel. However, filters known in the prior art do not enable satisfactory filtering to be obtained while simultaneously conveying high power. Waveguide filters adapted for these applications, such as filters of the waffle iron type or corrugated waveguide type present interference passbands above the nominal cutoff frequency, and in particular at frequencies that are harmonics thereof. The magnitudes of these interfering passbands increase with increasing spacing or gap between the walls of the waveguide in the electric field direction of the waves being conveyed, which leads to operation of multimode type: consequently, in order to be effective in eliminating the undesirable frequencies, it is necessary to use filters with a small gap, but that is not possible in high power applications (power of kilowatt or greater order), in particular when the filter is to be used in a vacuum, because of the risk of electron avalanche discharges ("multipaction"). A discussion of the electron avalanche discharge phenomenon can be found in the article by M. Ludovico, G. Zarba, L. Accatino, and D. Raboso "Multipaction analysis and power handling evaluation in waveguide components for satellite antenna applications", exp, Vol. 1, No. 1, December 2001.

OBJECTS AND SUMMARY OF THE INVENTION

An object of the present invention is to make it possible to achieve effective filtering over a broad band at high frequencies even in high power applications, and to do using a device that presents a structure that is particularly simple and easy to make. By way of example, the invention makes it possible to obtain attenuation of at least 25 decibels (dB) over a band having a width of several gigahertz at frequencies greater than 15 GHz, while making use solely of a passive structure in the form of a waveguide.

The invention relies on the principle of Bragg reflection, which is already used in the field of microwaves for producing mode converters and filters, but has never been used in high power and broadband multimode filters, as in the present circumstances.

For example, the article "Wave transformation in a multimode waveguide with corrugated walls" by N. F. Kovalev, I. M. Orlova, and M. I. Petelin, Radiophysics and Quantum Electronics, Vol. 11, No. 5, pages 449-450 (1968) discloses using a waveguide with corrugated walls as a narrowband filter. The corrugations of the walls have a sinusoidal profile and a peak-to-peak amplitude that is approximately equal to 3.8% of the mean cross-section of the waveguide.

The use of waveguides with walls presenting sinusoidal disturbances as mode converters operating in narrow band and in overmoded or quasi-optical regime, is also described in the work by B. Z. Katsenelenbaum, L. Mercader del Rio, M. Pereyaslavets, M. Sorolla Ayza, and M. Thumm "Theory of non-uniform waveguides—the cross-section method", IEEE Electromagnetic Waves Series, Vol. 44, London (1998).

In addition, U.S. Pat. No. 5,600,740 discloses using a corrugated waveguide presenting a 180° phase jump as a narrow band bandpass filter.

The invention provides a microwave bandstop filter comprising a waveguide segment of cross-section that presents longitudinal variation of the sinusoidal type that is modulated by an amplitude function that is continuous, the period of said longitudinal variation of sinusoidal type being the Bragg period for the fundamental guided mode at a center frequency of the band to be stopped.

According to advantageous characteristics of the invention:

The waveguide segment may be a metal waveguide segment of rectangular cross-section, the longitudinal variation in said cross-section being obtained by symmetrical deformation of two opposite faces thereof, and preferably of the two opposite faces of the greatest length;

- the maximum amplitude of the variation of said cross-section may be such that the minimum spacing or gap between said two opposite walls lies in the range 30% to 70%, and preferably in the range 40% to 60% of the mean gap;
- said waveguide segment may extend over a length lying in the range ten periods to 30 periods of said longitudinal variation of sinusoidal type of the cross-section;
- said amplitude function may present a rising front and a falling front of slope that is sufficiently small for the coefficient of reflection at the input of said waveguide section is less than or equal to −20 dB for frequencies lower than those of said band that is to be stopped;
- said amplitude function may be selected from: a cosine-squared function, a cosine even-power function, a Gaussian function, and a Hamming, Kaiser-Müller, or Black window;
- said longitudinal variation of sinusoidal type in the cross-section of the waveguide segment may also present continuous phase modulation (or frequency modulation, since that constitutes a special case of phase modulation).

In a particular embodiment:

the mean transverse dimensions of the waveguide section constituting said or each bandstop filter and the maximum amplitude of the longitudinal variation of its cross-section are such that they enable power of at least 0.5 kW to be conveyed in the microwave region of the spectrum without any danger of electron avalanche discharges occurring in a vacuum; and

the amplitude and the period of said longitudinal variation, and the length over which it extends, are such that they produce attenuation of at least 25 dB by Bragg reflection in a band having a width of at least 1 GHz.

Even more particularly, the mean transverse dimensions of the waveguide segment and the maximum amplitude of said longitudinal variation in its cross-section may be such that they enable power of at least 1 kW to be transmitted in the X and Ku bands without electron avalanche discharges occurring in a vacuum, and the amplitude and the period of said longitudinal variation, and the length over which it extends may be such that they produce attenuation of at least 25 dB by Bragg reflection in a band having a width of at least 1 GHz in bands K and higher.

The invention also provides a filter assembly comprising:

a microwave lowpass filter presenting a cutoff frequency and at least one interfering passband at frequencies higher than said cutoff frequency; and

at least one band stop filter as defined above, connected to the output of said lowpass filter, in which the amplitude and the period of said longitudinal variation, and the length over which it extends are such that they stop said interfering passband of said lowpass filter.

Advantageously:

the mean transverse dimensions of the waveguide segment constituting said or each bandstop filter, and the maximum amplitude of the longitudinal variation in its cross-section are such that they enable power to be conveyed that is not less than the maximum output power from said lowpass filter without electron avalanche discharges occurring in a vacuum;

the cutoff frequency of said lowpass filter is situated in the Ku band, and said interfering band is situated in the K or Ka band; and

said filter assembly comprises at least two filters as defined above, dimensioned to stop the interference band of said lowpass filter centered to correspond with the second and the third harmonics of its cutoff frequency.

The invention also provides an output multiplexer for a microwave multichannel transmitter including an output filter, wherein said output filter comprises such a filter assembly.

BRIEF DESCRIPTION OF THE DRAWINGS

Other characteristics, details, and advantages of the invention appear on reading the following description made with reference to the accompanying drawings, in which:

FIG. **1**A is a perspective view of a first filter of the invention, constituted by a waveguide segment of cross-section that presents longitudinal variation of sinusoidal type modulated in amplitude and in frequency;

FIGS. **1**B, **1**C, and **1**D are graphs showing the filter properties of the FIG. **1**A device;

FIG. **2**A is a perspective view of a filter assembly of the invention constituted by a cascade connection of a prior art lowpass filter and two waveguide segments of cross-section presenting longitudinal variation of amplitude modulated sinusoidal type;

FIGS. **2**B and **2**C are graphs showing the filter properties of the FIG. **2**A assembly;

FIG. **3** is an output multiplexer comprising a filter assembly of the type shown in FIG. **2**A; and

FIGS. **4**A and **4**B are diagrams showing a method of designing a bandstop filter of the invention.

MORE DETAILED DESCRIPTION

A bandstop filter of the invention is essentially constituted by a waveguide segment of cross-section that presents longitudinal variation of sinusoidal type, modulated by a continuous amplitude and/or phase function. If the cross-section of the waveguide segment is written S(x), where x is a longitudinal coordinate, it is then possible to write:

$$S(x)=S_0+P(x)\cdot\sin[\Omega_0\cdot x+\Phi(s)] \quad [1]$$

where:

S_0 is the mean section; and

$P(x)\cdot\sin[\Omega_0\cdot x+\Phi(x)]$ represents the modulated sinusoidal variation.

Advantageously, the filter can be obtained from a waveguide of rectangular section such as, for example, a WR75 waveguide having sides of length a=19.05 millimeters (mm) and b=9.525 mm. Such a waveguide is generally used for propagating TE modes in which the electric field is perpendicular to the longest walls, which are consequently said to be "E-planes". It is observed that when such a waveguide is used in a band lying in the range 10 GHz to 15 GHz and above, it presents a multimode character.

In the embodiment of the invention shown in FIG. **1**A, the distance b between the E-planes of a segment **10** of a WR75 type waveguide, known as the spacing or "gap", depends on the longitudinal coordinate x in application of a relationship of the form:

$$b(x)=b_0+P(x)\cdot\sin[\Omega_0\cdot x\Phi(x)] \quad [2]$$

This disturbance is obtained by deforming the E-planes of the waveguide in symmetrical manner.

In this embodiment, the phase function $\Phi(x)$ is kept constant in a first region **11** of the segment **10**, and then it increases linearly in a second region **12**. That means that the almost sinusoidal disturbance period of the gap presents a first space period $\Lambda_1=2\pi/\Omega_0$ in the first region **11** and a second space period $\Lambda_2=2\pi/(\Omega_0+d\Phi/dx)$ in the second region **12**, the connection between said regions taking place without phase discontinuity. More precisely, the first period Λ_1=7.142 mm corresponds to the Bragg period for an electromagnetic wave of frequency f_1=23 GHz propagating in the waveguide in the fundamental TE_{10} mode, and the second period Λ_2=5.26 mm corresponds to the Bragg period for a wave of frequency f_2=30 GHz also propagation in TE_{10} mode. It is recalled that the Bragg period Λ_B for an electromagnetic wave of frequency f propagating with a guided wave number β (f) is given by $\Lambda_B=\pi/\beta(f)$. When this condition is satisfied, the reflection coefficient of the wave is maximized.

The function of amplitude P(x) is a cosine-squared function of maximum amplitude equal to about $b_0/2$=4.7625 mm. The peak of the function P(x) corresponds to the interface between the first and second regions of the segment **10** and its first zeros to the level at the ends of said regions, beyond which it is truncated. Each region **11**, **12** has fourteen periods of the corresponding disturbance.

Such a structure can accommodate conveying power of the order of 1 kW at a frequency of 10 GHz to 15 GHz without there being any risk of an electron avalanche discharge occurring.

FIG. **1**B shows the way the scattering parameters S_{11} and S_{21} for the TE_{10} fundamental mode of the FIG. **1**A device depend on frequency. The physical significance of these terms is recalled initially: if it is considered that an electromagnetic wave is injected at an input end **13** of the waveguide segment **10** in the form of a TE_{10} mode wave, and that the output end **14** of said segment **10** is looped on a matched load, then S_{11} represents the reflection coefficient and S_{21} the transmission coefficient, for the TE_{10} component of said wave.

The curves $S_{11\text{-}TE10}$ and $S_{21\text{-}TE10}$ show that the disturbance to the E-planes of the waveguide segment **10** reflects the spectral components of the input signal that lie in the range approximately 16 GHz to approximately 39 GHz, inducing attenuation that can reach 100 dB around 25 GHz. However, losses in the payload band of 10 GHz to 15 GHz remain very low ($S_{21\text{-}TE10}$ greater than −0.2 dB, even though this is not visible in the figure).

At around 33 GHz to 35 GHz, the curve $S_{11\text{-}TE10}$ presents a local minimum: in this region of the spectrum, conversion to higher modes contributes strongly to attenuation of the TE_{10} mode being conveyed. FIGS. **1**C and **1**D show the parameters S_{11} and S_{21} for conversion of TE_{10} to TE_{12} mode and to TM_{12} mode respectively (curve S_{11}^{TE12} and S_{21}^{TE12} on FIG. **1**C, S^{21TM12} and S_{21}^{TM12} in FIG. **1**C). It can be seen that mode conversion is negligible in the payload band of 10 GHz to 15 GHz, and up to about 30 GHz.

A filter of the above-described type can be dimensioned in such a manner as to stop a band that extends, for example, from 13 GHz to 39 GHz, and can be used directly as an output lowpass filter for a multiplexer for a microwave transmitter. However, such a filter would be large in size: the Bragg period becomes longer with reduction in the frequency of the radiation that is to be stopped, and consequently it would be necessary to use a waveguide segment that is relatively long, which is not desirable, particularly in space applications. Consequently, it is preferable to use a conventional filter, e.g. of the waffle-iron or corrugated waveguide type so as to eliminate frequencies in the range approximately 13 GHz to approximately 20 GHz. Unlike filters of the invention, which are characterized by quasi-sinusoidal corrugations distributed over a relatively long length, such structures present sudden changes of section, making it possible to obtain large attenuation over a short length. Nevertheless, and as mentioned above, such conventional filters inevitably present interfering passbands above the nominal cutoff frequency, particularly when they are adapted to operate at high powers (large gap). The Bragg filters of the invention are particularly suitable for stopping said interfering passbands: since those bands occur at high frequencies, their Bragg period is relatively short, thus leading to structures that are compact. For example, for transmission in X band (8 GHz to 12 GHz) or in KU (12 GHz to 18 GHz), filters of the invention can be dimensioned to operate in the K band (18 GHz to 26 GHz) and in the Ka band (26 GHz to 40 GHz).

FIG. **2**A thus shows a filter assembly **20** comprising: an input waveguide segment **21**, a lowpass filter having a corrugated waveguide **23** provided with two impedance-matching sections **22** and **24**, first and second bandstop filters of the invention (respectively **25** and **26**), and an output waveguide segment **27**.

The lowpass filter **22** is known in the prior art and presents a cutoff frequency at 13 GHz; in order to be capable of accommodating powers of the order of several kW, the minimum gap between the E-planes is relatively large (4.75 mm), thus causing interfering passbands to appear at frequencies greater than 20 GHz. The two filters **25** and **26**, both constituted by a segment of WR75 waveguide with gap presenting longitudinal variation in application of equation [2], are dimensioned in such a manner as to eliminate said interfering passband up to a frequency of 39 GHz, which corresponds to the 3rd harmonic of the "primary" filter **22**. More precisely, the quasi-sinusoidal disturbance of the filter **25** presents 17 periods of length Λ_{25}=7 mm, corresponding to the Bragg period for radiation of 21 GHz propagating in TE_{10} mode, modulated by a cosine-squared amplitude function having a maximum amplitude of 2.1 mm. In similar manner, the quasi-sinusoidal disturbance of each E-plane of the filter **26** consists in 22 periods of length Λ_{26}=5.26 mm (Bragg period for radiation at 30 GHz), likewise modulated by a cosine-squared amplitude function having a maximum amplitude equal to 1.3 mm. With a WR75waveguide, this leads to a minimum gap of 5.325 mm, which is greater than that of the filter **22** (4.75 mm). In both configurations, the phase function $\Phi(x)$ is constant, which means that the longitudinal disturbance does not present any phase modulation.

FIG. **2**B shows how the parameters S_{11} and S_{21} for the TE_{10} fundamental mode of the filter assembly **20** depend on frequency (curves $S_{11\text{-}TE10}$ and $S_{21\text{-}TE10}$). It can be seen that the interfering passbands are stopped efficiently (attenuation greater than 25 dB) up to a frequency of 39 GHz, corresponding to the 3rd harmonic of the cutoff frequency of the filter **23** (13 GHZ) . At the same time, losses in the passband (10 GHz to 13 GHz) remain limited to less than −20 dB.

Since the waveguide segments **25** and **26** present a gap that is greater than $b_0/2$ at all points, and furthermore they do not include any sudden changes of section, these elements of the filter assembly present little tendency to cause electron avalanche discharges. The element which limits the maximum power that can be conveyed by the assembly to about 1 kW is the lowpass filter **22** because of its small minimum gap and its corrugations of rectangular profile.

FIG. **2**C shows the result of measurements of the parameters S_{11} (curve $S_{11\text{-}exp}$) and S_{21} (curve $S_{21\text{-}exp}$) taken on a prototype of the filter assembly **20** of FIG. **2**A. It can be seen that attenuation of more than 40 dB is obtained in a band extending from about 13.75 GHZ to about 39 GHz, which frequency corresponds to the third harmonic of the upper limit of the payload band (13 GHz). Attenuation drops to below 40 dB only over two very narrow bands around 25 GHz and 37 GHz, and always remains greater than 20 dB.

As explained above, a filter assembly of the FIG. **2**A type is particularly well adapted for use in making output multiplexers for microwave multichannel transmitters. FIG. **3** is a diagram of such a multiplexer **30**, which is constituted essentially by a manifold **31** having connected thereto microwave signal generators **32***a*-**32***h*, each corresponding to one transmission channel. In the prior art, between each generator **32***a*-**32***h* and the manifold **31**, it is necessary to interpose a lowpass filter for stopping the harmonics of the payload signal so as to prevent parasitic intermodulation signals appearing; the invention makes it possible to eliminate these filters, or at least to simplify them considerably. A multiplexer **30** of the invention comprises, at the outlet from the manifold **31**, a filter assembly **20** of the kind described with reference to FIG. **2**A. Such a filter assembly comprises a single lowpass filter **23** replacing the filters that used to be provided for each of the individual transmitters; compared with those filters, the filter **23**, which must be capable of conveying much higher power, inevitably presents a transfer function that is less good, characterized by relatively large interfering passbands. The bandstop filters **25** and **26** make it possible to stop those interfering passbands without limiting the maximum power that can be conveyed. The use of a single filter assembly **20** replacing the plurality of filters associated with the generators **32***a*-**32***h*

makes it possible significantly to reduce the weight and the size of the multiplexer **30**, and that is particularly important for space applications.

When designing a bandstop filter of the invention, the type of waveguide that needs to be used is generally imposed by the specific application under consideration: it will generally be a rectangular waveguide, however waveguides of circular section or ridged waveguides may also be used. Under such circumstances, dimensioning consists essentially in determining:

- the spatial frequency Ω_0 of the quasi-sinusoidal disturbance;
- the form of the amplitude function P(x), e.g. a cosine-squared function or a Gaussian function;
- its longitudinal scale factor, i.e. the length over which $P(x)\neq 0$, and consequently the number of periods of the disturbance;
- its peak amplitude, which in turn determines the maximum reduction in the cross-section of the waveguide; and
- the possible presence of any phase modulation $\Phi(x)$ in such a manner as to satisfy certain conditions:
  - minimum attenuation over a band of determined width;
  - maximum acceptable level of losses in the payload band; and
  - maximum power level that can be conveyed without risk of an electron avalanche discharge.

Determining the "spatial frequency" Φ_0 generally does not pose any particular problem: it is determined so as to satisfy the Bragg condition $\Omega_0=2\beta(f_{CB})$ for a frequency f_{CB} situated approximately in the middle of the band to be stopped.

The number of periods of the disturbance constitutes a compromise between two contradictory requirements: a high number of periods makes it possible to reflect effectively the radiation at the center frequency f_{CB} even in the presence of disturbances of small amplitude, but it also determines filtering over a narrow band. In order to stop a band that is of sufficient width (1 GHz and more) centered about f_{CB}, it is therefore necessary to use a limited number of periods, but that reduces the reflection coefficient for a disturbance of given amplitude. Simultaneously, it is not possible to increase said amplitude of the disturbance beyond a certain limit without running the risk of electron avalanche discharges appearing at the maximum operating power. Typically, it is therefore necessary to use disturbances extending over ten to 30 periods with a maximum amplitude lying in the range 30% to 70% and preferably in the range 40% to 60% of the mean gap b_0 of the waveguide.

The amplitude function P(x) generally cannot be a simple rectangular function since that would induce losses by reflection in the passband and lead to excessive conversions to higher order modes. It is therefore appropriate to use continuous functions presenting "gentle" transitions and rising and falling fronts having slopes that are small enough. It is observed that in high power applications, reflection losses in the passband are particularly harmful since as well as attenuating the signals being conveyed, they can damage the transmitters by reflecting back to them too great a fraction of the power they transmit. In the embodiments described above, the amplitude function P(x) has a cosine-squared form. Other suitable forms are cosine even powers greater than 2, giving steeper rising and falling fronts and a central region that is almost constant, Gaussian functions, and Hamming, Kaiser-Müller, or Black windows. Generally, the particular form chosen is not critical.

Phase modulation $\Phi(x)$ can be used subsequently to enlarge the filter band. To limit losses in the payload band and conversions to higher order modes, this function must also be continuous and present transitions that are "gentle". Phase modulation can impart linear frequency modulation ("chirp") or a continuous connection between two sinewaves of different periods, as in the example of FIG. **1**A.

A rational method of dimensioning a filter of the invention can be described with the help of the flow chart of FIG. **4**A and the table of FIG. **4**B.

The first step E**1** consists in determining a "center" frequency f_{CB} of the band to be stopped, and in determining its guided wave number at the fundamental mode of the guide, $\beta(f_{CB})$. This makes it possible to calculate the "spatial frequency" Ω_0 of the disturbance.

The following step, E**2**, consists in determining the maximum amplitude P_{max} of the quasi-sinusoidal disturbance of the waveguide that is compatible with the requirements in terms of power conveyed.

Step E**3** consists in selecting a form, a peak value, and a longitudinal scale factor for an amplitude function P(x), said peak value being less than the maximum amplitude P_{max} as determined in the preceding step. This selection can be made in relatively random manner, however it is clear that experience can be a guide towards determining initial values that enable the dimensioning method to converge quickly. The exact form of the amplitude function P(x) is rarely critical, at least during the initial design stage. optionally, the dimensioning method can be repeated for different forms of P(x) in order to optimize the response of the filter for a determined application.

For reasons of simplicity, it is appropriate to assume initially that $\Phi(x)$=constant.

Step E**4** comprises using numerical simulations to calculate the transfer function of the filter as obtained and to compare it with requirements in terms of the filter properties that are to be achieved. If the result is satisfactory, the method is terminated, otherwise it is necessary to modify at least some of the parameters in step E**5**.

Table **4**B shows how the longitudinal scale factor of P(x), its peak value, and phase modulation $\Phi(x)$ can be modified. To do this, it is determined whether the attenuation in the center of the band $A(f_{CB})$ and the width LB of the stopband are substantially greater than, approximately equal to, or less than the required minimum values $A(f_{CB})'$ and LB'.

If $A(f_{CB})\geqq A(f_{CB})'$ and $LB\geqq LB'$, it is not necessary, at least initially, to modify the longitudinal scale factor of P(x), or its peak value, nor is it necessary to introduce a term in $\Phi(x)$.

If the attenuation in the center of the band $A(f_{CB})$ is insufficient while the width of the attenuated band is wider than necessary, it is possible to increase the scale factor P(x) and thus the number of disturbance periods. It is also possible to increase the peak value of P(x), providing the maximum value P_{max} is not exceeded.

If the attenuation at the center of the band $A(f_{CB})$ is insufficient while the width of the attenuated band is itself hardly sufficient, it is necessary to increase the peak value of P(x). If that is not possible, it is necessary to increase the scale factor and to correct the resulting band narrowing by introducing phase modulation $\Phi(x)$. This phase modulation can be determined by selecting additional frequencies within the band to be stopped, by determining the corresponding Bragg periods, and by connecting together sinusoidal disturbances presenting said periods while guaranteeing phase continuity. Additional frequencies are added until a band of desired width is obtained. The device of FIG. **1**A shows phase modulation of this type.

If the width of the attenuation band is insufficient and the attenuation at the center of the band is greater than required,

it is possible to reduce the scale factor of P(x) and thus the number of disturbance periods, without modifying the amplitude.

In contrast, if the width of the attenuation band is insufficient, but the attenuation at the center of the band is hardly sufficient, or even insufficient, it is necessary to decrease the scale factor of P(x) and simultaneously to increase its peak value. If that is not possible because of the power limitations that would then arise, it is necessary to keep the number of disturbance periods constant and to introduce frequency modulation in order to broaden the attenuated band.

If both $A(f_{CB})$ and LB present values that are satisfactory, but the losses in the passband or the conversion coefficients to higher order modes are excessive, it is necessary to change the form of the amplitude function P(x), and possibly also of the phase function Φ(x), by selecting a function that presents transitions that are "gentler" with rising and falling fronts presenting smaller slopes.

Modifications are carried out iteratively, with the transfer function of the structure being recalculated on each occasion.

What is claimed is:

1. A microwave bandstop filter comprising a waveguide segment of cross-section that presents longitudinal variation of the sinusoidal type that is modulated by an amplitude function that is continuous, a period of said longitudinal variation of sinusoidal type being the Bragg period for a fundamental guided mode at a center frequency of a band to be stopped, wherein a maximum longitudinal variation in the cross-section of the waveguide lies in the range 30% to 70% of the mean gap of the waveguide segment.

2. A filter according to claim **1**, in which the longitudinal variation in the cross-section of the waveguide lies in the range 40% to 60% of the mean gap of the waveguide segment.

3. A filter according to claim **1**, in which the waveguide segment is a waveguide segment suitable for conveying a plurality of transverse modes in the spectral band to be stopped.

4. A filter according to claim **1**, in which the waveguide segment is a metal waveguide segment of rectangular cross-section, the longitudinal variation in said cross-section being obtained by symmetrical deformation of two opposite faces thereof.

5. A filter according to claim **4**, in which the longitudinal variation of said cross-section is obtained by symmetrical deformation of the two opposite faces of greatest length.

6. A filter according to claim **1**, in which said waveguide segment extends over a length lying in the range ten periods to 30 periods of said longitudinal variation of sinusoidal type in its cross-section.

7. A filter according to claim **1**, in which said amplitude function presents a rising front and a falling front of slope that is sufficiently small for the reflection coefficient at the input of said waveguide segment to be less than or equal to −20 dB for frequencies below those of said band to be stopped.

8. A filter according to claim **1**, in which said amplitude function is selected from: a cosine-squared function, a cosine even-power function, a Gaussian function, and a Hamming, Kaiser-Müller, or Black window.

9. A filter according to claim **1**, in which said longitudinal variation of sinusoidal type in the cross-section of the waveguide segment also presents phase modulation that is continuous.

10. A filter according to claim **1**, in which;

mean transverse dimensions of the waveguide segment and the maximum amplitude of said longitudinal variation of the waveguide segment cross-section are such as to enable the waveguide segment to convey a power of at least 0.5 kW in the microwave region of the spectrum without electron avalanche discharges occurring in a vacuum; and

an amplitude and a period of said longitudinal variation, and also a length over which a said longitudinal variation extends are such to produce attenuation of at least 25 dB by Bragg reflection in a band having a width of at least 1 GHz.

11. A filter according to claim **10**, in which:

mean transverse dimensions of the waveguide segment and the maximum amplitude of said longitudinal variation of the waveguide segment cross-section are such to enable power of at least 1 kW to be conveyed in the X and Ku bands without electron avalanche discharges occurring in a vacuum; and

an amplitude and a period of said longitudinal variation, and a length over which said longitudinal variation extends, are such to produce attenuation of at least 25 dB by Bragg reflection in a band having a width of at least 1 GHz in the K and higher bands.

12. A filter assembly, comprising:

a microwave lowpass filter presenting a cutoff frequency and at least one interfering passband at frequencies higher than said cutoff frequency; and

at least one band stop filter according to claim **1**, connected to the output of said lowpass filter, in which an amplitude and a period of said longitudinal variation, and a length over which said longitudinal variation extends are such to stop said interfering passband of said lowpass filter.

13. A filter assembly according to claim **12**, in which mean transverse dimensions of the waveguide segment constituting said or each of said bandstop filter, and a maximum amplitude of the longitudinal variation in the waveguide segment cross-section are such to enable power to be conveyed that is not less than a maximum output power from said lowpass filter without electron avalanche discharges occurring in a vacuum.

14. A filter assembly according to claim **12**, in which the cutoff frequency of said lowpass filter is situated in the Ku band, and said interfering band is situated in the K or Ka band.

15. A filter assembly according to claim **12**, comprising at least two filters, each filter comprising a waveguide segment of cross-section section that presents longitudinal variation of the sinusoidal type that is modulated by an amplitude function that is continuous, the period of said longitudinal variation of sinusoidal type being the Bragg period for the fundamental guided mode at a center frequency of the band to be stopped, wherein the maximum longitudinal variation in the cross-section of the waveguide lies in the range 30% to 70% of the mean gap of the waveguide and dimensioned to stop the interfering bands of said lowpass filter centered to correspond with the second and third harmonics of lowpass filter cutoff frequency.

16. An output multiplexer for a multichannel microwave transmitter having an output filter, wherein said output filter comprises a filter assembly according to claim **12**.

* * * * *

2.2 Waveguide Filter based on Discrete Elements

The waveguide filter based on discrete elements presented in this thesis is based on the Complementary Split Ring Resonator. This section is devoted to the design of very compact waveguide filters based on CSRR particles. This design is then validated in the paper [4] by the author of this thesis.

2.2.1 CSRR Particle Discovery. Motivation

The Complementary Split Ring Resonator is firstly presented in [5] as the complementary particle of the Split Ring Resonator. Based on complementarity, E and H field lines can be interchanged, as well as metal and air slots, leading to CSRR particles that are similar to media that exhibit in this case, negative values of dielectric permittivity.

The motivation which leads to the discovery of CSRR particle is related to the constraints that the excitation of SRR particles present in Microstrip technology, due to the high confinement of the H-field component. CSRR particles are the good solution to overcome this handicap. Furthermore, in [5] the CSRR particle is presented as a unit cell for the design of metasurfaces with high frequency selectivity and planar metamaterials with negative dielectric permittivity. The applications using SRR and CSRR particles in filters, couplers and antenna designs allow to take advantage of the small electrical size of these particles at their self-resonance, thus resulting in a significant miniaturization.

2.2.2 CSRR based Waveguide Filters

This sub-section is an overview of the main research results based on standard Waveguide Filters using Complementary Split Ring Resonators. It is remarkable that research work on standard waveguides has not been very fruitful over the last decade. In the contrary, most of the research results have been focused on substrate integrated waveguides.

The first work on standard waveguide filter design based on CSRRs is presented in 2005 by the author of this thesis in [4]. The content of this paper is presented in *Section 2.2.3*. To the best of the author's knowledge, the author's contributions on this topic do precede to the other works.

In 2008, [6] refers to the author's work presented in [4] (see *Section 2.2.3*). In [6] CSRRs are used to design a compact Bandpass Waveguide filter in X-Band, where the CSRRs are etched in metal sheets, as in the authors design presented in [4]. Those metal sheets are combined with proper admittance inverters. As a result, the presented waveguide filter is compacted by 66%.

In 2013 the work in [7] presents models of the bandpass waveguide filters using novel Complementary Split Ring Resonators. The filter response is analyzed in terms of various parameters of the resonators.

From 2013 to present, no relevant works have been published on this topic.

2.2.3 Paper: CSRR for Compact Waveguide Filter Design

As it is explained in the section above (*Section 2.2.1*), the results shown in [5] demonstrate the feasibility of using CSRR particles as unit cells for metasurfaces thanks to the analysis of the excitation of SRR and consequently CSRR particles. Based on that analysis, the CSRR can be excited by two different ways; by an electric field normal to the particle plane or by magnetic field properly applied in the plane of the particle.

The capability of exciting the CSRR particle by magnetic field properly applied in the plane of the particle, brought the possibility to excite such particle inside of a rectangular waveguide. This excitation is achieved by etching a CSRR particle in the center of a metallic sheet traversal to the rectangular waveguide. This original layout reduces the dimensions of the well-known resonant-cavity waveguide filters coupled by irises. This has been made feasible due to the self-resonance property of the CSRR. Thus, it is possible to design waveguide filters with lengths equal to the thickness of a metallic sheet. Consequently, this technique paves the way for the design of miniaturized waveguide filters, in contrast to conventional waveguide filters. The paper I submitted on this topic [4]is presented below.

The contribution of this filter in this field is summarized as follows:

- The usefulness of a CSRR for the design of narrow bandpass filter in a rectangular waveguide has been proved by the design, manufacturing and testing of a prototype.
- The filter design is very simple and it consists in a CSRR particle etches in the center of a metallic sheet placed in a rectangular waveguide. In *Fig. 4.* of the paper a picture of the prototype is depicted.
- The frequency response of the measured prototype exhibits a maximum transmission of -5dB at its resonance with a rejection of -20dB in the interval of +/-100MHz, within a fractional bandwidth of 0.73
- The frequency shift between the simulated and measured results can be attributed to the tolerances of the fabrication process. The measured transmission level is predicted by simulated results.
- The presented filter has a very small length and it exhibits a high tenability by changing the dimensions of the CSRR or by increasing the thickness of the metal sheet.

- It is believed that the proposed structure can be of practical interest for the fabrication of very compact waveguide bandpass filters, with a length equal to the thickness of the metallic sheet.

Complementary split-ring resonator for compact waveguide filter design

N. Ortiz J. D. Baena M. Beruete F. Falcone M. A. G. Laso T. Lopetegi R. Marqués F. Martín J. García‐García M. Sorolla

First published: 18 May 2005 https://doi.org/10.1002/mop.20909

Abstract

In this paper, the potential use of complementary split‐ring resonators (CSRRs) to design very compact waveguide filters, by etching a CSRR in the center of a metallic sheet, is demonstrated. This original layout reduces the dimensions of the well‐known resonant‐cavity waveguide filters coupled by irises. This has been made feasible due to the self‐resonance property of the CSRR. Thus, it is possible to design waveguide filters with lengths equal to the thickness of a metallic sheet. Consequently, this technique paves the way for the design of miniaturized waveguide filters, in contrast to conventional waveguide filters, based on bulk resonators. © 2005 Wiley Periodicals, Inc. Microwave Opt Technol Lett 46: 88–92, 2005; Published online in Wiley InterScience (www.interscience.wiley.com). DOI 10.1002/mop.20909

Ortiz, N., Baena, J. D., Beruete, M., Falcone, F., Laso, M. A. G., Lopetegi, T., … Sorolla, M. (2005). Complementary split-ring resonator for compact waveguide filter design. *Microwave and Optical Technology Letters,* 46(1), 88-92. http://doi.org/10.1002/mop.20909

3. Single CSRR Application in Simple Radiating Structures

Dream deep, for every dream proceeds the goal.

Mother Teresa of Calcuta

Complementary Split Ring Resonator particle was originally considered as a unit cell for the design of metasurfaces and then it was applied to the design of compact waveguide filters, as presented in *Chapter 2*. Likewise, the aforementioned particle was also thought to be used as an stand-alone radiating element. In that sense, simulations of the stand alone resonator particle were carried out throughout 2005 in order to characterize the radiating properties of such resonator. These simulations showed that such particle behaves like a dipole and unfortunately due to its reduced electrical volume, it exhibits a low radiation efficiency. Consequently, in order to overcome that limitation, at beginning of 2006 together with my thesis directors, we decided to insert the Complementary Split Ring Resonator in the patch of a rectangular patch antenna. As the electrical volume of the resulted structure is larger, the radiation efficiency improves.

On the other hand, the Complementary Split Ring Resonator can be considered as a perturbation inside the conventional rectangular patch. However, for the author and directors of this thesis, the Complementary Split Ring Resonator is considered as a stand-alone radiating element, which is excited by the currents presented in the conventional patch.

The research results based on the proposed structure are summarized in the author's four contributions presented throughout this chapter. The proposed structure is firstly presented by the author in the Asia-Pacific conference in 2009. To the best of the author's knowledge, this contribution precede to other works presented by other authors on this topic. The following two author's contributions published in 2011 and 2012; respectively, are centered on the characterization of radiation efficiency of the CSRR particle inside the rectangular patch antenna, while the last contribution, published in 2015, shows the equivalent circuit model of the radiating structure.

3.1 CSRR as Stand alone Radiating Element

As it is explained in the previous chapters of this thesis, in [1] the Complementary Split Ring Resonator is proposed as a unit cell for the design of metasurfaces. Following the theoretical discussion in [1], the considered metallic surface with CSRRs etched on it can be seen - from the source side- as an electric dipolar sheet on top of a flat metallic screen. This is possible since we are in the long wavelength limit; as the CSRRs are electrically small resonators, then the distance between them can be made much smaller than the incident radiation wavelength.

Based on the results obtained in [1], the idea of implementing a CSRR as an stand alone radiating element came naturally to the directors and author of this thesis in 2005. From that moment, we were focused to design a miniaturized metamaterial antenna. Consequently, throughout 2005 an stand along Complementary Split Ring Resonator is simulated by the author. Simulation results showed poor radiation efficiencies. These results are in accordance with the reduced electrical volume of the radiation element; which is in the order of 0.1 free-space wavelengths at its quasi-static resonance. Additionally, these results are also in alignment to the theoretical discussions presented in [2], [3], [4] and more recently in 2012 in [5].

Accordingly, in order to improve the radiation efficiency of the stand alone Complementary Split Ring Resonator particle, at beginning of 2006 we decided to insert the CSRR particle in a larger radiating structure; such as a conventional rectangular patch antenna. As that novel structure exhibit larger electrical dimensions compared to the ones of the stand alone radiating element, the radiation efficiency is improved. Moreover, the novel structure exhibits a dual band behavior. Since then, the goal of this thesis is focused in the design of Metamaterial Antennas based on CSRR particles, laying aside the design of miniaturized antennas. In the section below, in *Section 3.2*, the author's contributions and then the achievements on this topic are presented.

3.2 Novel Metamaterial Structure: CSRR etched in the patch antenna

3.2.1 Motivation and Context

The novel radiating structure proposed in order to improve the radiation efficiency obtained by the Complementary Split Ring Resonator as a stand along radiating element, is to etch the aforementioned particle in the patch of a conventional patch antenna. The resulting structure allows the

author to design a dual band Metamaterial Antenna, which exhibits higher radiation efficiencies compared to the ones of the stand alone radiating structure. At beginning of 2006 we started studying and simulating this novel structure. Here-below a chronological order of author's contributions and achievements on this novel structure is presented.

Beginning 2006: The novel radiating structure is proposed by the directors and author of this thesis. The author starts studying and simulating this structure.

End 2006: The first prototypes of the aforementioned structure are manufactured. The impedance matching at antenna port is measured and characterized. See *Fig. 3.* in my paper published in 2009, *Figure 2* in my paper published in 2011 and *Figure 7* in my paper published in 2012. Those papers are presented in *Section 3.2.3*, *Section 3.2.4* and *Section 3.2.5*; respectively.

End 2007: Radiation parameters of the first prototypes manufactured in 2006 are measured. These measurements comprise radiation patterns (co- and cross-polar components) and directivity. See *Fig. 4.* and *Fig. 5.* in my paper published in 2009, *Figure 4* in my paper published in 2011 and *Figure 9* in my paper published in 2012. Those papers are presented in *Section 3.2.3*, *Section 3.2.4* and *Section 3.2.5*; respectively.

2009: The results of the first prototypes manufactured at the end of 2006 are published by first time in the Asia-Pacific APMC conference. See paper presented in *Section 3.2.3*.

2010: The equivalent circuit model of the aforementioned novel structure is proposed based on simulation results. A second batch of prototypes is designed and it is prepared for manufacturing in order to validate the proposed equivalent circuit model.

2011: Higher radiation efficiency values for the CSRR resonance are computed from simulation results for reduced CSRR area when the CSRR is etched in the center of the rectangular patch antenna. The paper that includes these results is published in the magazine "Microwave and Optical Technology Letters". See this paper in *Section 3.2.4*.

2012: A parametric study shows higher radiation efficiencies based on the position of the CSRR inside the rectangular patch. The paper that includes these results is published in the magazine "International Scholarly Research Network ISRN Communications and Networking". See this paper in *Section 3.2.5*.

2014: The second batch of prototypes designed in 2010 is manufactured. Based on the measurement results of those prototypes, the proposed equivalent circuit model is validated. The impedance matching at antenna port and radiation parameters (co- and cross-polar components) are measured. See *Figure 6*, *Figure 7* and *Figure 8* in the paper presented in *Section 3.2.6*.

2015: The circuital model of the manufactured prototypes in 2014 is validated. The paper that

includes this validation is published in the magazine "Waves in Random and Complex Media". See this paper in *Section 3.2.6*.

It is remarkable that to the best of the author's knowledge, the author's first contribution published in 2009, precede to other works presented by other authors on the topic of Metamaterial Antennas based on Complementary Split Ring Resonators. In particular, until 2009 the use of Metamaterial concepts in practical miniaturized antennas is a very challenging research topic which is in its infancy, see the related works that are published until 2009, [6], [7], [8], [9], [10], [11] and [12]. Among these works, only the works presented in [8], [9], [10], [11] and [12] use single or multiples Complementary Split Ring Resonators. In particular, in [8], [9] and [10] single and/or multiple CSRRs are etched in the ground plane of a microstrip antenna. This solution allows a significant miniaturization of the patch antenna. Secondly, in the work [11] the CSRR is implemented in a ultra-wideband monopole antenna to generate dual band notched characteristics. On the other hand, in the work in [12] in accordance with the novel structure presented in this section by the author of this thesis, the CSRR is etched in the patch of a rectangular antenna. Both works show a dual band antenna performance. However, the achieved results in [12] exhibit very low efficiencies driving to low gain antennas designed by metamaterial concepts based on CSRR particle comparing to the design based on the novel structure presented in the chapter of this thesis.

3.2.2 Radiating Structure Description

As explained in the previous section, see *Section 3.2.1*, the radiating structure is composed of a CSRR particle etched in the patch of a rectangular patch antenna. This structure allows a Dual Band antenna behavior. The first resonance of the dual band Metamaterial antenna is produced by the excitation of the CSRR in the patch, while the second resonance is originated by the rectangular patch itself. Going further the presence of the CSRR etched in the patch, also introduces a miniaturization of both patch antenna resonances, leading to a miniaturized dual band antennas. Comparing the first resonance produced by a CSRR particle within an iris of its same external dimensions, the iris does not exhibit a resonance at the same frequency of the CSRR, but at higher frequencies. The resonance frequency of a rectangular iris on a dielectric is approximately given by $c_0/\left(a+b\right)\sqrt{\varepsilon_r}$; where c_0, ε_r, a, and b are the speed of light in vacuum, dielectric relative permittivity and the external dimensions of the rectangular iris, respectively. In opposition to the resonance frequency of a rectangular iris, the resonant frequency of the CSRR is much lower for the same physical size. Hence, the lowest frequency of the dual band antenna is easily designed by exciting the CSRR etched in a patch of a conventional patch antenna.

The author's contributions on the presented radiating structure in this section are presented in the next sections of this chapter.

3.2.3 Paper: Dual Band Patch antenna based on Rectangular CSRR

This paper is key because in this paper the aforementioned metamaterial structure, which is described in the previous section (*Section 3.2.2*), is presented for the first time. The contributions of this work are summarized as follows:

- The aforementioned Metamaterial antenna exhibits a dual band performance. Moreover, this antenna is easy to design.
- The dual performance is feasible due to the excitation of the quasi-static resonance of the Complementary Split Ring Resonator, which represents the first resonance of the dual band antenna. The second resonance is driven by the resonance of the rectangular patch itself.
- In the design presented in the paper the CSRR particle is etched in the center of the rectangular patch. At this position the CSRR is excited by the magnetic field tangent to the resonator axis. This position of the CSRR allows miniaturization of the rectangular patch antenna.
- The impedance matching and radiation patterns of the fabricated prototype are measured. The frequency shift in the impedance response is due to the mechanical manufacturing process technique. Simulated and measured radiation results show good agreement.
- As expected, simulated and measured radiation efficiency is higher than the radiation the efficiency obtained in the simulations of the CSRR as stand alone radiating element (see *Section 3.1*).
- This work has been cited in 2012 by the authors of the work [13]. This last work presents different CSRR particle configurations etched in a rectangular patch antenna.

Dual band patch antenna based on Complementary Rectangular Split-Ring Resonators

N. Ortiz, F. Falcone, M. Sorolla

Millimeter Wave Laboratory, Public University of Navarra
Campus Arrosadía, E-31006 Pamplona, Spain
ortiz.25739@e.unavarra.es
francisco.falcone@unavarra.es
mario@unavarra.es

Abstract — A simple and successful dual band patch rectangular antenna design is presented. The dual band antenna is designed etching a complementary rectangular split ring resonator in the patch of a conventional rectangular patch antenna, achieving a miniaturization of the conventional antenna. The dual band antenna design has been made feasible due to the quasi-static resonance property of the complementary split ring resonators. Simulated results are compared with measured data and good agreement is reported.

Index Terms — Dual Band Patch antenna, Complementary Split Ring Resonator, Metamaterials.

Ortiz, N., Falcone, F., y Sorolla, M. (2009). Dual band patch antenna based on complementary rectangular split-ring resonators. *APMC 2009 - Asia Pacific Microwave Conference 2009,* 2762-2765. http://doi.org/10.1109/APMC.2009.5385367

978-1-4244-2802-1/09/$25.00 ©2009 IEEE

3.2.4 Paper: Enhanced gain dual Band patch antenna based on CSRR

The contributions of this work are summarized as follows:

- The antenna structure presented in this paper is the same prototype showed in the previous section (see *Section 3.2.3*).
- The novelty of this paper is the radiation efficiency study presented in *Figure 5* and *Figure 6*. This study shows that by optimizing the design parameters a and b of the CSRR, radiation efficiencies of approximately 50% are achieved for an area occupied by the CSRR of approximately 17.mm^2. These design parameters are defined in *Figure 1*. The occupied area by the fabricated prototype is 19.3mm^2.
- As predicted the radiation efficiency of the CSRR is increased when it is implemented in the proposed antenna structure.
- Moreover, as the CSRR is placed in the center of the rectangular patch a miniaturization of the rectangular patch antenna is achieved.

Enhanced gain dual band patch antenna based on complementary rectangular split-ring resonators

N. Ortiz F. Falcone M. Sorolla

First published: 19 January 2011 https://doi.org/10.1002/mop.25797

Abstract
A simple and successful dual band patch vertical polarized rectangular antenna design is presented. The dual band antenna is designed etching a complementary rectangular split ring resonator in the patch of a conventional rectangular patch antenna. Furthermore, a miniaturization of the conventional rectangular patch antenna and an enhancement of the complementary split ring resonator resonance gain are achieved. The dual band antenna design has been made feasible due to the quasi - static resonance property of the complementary split ring resonators. The simulated results are compared with measured data and good agreement is reported. © 2011 Wiley Periodicals, Inc. Microwave Opt Technol Lett 53:590–594, 2011; View this article at wileyonlinelibrary.com. DOI 10.1002/mop.25797

Ortiz, N., Falcone, F., y Sorolla, M. (2011). Enhanced gain dual band patch antenna based on complementary rectangular split-ring resonators. *Microwave and Optical Technology Letters*, 53(1), 3872-3875. http://doi.org/10.1002/mop

3.2.5 Paper: Gain Improvement of dual Band Antenna based on CSRR

The contributions of this work are summarized as follows:

- The antenna structure presented in this paper is the same prototype showed in the previous two sections (see *Section 3.2.3* and *Section 3.2.5*).
- The novelty of this paper is the parametric study that has been carried out in order to analyze the mutual interaction between the radiation efficiency of the CSRR and the rectangular patch. The parametric study shows how the radiation efficiency of both antenna resonances varies depending on the position of the CSRR in the patch. Design parameters of the CSRR do not change in the parametric study.
- *Figure 4* shows that there are positions in the rectangular patch where the radiation efficiencies generated by the patch and the CSRR increase up to 50%. In particular, these positions are where the CSRR is located further from the center of the rectangular patch; i.e. closer to the non radiating and radiating edges of the rectangular patch.
- For the locations where the CSRR is placed around the center of the rectangular patch, there is a miniaturization in the dimensions of the CSRR and the rectangular patch. On the contrary, when the CSRR is located further from the center of the patch, there is no miniaturization of the antenna dimensions.

International Scholarly Research Network
ISRN Communications and Networking
Volume 2012, Article ID 951290, 9 pages
doi:10.5402/2012/951290

Research Article

Gain Improvement of Dual Band Antenna Based on Complementary Rectangular Split-Ring Resonator

Noelia Ortiz, Francisco Falcone, and Mario Sorolla

Millimeter Wave Laboratory, Electrical and Electronic Engineering Department, Public University of Navarra, Arrosadía Campus, 31006 Pamplona, Spain

Correspondence should be addressed to Mario Sorolla, mario@unavarra.es

Received 7 October 2011; Accepted 9 November 2011

Academic Editors: C. Luxey and J. K. Muppala

A simple and successful dual band patch linear polarized rectangular antenna design is presented. The dual band antenna is designed etching a complementary rectangular split-ring resonator in the patch of a conventional rectangular patch antenna. Furthermore, a parametric study shows the influence of the location of the CSRR particle on the radiation characteristics of the dual band antenna. Going further, a miniaturization of the conventional rectangular patch antenna and an enhancement of the complementary split-ring resonator resonance gain versus the location of the CSRR on the patch are achieved. The dual band antenna design has been made feasible due to the quasistatic resonance property of the complementary split-ring resonators. The simulated results are compared with measured data and good agreement is reported.

1. Introduction

The possibility of obtaining media with simultaneously negative permeability and permittivity was hypothesized by Veselago in the late 1960s [1]. In spite of the interesting properties presented by such media, it was not until 2000 that the first experimental evidence of a medium with simultaneously negative permeability and permittivity was demonstrated [2]. The original medium proposed in [2] consists of a bulky combination of metal wires and split-ring resonators (SRRs) [3].

The SRR electromagnetic properties have been already analyzed in [4, 5]. This analysis shows that the SRR behaves as an LC resonant tank that can be excited by an external time-varying magnetic field applied parallel to the particle axis, thus producing a quasi-static resonant effect [4]. Therefore, the SRR has subwavelength dimensions at its quasi-static resonance, allowing very compact device designs. Up to now, these self-resonant particles have been used in the design of microwave filters in planar technology [6, 7]. However, in this paper, we have taken advantage of the complementary split-ring resonator (CSRR) concept [8] to design a miniaturized dual band patch antenna with vertical polarization, also studying how to improve radiation efficiency for the resonance produced by the CSRR in this kind of antennas. The CSRR is inspired on Babinet principle [9], and, as occurs with the SRR, it also exhibits a quasi-static resonance, which enables the particle to be electrically small [8, 9].

Up to now, the use of metamaterial concepts in practical miniaturized antennas is a very challenging research topic [10–16] and the achieved results based on self-resonance particles as SRRs or CSRRs [16] exhibit low radiation efficiencies driving to low-gain antennas comparing to the results of the parametric study presented in this paper. In this sense, the excitation of a CSRR etched in the patch of a conventional patch antenna allows us to design dual band patch antennas. Going further, the presence of the CSRR etched in some positions of the path also produces a miniaturization of both patch antenna resonances, leading to miniaturized dual band antennas. Replacing the CSRR within a slot of its same external dimensions, the slot does not exhibit a resonance at the same frequency of the CSRR, but at higher frequencies and more than one slot should be placed in the patch depending on their position in order to achieve a dual band response. The resonance frequency of a rectangular slot on a dielectric is approximately given by $c_{\text{light}}/(a+b)\cdot\sqrt{\varepsilon_r}$, where c_{light}, ε_r, a, and b are the speed of light in vacuum, dielectric relative permittivity, and the external dimensions

of the rectangular iris, respectively. In opposition to the resonance frequency of a rectangular slot, the resonant frequency of the CSRR is much lower for the same physical size. Hence, it can be designed to exhibit a resonance at lower frequencies comparing to different shapes of slots that can also be etched in a conventional patch. The design presented in this paper gives an alternative solution to the existing dual band antenna designs [17], as the ones carried out by loading a rectangular patch antenna with a pair of bent slots or embedded step slots close to the patch nonradiating edges, or the ones done by spur lines or shorted microstrip antenna with rectangular patch. Overall, as it can be shown in this paper, the properties of the CSRR allow us to design dual band miniaturized antennas based on the anisotropic properties of the CSRR as indicated by the measurements of a fabricated prototype and the parametric studies of the presented design in opposition to dual band antennas produced by the radiation of slots, whose resonances are dependent on their physical length. The prototype has been designed to exhibit a dual band behaviour in two frequency bands in the range from 4 GHz to 5 GHz for wireless applications. Nowadays, there is a growing trend to integrate different wireless communication systems in one single user terminal as long as to reduce the overall size. Since all these systems work at different frequency bands, dual and multiband antennas with frequency ratios around 1.2 between different bands are desirable. For this application, the type of antennas presented in this paper are a good alternative as introducing different CSRRs on the patch multiband antennas can be obtained very easily taking as a starting point the dual band antennas presented in this paper. The dual band antenna design presented has been validated, and a parametric study of the CSRR location and its influence on antenna radiating characteristics is presented and analyzed.

2. CSRR Excitation in a Rectangular Patch

The excitation of CSRRs has been usually driven by an incident electric field normal to the particle plane. In order to understand the excitation of these particles, let us consider the CSRR presented in Figures 1(b) and 1(c). Comparing the excitation of an SRR with a CSRR, the CSRR particle should be rotated 90° from the position of the SRR particle, as it is shown in Figure 1(a). Following the theoretical discussion shown in [4, 5], the operation of the SRR near its first resonance frequency obeys the effect of resonant polarizabilities, which gives the resonant magnetic and electric dipolar moments m_z, p_x, and p_y as a function of the exciting field components B_z^{inc}, E_x^{inc}, and E_y^{inc}. Complementarily, using the Babinet principle [9], the CSRR can be excited by the incident complementary fields E^{incc} and B^{incc}, which are related to E^{inc} and B^{inc} by $E^{\text{incc}} = c \cdot B^{\text{inc}}$ and $B^{\text{incc}} = -(1/c) \cdot E^{\text{inc}}$ by means of another set of resonant polarizabilities, thus given an electric dipole p_z^c and magnetic dipoles m_x^c and m_y^c. Then, as seen in Figures 1(b) and 1(c), depending on the CSRR position inside the patch, it will be excited by incident electric field normal to the particle plane (E_z) and by incident magnetic field tangent to the particle plane (B_x). For the excitation of the CSRR by the magnetic field (B_x), the CSRR should be rotated 90° in the patch as it is shown in Figure 1(c) comparing to the orientation of the CSRR in Figure 1(b).

In order to show graphically the excitation of the CSRR by the existing fields inside a rectangular patch antenna, Figures 2 and 3 show the electric fields and surface current distributions at the resonance frequency of the CSRR for the locations of this particle according to the layouts of Figures 2(a) and 3(a). In Figure 2, the CSRR particle has been located for its proper excitation by E_z electric field component, placed in one position inside the area where E field distributions are higher. Otherwise, in Figure 3, the CSRR particle has been located where magnetic field distributions are more concentrated, for the best suitable CSRR excitation by B_x magnetic field component. Though, for this case, the CSRR is also excited by E_z. The simulations of the structures presented in this paper have been performed with the commercial finite-integration time-domain CST Microwave Studio Code.

3. Parametric Study

The parametric study carried out in this work shows how the position of the CSRR (without changing its dimensions) has influence on the radiation efficiency of both antenna resonances for the orientation of the particle as it is in Figure 1(b). On this way, for some locations of the CSRR in the patch, radiation efficiencies up to 50% are achieved for both resonances. These results together with the measurement results of the prototype comparing to the simulated results show the usefulness of this kind of dual band patch antennas. The simulated antenna in the parametric study has the same dimensions as the fabricated one, excluding the placement of the CSRR inside the patch, which varies from Pos $= -9$ mm to Pos $= 9$ mm in the y-axis direction and from $u = 1$ mm to $u = 13$ mm in the x-axis direction. In Figure 1(b), the references of both Pos and u parameters are specified. The substrate employed in the simulated and fabricated prototype is the commercially available Arlon 250-LX-0193-43-11 ($\varepsilon_r = 2.43$ and thickness $h = 0.49$ mm). The physical width and length of the rectangular patch antenna are 18.43 mm and 23.68 mm, respectively [18]. Then, its resonance has been set around 5 GHz. The width of the micro strip line is 1.34 mm, corresponding to a characteristic impedance of 50 Ω. This line exhibits an offset from the centre of the patch antenna in order to match its reflection coefficient at its working frequency. The offset is ($X1 = -13.37$ mm and $Y1 = 0$ mm) (see Figure 1(b)).

The CSRR particle has been designed to exhibit its quasi-static resonance frequency below the resonance frequency of the patch, obtaining more compact devices highlighting the advantages of the resonance properties of anisotropic particles comparing to other slots already used for dual band antenna designs. The radiation produced by conventional slots does not have the same origin comparing to the radiation produced by a CSRR particle, and their electric length should be longer comparing to the electric length of the CSRR. The necessary physical dimensions of the CSRR to achieve a radiation frequency below the resonant frequency

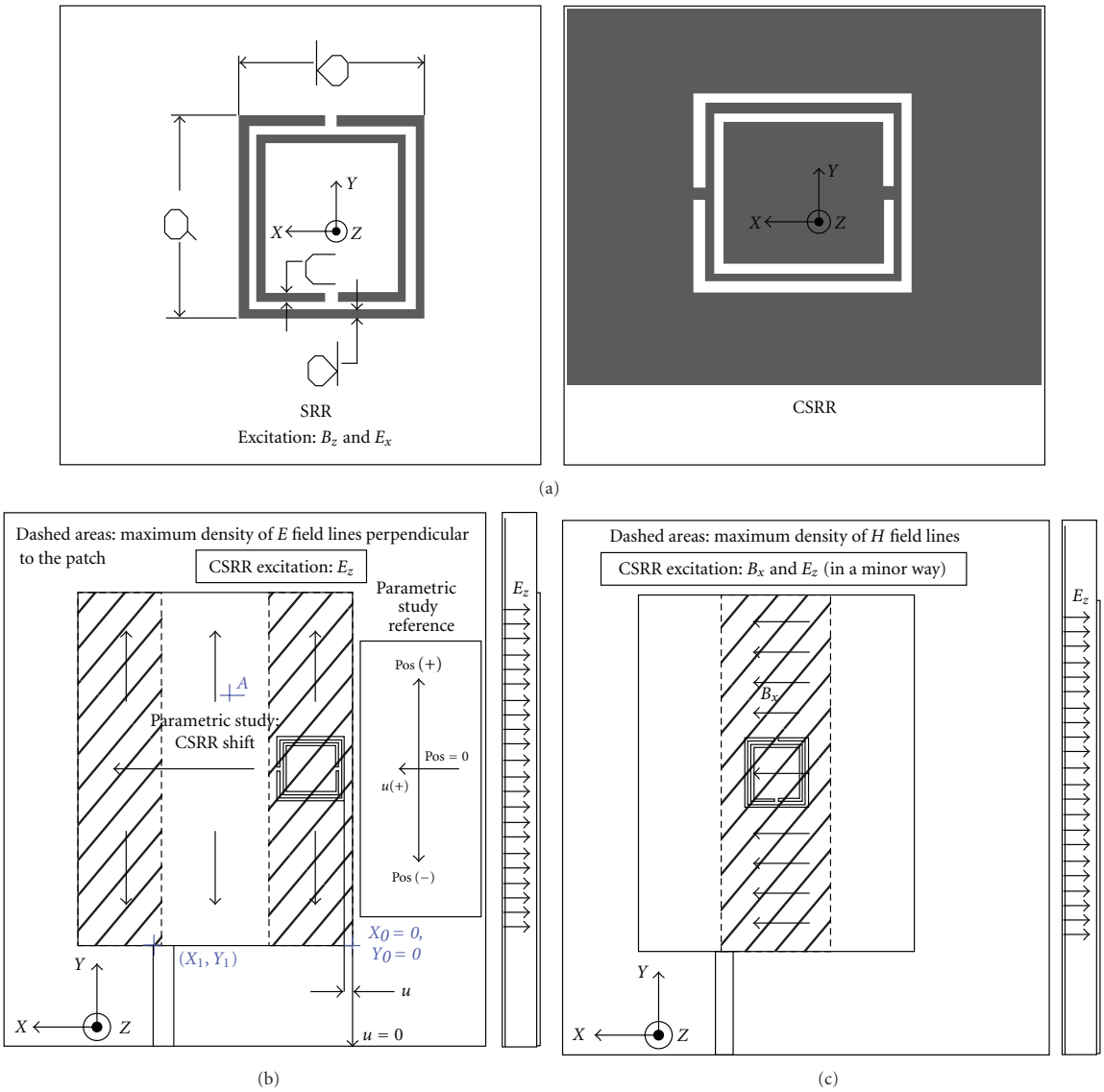

Figure 1: (a) SRR and CSRR topologies relevant dimensions. (b) Configuration of dual band CSRR-rectangular patch antenna. CSRR excitation by incident electric field normal to the particle plane, E_z. (c) Configuration of dual band CSRR-rectangular patch antenna. CSRR excitation by magnetic field tangent to the particle plane, B_x, and by electric field normal to the particle plane, E_z.

of the designed rectangular patch have been calculated using the design formulas for SRR reported in [4], resulting in this case in $a = 4.6$ mm, $b = 4.2$ mm, and $c = d = 0.2$ mm. In all the results presented in this paper, the first resonance of the dual band antenna is the one produced by the excitation of the CSRR, while the second resonance is produced by the conventional patch itself.

In Figures 4(a) and 4(b) radiation efficiencies as results from the parametric study are shown for both resonances. Figure 4(a) shows how the radiation efficiency of the resonance produced by the excitation of the CSRR increases while the anisotropic particle is placed at the radiating edges of the rectangular patch (*Pos parameter* values of −9 mm and 9 mm). However, there are some positions for the CSRR inside the patch where the radiation due to the CSRR is cancelled. These positions correspond to values around *Pos parameter of 0* mm and values around this value. This means that when the CSRR is etched in the centre of the rectangular patch its resonance is cancelled leading to a single resonance antenna.

Figure 4(b) shows how the radiation efficiency of the resonance produced by the patch decreases for some

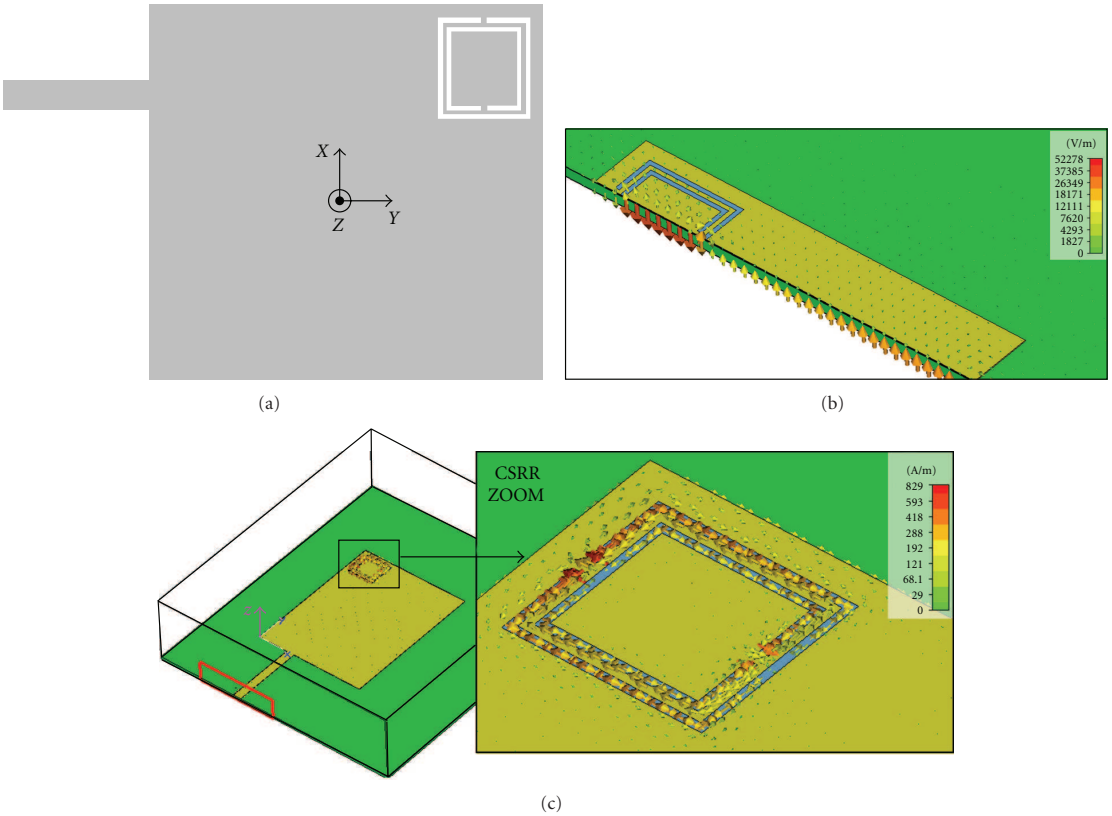

FIGURE 2: (a) Top view of the layout for E field and current distributions analysis in reference with Figure 1(b). (b) Simulated E_z field distribution in the CSRR at its resonant frequency. (c) Simulated current distributions in the CSRR at its resonant frequency.

u positions when the CSRR is placed at the radiating edges of the conventional patch antenna. However, there are other u positions at these edges where both resonances exhibit radiation efficiencies up to 50%. The position values where radiation efficiency has been set to zero mean that the resonance produced by the CSRR particle or by the patch has been cancelled as explained before. The results of the parametric study for radiation efficiencies of both resonances show that the results are not symmetric, these differences are due to the asymmetric microstrip line excitation of the rectangular patch.

In Figures 5(a) and 5(b) gain values for u parameter values ($u = 3, 4, 11, 12$, and 13), which drive to the highest radiation efficiencies for both resonances, are depicted. The discontinuities with no values in the curves of Figures 5(a), 6(a), and 6(b) are because there is no resonance of the CSRR for those positions.

For the locations where the CSRR is etched around the centre of the rectangular patch, $u = 6$ mm, $u = 7$ mm, and $u = 8$ mm, both resonances, the one produced by the CSRR and the one produced by the patch, are shifted to lower frequencies, resulting in a miniaturization of both frequency bands of dual band patch antenna comparing to a conventional rectangular patch antenna of the same dimensions. By contrast, as the CSRR moves away from the centre of the patch towards the nonradiating edges (in u direction for all its *Pos parameter* values), the resonance produced by the rectangular patch shifts to higher frequencies comparing to the resonant frequency of the conventional rectangular patch itself. In Figures 6(a) and 6(b) the resonant frequencies for the first and second resonances versus *Pos parameter* and $f2/f1$ ratio are shown for $u = 1$, $u = 6$, and $u = 13$ parameter values, where $f1$ and $f2$ are the resonance produced by the CSRR and the one produced by the rectangular patch, respectively. The miniaturization ratio of this type of antennas based on this design is around 1.2, but it also depends on the position of the CSRR on the patch, as the resonance frequencies are shifted. This behaviour is clearly shown in Figures 6(a) and 6(b).

From Figures 6(a) and 6(b) the miniaturization factor has been calculated for two different positions of the CSRR on the patch. In the first case, for particle location parameters of $u = 13$ mm and Pos $= -9$ mm the miniaturization factor is 1.16, corresponding to a radiation efficiency of 45.37% and gain of 3.59%. For the second case, the position parameters values are $u = 6$ mm and Pos $= 0$ mm. In this case the resonance produced by the CSRR has been cancelled and a single-band antenna is achieved. The miniaturization factor

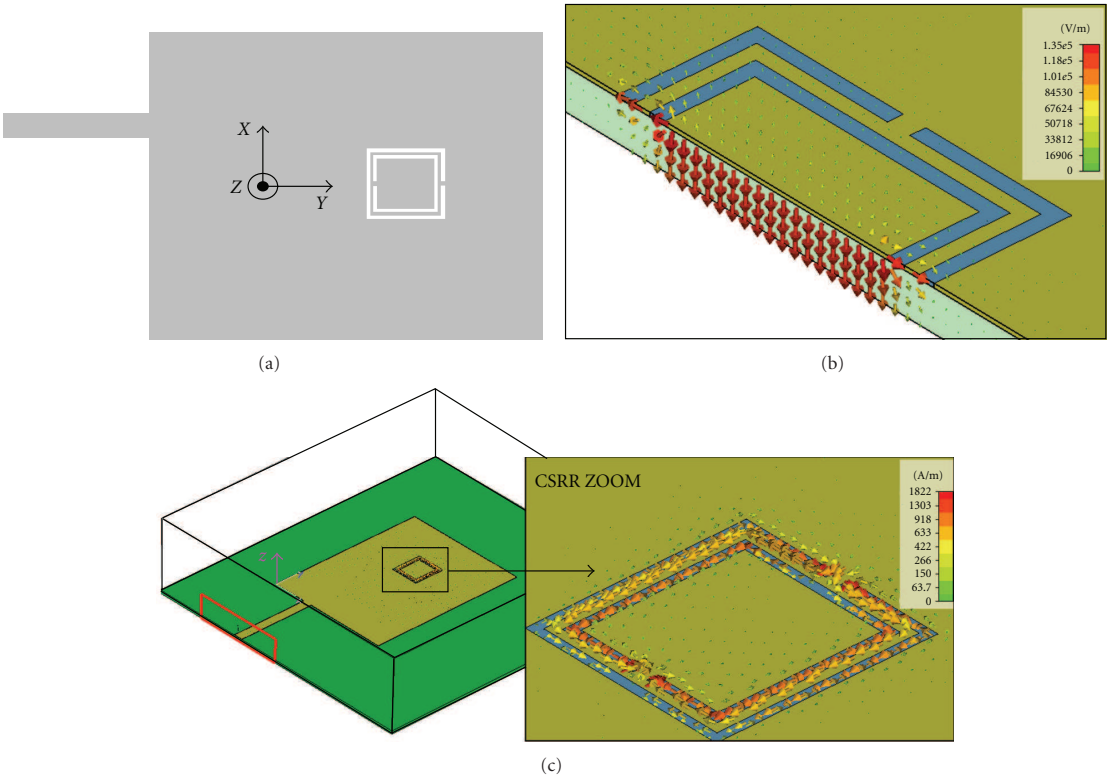

FIGURE 3: (a) Top view of the layout for E field and current distributions analysis in reference with Figure 1(c). (b) Simulated E_z field distribution in the CSRR at its resonant frequency. (c) Simulated current distributions in the CSRR at its resonant frequency.

is 1.1, corresponding to a radiation efficiency of 84.36% and gain of 6.56 dB.

4. Experimental Results

In order to demonstrate the usefulness of this dual band antenna design, a prototype has been fabricated. The fabricated prototype has been chosen from the parametric study in a case where the radiation efficiency is low comparing to the highest values obtained of this parameter. This case has been chosen to validate the usefulness of this design in a worst case condition. The prototype has been fabricated using a laser drilling machine. The design parameters of the CSRR particle are $a = 4.6$ mm, $b = 4.2$ mm, and $c = d = 0.2$ mm (the same ones of those of the CSRR used in the parametric study). In the fabricated prototype the CSRR has been placed at A point (see Figure 1(b)) being the coordinates of this point (X = −9.3 mm, Y = 15.54 mm).

In Figure 7 simulated and measured reflection coefficient results of the fabricated prototype are shown. For matching measurements data has been collected by using an HP8510 network analyzer. As it can be seen in Figure 7, there is a frequency shift of 162 MHz to lower frequencies for the lower resonance. The upper resonance presents a frequency shift of 84 MHz, shifted to lower frequencies. Although there is a frequency shift between simulated and measured results, the matching values achieved are properly predicted by simulations. The discrepancies between simulated and measured results are due to the manufacturing process as the CSRR manufacturing tolerances are critical, changing slightly its frequency resonance. In simulations, materials have been simulated considering their corresponding finite conductance and substrate has been simulated considering its dielectric losses. In Figure 8 a picture of the fabricated prototype is shown.

In Figures 9(a) and 9(b) measured results for normalized gain radiation patterns for 0° and 90° phi cut planes for both resonant frequencies are shown. Besides, simulated results just for 90° phi cut are shown. No more simulated cuts are introduced to maintain the figures legible. These frequencies are $F1 = 4.19$ GHz and $F2 = 4.808$ GHz, the resonant frequencies produced by the CSRR particle and conventional patch, respectively. The radiation pattern measured results show the feasibility of this type of dual band antenna design. Both resonances show cross-polar levels around −20 dB for theta 0°.

Table 1 shows a comparison between simulated and measured results of the fabricated prototype from impedance matching and radiation point of views. This table shows that both resonances have similar characteristics. From matching

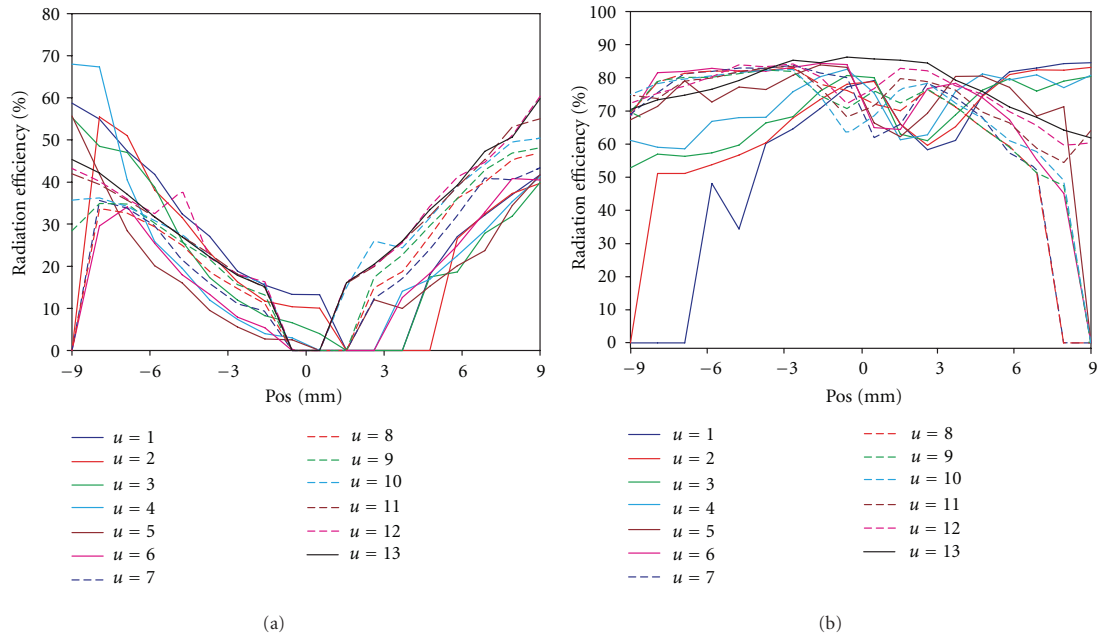

FIGURE 4: (a) Simulated radiation efficiency for the resonance produced by the CSRR. (b) Simulated radiation efficiency for the resonance produced by the rectangular patch antenna.

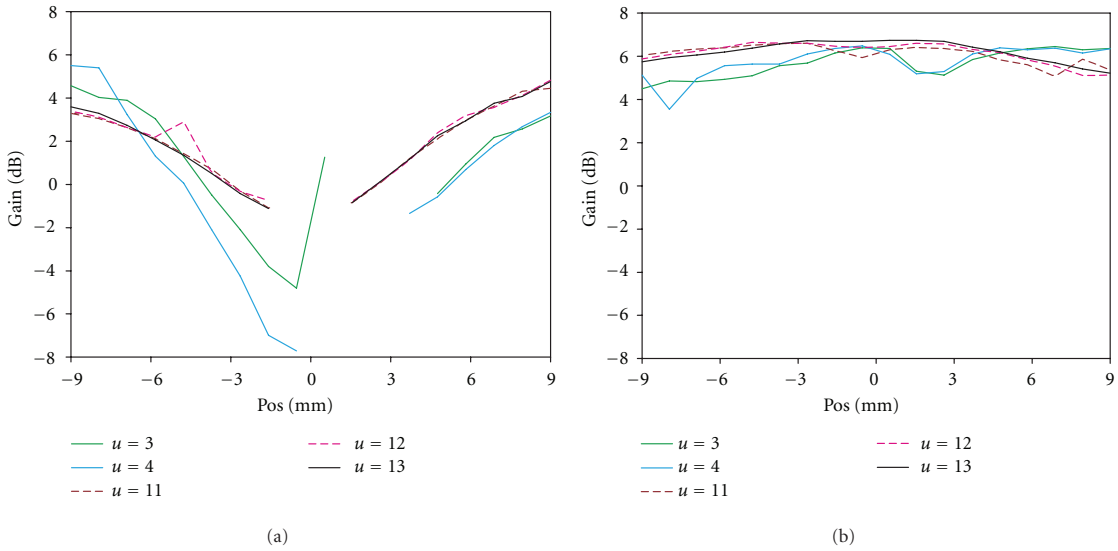

FIGURE 5: (a) Simulated gain values for the resonance produced by the CSRR. (b) Simulated gain values for the resonance produced by the rectangular patch antenna.

point of view, the parameters shown in Table 1 are reflection coefficient values for both resonant frequencies. From radiation point of view, parameters shown in Table 1 are peak directivity, peak gain, and radiation efficiency. Directivity values have been calculated [18] from measured gain radiation patterns for both resonances in order to calculate efficiency and verify the good agreement between simulated and measured data. Within the fabricated prototype the parametric study made in this work has been validated due to the good agreement between simulations and measured results. Although gain and radiation efficiency obtained by the resonance produced by the CSRR is low comparing to the second resonance in the fabricated prototype, these values are in accordance with the simulated results. Furthermore,

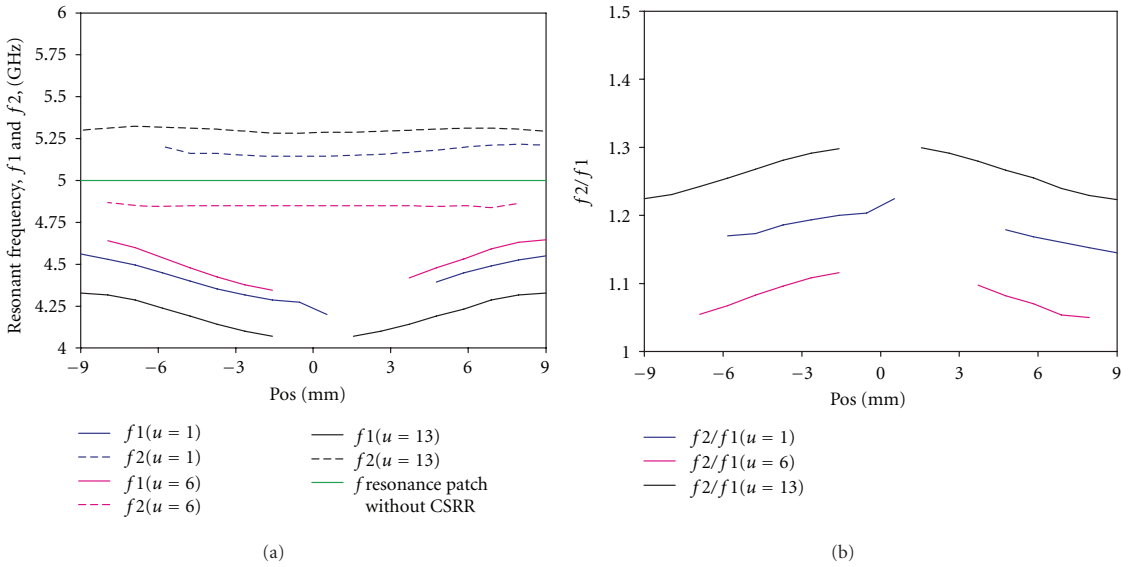

Figure 6: (a) Parametric study results. $f1$ and $f2$ resonant frequencies. (b) Parametric study results. $f2/f1$ ratio.

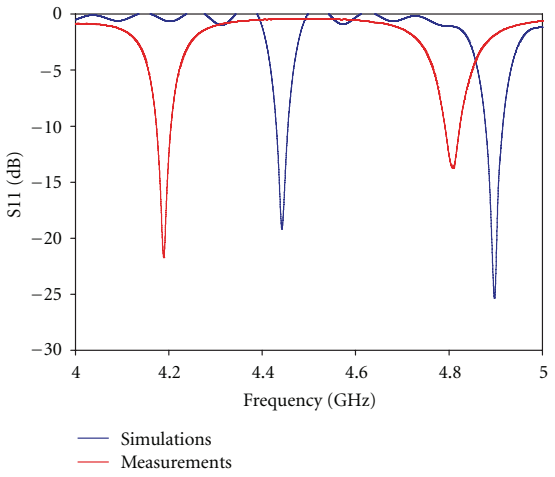

Figure 7: Simulated and measured reflection coefficient results.

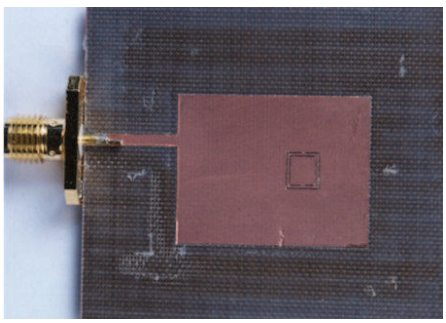

Figure 8: Fabricated prototype.

Table 1

Parameters	Simulated results	Measured results
Matching characteristics		
First resonance ($F1$)		
$F1$, (GHz)	4.352	4.19
Reflection coefficient, (dB)	−16.75	−21.25
Effective bandwidth at −5 dB (%)	1.60	1.52
Second resonance ($F2$)		
$F2$, (GHz)	4.892	4.808
Reflection coefficient, (dB)	−15.15	−13.86
Effective bandwidth at −5 dB (%)	1.79	1.72
Radiation characteristics		
First resonance ($F1$)		
Peak directivity, (dBi)	7.16	7.36
Peak gain, (dB)	−0.97	−0.11
Radiation efficiency (%)	15.38	17.92
Second resonance ($F2$)		
Peak directivity, (dBi)	7.243	7.74
Peak gain, (dB)	5.946	5.85
Radiation efficiency, (%)	74.18	64.83

it is remarkable that gain values obtained for the positions of the CSRR in the patch studied in this work are higher compared to previous works [16].

Up to this point, in order to compare the performances of the dual band antenna topology presented in this paper with those of the same conventional patch antenna without a CSRR etched in its centre, in Table 2 measured data of the conventional rectangular patch antenna is shown.

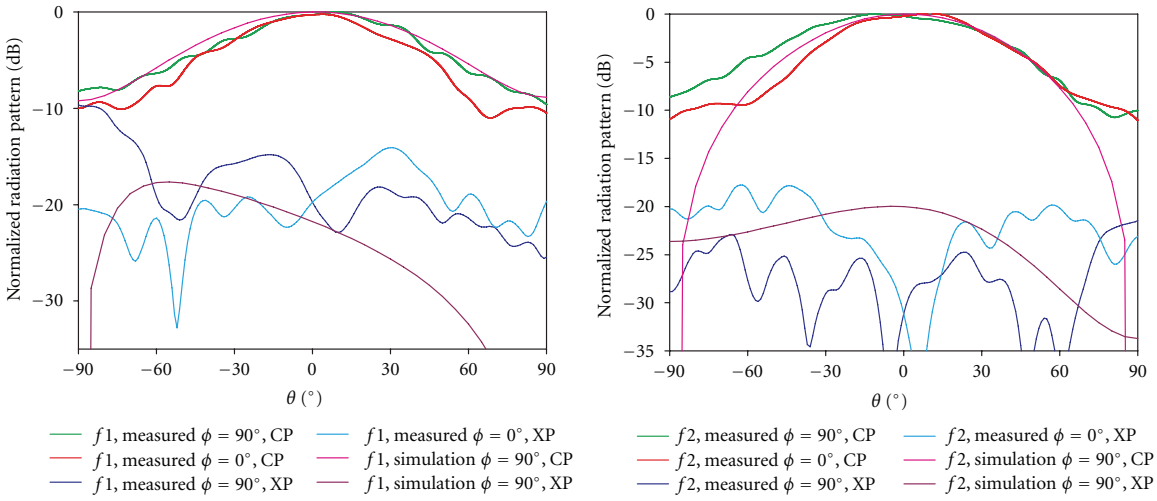

(a) (b)

Figure 9: (a) Measured normalized copolar and cross-polar gain radiation patterns for 0° and 90° phi cuts. Simulated normalized copular and cross-polar gain radiation pattern for 90° phi cut at $F1 = 4.19$ GHz. (b) Measured normalized copolar and cross-polar gain radiation patterns for 0° and 90° phi cuts. Simulated normalized copular and cross-polar gain radiation pattern for 90° phi cut at $F2 = 4.808$ GHz.

Table 2

Parameters	Measured results
Patch antenna	
Matching characteristics	
Frequency, (GHz)	5.16
Reflection coefficient, (dB)	−22.3
Effective bandwidth at −5 dB (%)	1.9
Radiation characteristics	
Peak directivity, (dBi)	7.55
Peak gain, (dB)	6.08
Radiation efficiency (%)	71.3

Comparing Tables 1 and 2, the designed prototype presents similar performances to those of the conventional patch antenna from matching point of view (effective bandwidth and reflection coefficient values). On the other side, from radiation point of view, the designed and fabricated dual band antenna resonances show lower radiation efficiencies as it has been mentioned before.

Finally, to understand in an oversimplified way the radiation mechanism of the proposed antenna, one needs to consider the pair of electric dipoles that are described in [9] and the effect of the finite ground plane. In a recent work a refined equivalent circuit model for the CSRR which explains more accurately the physical interpretation of the influence of reactive parameters [19] is presented. This circuit model will be developed in further works in order to take into account the radiation resistance and the internal coupling to the patch and ground plane.

5. Conclusions

In this work a dual band patch antenna based on a CSRR has been proposed, studied, and successfully tested, demonstrating the feasibility of this type of dual band antennas, adding a miniaturization of patch dimensions for some locations of the CSRR inside the patch. A good agreement between simulated and measured results is shown. The parametric study shows the influence of the location of the CSRR on the patch on the radiation characteristics. The design of the dual patch antenna is simple as the only design parameters comparing to a conventional path antenna are the ones of the CSRR particle design parameters. Also, multiband antennas can be designed in a similar way by simply adding different CSRRs on the patch.

Acknowledgments

This work has been supported by the Spanish Government and EU Feder by the Contracts Consolider "Engineering Metamaterials" CSD2008-00066 and TEC2008-06871-C02-01.

References

[1] V. G. Veselago, "The electrodynamics of substances with simultaneously negative values of ε and μ," *Soviet Physics Uspekhi*, vol. 10, pp. 509–514, 1968.

[2] D. R. Smith, W. J. Padilla, D. C. Vier, S. C. Nemat-Nasser, and S. Schultz, "Composite medium with simultaneously negative permeability and permittivity," *Physical Review Letters*, vol. 84, no. 18, pp. 4184–4187, 2000.

[3] J. B. Pendry, A. J. Holden, D. J. Robbins, and W. J. Stewart, "Magnetism from conductors and enhanced nonlinear

phenomena," *IEEE Transactions on Microwave Theory and Techniques*, vol. 47, no. 11, pp. 2075–2084, 1999.

[4] R. Marqués, F. Mesa, J. Martel, and F. Medina, "Comparative analysis of edge- and broadside-coupled split ring resonators for metamaterial design—theory and experiments," *IEEE Transactions on Antennas and Propagation*, vol. 51, no. 10, pp. 2572–2581, 2003.

[5] R. Marqués, F. Medina, and R. Rafii-El-Idrissi, "Role of bianisotropy in negative, permeability and left-handed metamaterials," *Physical Review B*, vol. 65, no. 14, pp. 1444401–1444406, 2002.

[6] F. Martín, F. Falcone, J. Bonache, T. Lopetegi, R. Marqués, and M. Sorolla, "Miniaturized coplanar waveguide stopband filters based on multiple tuned split rin resonators," *IEEE Microwave and Wireless Components Letters*, vol. 13, no. 12, pp. 511–513, 2003.

[7] F. Falcone, F. Martín, J. Bonache, R. Marqués, T. Lopetegi, and M. Sorolla, "Left handed coplanar waveguide band pass filters based on Bi-layer split ring resonators," *IEEE Microwave and Wireless Components Letters*, vol. 14, no. 1, pp. 10–12, 2004.

[8] F. Falcone, T. Lopetegi, J. D. Baena, R. Marqués, F. Martín, and M. Sorolla, "Effective negative-ε stopband microstrip lines based on complementary split ring resonators," *IEEE Microwave and Wireless Components Letters*, vol. 14, no. 6, pp. 280–282, 2004.

[9] F. Falcone, T. Lopetegi, M. A. G. Laso et al., "Babinet principle applied to metasurface and metamaterial design," *Physical Review Letters*. In press.

[10] R. W. Ziolkowski and A. D. Kipple, "Application of double negative materials to increase the power radiated by electrically small antennas," *IEEE Transactions on Antennas and Propagation*, vol. 51, no. 10, pp. 2626–2640, 2003.

[11] F. Qureshi, M. A. Antoniades, and G. V. Eleftheriades, "A compact and low-profile metamaterial ring antenna with vertical polarization," *IEEE Antennas and Wireless Propagation Letters*, vol. 4, no. 1, pp. 333–336, 2005.

[12] R. K. Baee, G. Dadashzadeh, and F. G. Kharakhili, "Using of CSRR and its equivalent circuit model in size reduction of microstrip antenna," in *Proceedings of the Asia-Pacific Microwave Conference (APMC '07)*, pp. 1–4, 2007.

[13] Y. Lee, S. Tse, Y. Hao, and C. G. Parini, "A compact microstrip antenna with improved bandwidth using complementary split-ring resonator (CSRR) loading," in *Proceedings of the IEEE Antennas and Propagation Society International Symposium*, pp. 5431–5434, June 2007.

[14] L. Meng, L. Mingzhi, and J. C. Tie, "Novel miniaturized dual band antenna design using complementary metamaterial," in *Proceedings of the International Workshop on Metamaterials (META '08)*, pp. 374–376, November 2008.

[15] J. Liu, S. Gong, Y. Xu, X. Zhang, C. Feng, and N. Qi, "Compact printed ultra-wideband monopole antenna with dual band-notched characteristics," *Electronics Letters*, vol. 44, no. 12, pp. 710–711, 2008.

[16] H. Zhang, Y. Q. Li, X. Chen, Y. Q. Fu, and N. C. Yuan, "Design of circular/dual-frequency linear polarization antennas based on the anisotropic complementary split ring resonator," *IEEE Transactions on Antennas and Propagation*, vol. 57, no. 10, Article ID 5196779, pp. 3352–3355, 2009.

[17] K.-L. Wong, *Compact and Broadband Microstrip Antennas*, John Wiley & Sons, New York, NY, USA, 2002.

[18] J. D. Kraus and R.J. Marhefka, *Antennas for all Applications*, McGraw-Hill, New York, NY, USA, 3rd edition, 2002.

[19] F. Aznar, M. Gil, J. Bonache, and F. Martín, "Revising the equivalent circuit models of resonant-type metamaterial transmission lines," in *Proceedings of the IEEE MTT-S International Microwave Symposium Digest (MTT '08)*, pp. 323–326, June 2008.

3.2.6 Paper: Design and Implementation of dual Band Antennas based on CSRR

The contributions of this work are summarized as follows:

- In this paper the equivalent circuit model of dual band-patch antennas based on a Complementary Split Ring Resonator is presented and validated. This equivalent circuit model is sound in order to understand the functionality of the radiating structure. In fact, the validation of the equivalent circuit model proofs that the CSRR particle behaves as a stand-alone radiating element; which is coupled to the rectangular patch antenna.
- The validation of the equivalent circuit model has been carried out by the manufacture and testing of three antenna prototypes; which have been printed on substrates with different permittivity values. Good agreement between simulation, equivalent circuit model and experimental results is shown and discussed.
- The designed and tested prototypes show radiation efficiencies of 62.5% and 64% for the radiation driven by the CSRR and rectangular patch; respectively. These values are in accordance to the parametric study presented in *Section 3.2.5* for the case where the CSRR is located in close to the non radiating edges of the rectangular patch. See *Figure 4* of the paper presented in *Section 3.2.5*.
- The experimental validation of the equivalent circuit model allows the equivalent circuit model to become a simple and straightforward tool for the design of this type of multiband antennas, of low cost and versatile operation for a broad range of wireless communication systems.
- In the *Table 3* of the paper presented in this section, a state of the art study of dual band patch antennas based on CSRRs is provided. This table shows that the design presented in this paper exhibits highest radiation efficiencies compared to other antennas, see designs in [13].

Waves in Random and Complex Media, 2015
http://dx.doi.org/10.1080/17455030.2015.1028577

Taylor & Francis
Taylor & Francis Group

Design and implementation of dual-band antennas based on a complementary split ring resonators

Noelia Ortiz, Juan Carlos Iriarte, Gonzalo Crespo and Francisco Falcone*

Electrical Engineering Department, Universidad Pública de Navarra, Pamplona, Spain

(*Received 2 November 2014; accepted 8 March 2015*)

A simple dual-band antenna design and implementation method is proposed in this work, based on the equivalent media properties inspired by resonant metamaterial elements. The equivalent circuit model of dual-band patch antennas based on a complementary split ring resonator (CSRR) is presented and validated. The dual-band patch antenna is designed etching a CSRR in the patch of a conventional rectangular microstrip patch antenna. The first resonance is governed by the quasi-static resonance of the CSRR while the second resonance is originated by the rectangular patch. The fact of etching a CSRR on a rectangular patch antenna also produces a miniaturization of a conventional patch antenna. The equivalent circuit model proposed in this letter is sound in order to understand the functionality of dual-band patch antennas based on a CSRR. Good agreement between simulation, equivalent circuit model and experimental results is shown and discussed. These results lead the equivalent circuit model to become a simple and straightforward tool for the design of this type of multiband antennas, of low cost and versatile operation for a broad range of wireless communication systems.

*Corresponding author. Email: francisco.falcone@unavarra.es

4. Multiple CSRR Application in Complex Radiating Structures

L'imagination est tout.
C'est un avant-gôut de ce que la vie nous réserve.
Albert Einstein

A novel Metamaterial antenna structure based on a CSRR particle etched in a rectangular patch antenna is presented in the previous chapter. This novel structure was proposed in 2006 in order to increase the radiation efficiency of the CSRR stand alone radiating element. Results presented in the previous chapter demonstrate radiation efficiency improvement for the CSRR. Hence, it came naturally to us to implement multiple CSRRs in the patch of a patch antenna in order to obtain a multi-band antenna.

When etching different CSRRs in the patch of a rectangular patch antenna, two distinct behaviors are observed in terms of impedance matching, radiation characteristics and polarization. These distinct behaviors have the origin in the coupling mechanism among the CSRRs. On the one hand a multi-band antenna is obtained when there is low coupling among the CSRRs. In this case, each CSRR acts as an isolate particle and the radiation properties of each CSRR can be predicted by the results of the parametric study presented in *Chapter 3*. Simulation and measurement results of these multi-band antenna structures are not shown in this memoir because these results are still under preparation. Preliminary outcomes are very encouraging and will probably be part of future publications.

On the other hand, when there is a strong electric coupling among the CSRRs part of a chain of resonators printed in the patch, an Electro-Inductive wave (EIW) propagation is supported by that chain. Then, the EIW propagation phenomenon is used to master the field distribution within the rectangular patch, and hence, to change the polarization of the patch antenna, which is shown to change from linear to circular polarization. Author's contribution in this direction is presented in this chapter.

4.1 Electro-Inductive-Wave Coupling to chain of CSRRs

Electro-Inductive waves (EIWs) can be interpreted as the dual counterpart of the so called Magneto-Inductive Waves (MIWs) (see [1], [2], [3]); which are due to the mutual inductance between chains of resonators.

Generally, EIWs are supported by chains of resonators drilled on a metallic substrate. Previously, chains of CSRR elements have been studied as supporting structures for EIWs, due to inter CSRR interaction given mainly by E-field coupling. This phenomenon has been employed in the implementation of devices such as delay lines (see [4]) or compact filters. The proposed structures enable power flow following the path of the CSRR elements. If unit CSRR elements are geometrically modified, in terms of their relative dimensions or of their position (e.g., relative resonator rotation), potential modification of wave polarization can be achieved. This concept has already been employed in order to implement lowloss waveguiding structures, by supporting so called spoof plasmon polaritons, which can be viewed as complex surface waves within the microwave and millimeter wave regime [5], providing alternative paths to device integration.

In the author's work presented in the section below, *Section* **??**, the EIW phenomenon is employed to define and characterize new structures based on CSRR configurations for generating circular polarization in a rectangular patch antenna.

4.2 Paper: Circularly polarized waves based on EIW coupling to chain of CSRRs

As it is explained in the previous section (see *Section* **??**), the work presented in this section show new structures based on CSRR configurations for generating circular polarization in a rectangular patch. In this work, a different principle to the one used in previous works [6], [7] and [**?**] for the generation of circular polarization in a rectangular patch antenna is presented.

In 2009 and 2012, in [6] and [7] respectively, the principle of circularly polarized patch antenna is to use the CSRR as an asymmetric perturbation in the patch of a linearly polarized fed square patch antenna. In 2012, in [**?**] the principle of the circularly polarized rectangular patch antenna is to overlap the two working frequencies of a dual band dual-linearly polarized rectangular patch antenna composed of two CSRRs elements side-by-side, reversely placed in the center of a rectangular patch

antenna and excite these two resonances with a 90° phase difference. The first resonance is generated by the two CSRRs, while the second resonance is the inherent rectangular patch resonance. Since the probe feed is in the center of the rectangular patch and wave propagation is directed towards the two diagonal lines oppositely with 45° phase delay, the 90° phase difference is automatically introduced.

In the author's work presented in this section, the circular polarization is generated by the propagation of an Electro-Inductive wave at the quasi-static resonant-frequency of a CSRR array printed in the rectangular patch. This work has been published in the journal of Applied Physics in 2016. The contributions of this work are summarized as follows:

- This work demonstrates a practical application of the EIW propagation phenomenon. Thanks to EIW propagation along a chain composed of CSRRs printed on the rectangular patch of a patch antenna, circular polarization is generated. Depending on the configuration of the Complementary Split Ring Resonator particles printed on the patch, Right or Left handed circularly polarized antennas are obtained.
- EIW propagation is demonstrated by the existence of electric coupling between CSRRs. In this paper the electric coupling is shown by the comparison of electric field x, y and z components with the ones of the reference conventional rectangular antenna. For futher detailed information, see computed results shown in *FIG. 11.*
- The principle of operation is demonstrated with the design, fabrication and measurement of antenna prototypes. Good agreement between simulation and measurement results is shown, considering the effect of fabrication tolerances in initial frequency shifts.
- The proposed design provides a simple, low cost alternative in order to provide polarization modification properties for multiple antenna communication systems.
- The coupling of EIW in order to provide polarization rotation capabilities can be extended in order to demonstrate the phenomena in different configuration, such as in guided wave structures, or with enhanced capabilities provided by the inclusion of active elements in order to achieve certain level of tunability in the frequency selective or phase response of the implemented devices.

JOURNAL OF APPLIED PHYSICS **120**, 174905 (2016)

Generation of circularly polarized waves based on electro inductive-wave (EIW) coupling to chains of complementary split ring resonators

Noelia Ortiz, Gonzalo Crespo, Juan Carlos Iriarte, and Francisco Falcone
Departamento de Ingeniería Electrica y Electronica, Universidad Publica de Navarra, 31006 Pamplona, Navarra, Spain

(Received 6 June 2016; accepted 18 October 2016; published online 7 November 2016)

In this work, Electro-Inductive wave (EIW) propagation phenomenon is employed in order to introduce a polarization rotation capability in a rectangular patch antenna. The EIW propagation phenomenon is used to master the field distribution within the rectangular patch, and hence, to change the polarization of a patch antenna, which is shown to change from linear to circular polarization. EIW propagation is supported by a chain of Complementary Split Ring Resonators printed in a rectangular patch antenna at specific locations. This principle of operation is demonstrated with the design, fabrication, and measurement of antenna prototypes. Experimental results confirm numerical analysis, providing a simple antenna configuration with polarization variation capabilities, extendable to multiple configurations, in radiated waves as well as in guided wave phenomena. *Published by AIP Publishing.* [http://dx.doi.org/10.1063/1.4966929]

I. INTRODUCTION

Complementary Split Ring Resonators (CSRRs)[1] are the dual particles of Split Ring Resonators (SRRs),[2] by direct application of Babinet's principle. SRRs were first introduced by Pendry[2] in order to produce artificial media with a strong magnetic response at microwaves and radio-frequencies. In his seminal work Pendry predicted that artificial media with negative permeability could be designed by using SRRs. In fact, this prediction was soon confirmed by Smith's experiments,[3] in which the experimental demonstration of a left handed medium, as a combination of an array of SRR and wire media for propagating waves in free space was presented.[3]

In the last decade, SRRs and CSRRs have become popular and powerful elements in the design of planar technology devices due to their versatile frequency response as well as their sub-wavelength dimensions.[4] SRR and CSRR electromagnetic properties have been deeply investigated.[1,5,6] Firstly, these particles have been solid constituents for planar microwave filter,[7–11] directional coupler,[12,13] frequency selective surfaces,[14] and Electromagnetic Band-GAP (EBG) structures designs.[15] Secondly, SRR and CSRR particles have also been used in conventional planar antennas. In particular, CSRR particles have been introduced in different types of conventional planar antennas in order to improve their bandwidth,[16–18] miniaturize antenna size,[19–22] generate multi-frequency band antennas,[20,23–28] enhance dual-band antennas radiation characteristics,[28] and generate circular polarization from conventional linear polarization patch antennas.[20,29–31] Other solutions have also been proposed in order to control radiation characteristics in multiple frequency ranges and device configurations, such as Metasurfaces and Metaradomes (which can be defined as a radome or superstrate, which exhibits engineered electromagnetic properties owing to the inclusion of metamaterial-inspired elements within the initial host material), providing effective mechanisms in a bi-dimensional single layer fashion or by means of multiple stacking.[32–36] Metasurfaces have been implemented by employing coupled bi-layer structures, exhibiting enhanced transmitted field distributions in the optical range.[32] Polarization conversion has also been demonstrated by employing self-complementary structures, such as strip gratings, SRR-CSRR arrays and hole/patch structures, enabling the implementation of compact polarizers.[33] Other works, such as those described in Refs. 34–36 exploit the use of active elements as well as non-linear behavior of certain materials in order to achieve certain degree of tunability, which can be observed in the location of quasi-static resonance frequencies or the corresponding phase response.

The phenomenon that allows polarization rotation and circular polarization generation in the present work is different from the principles presented and described in previous works.[20,29–31] Previously,[20] the principle of the circularly polarized rectangular patch antenna is to overlap the two working frequencies of a dual band dual-linearly polarized rectangular patch antenna composed of two CSRRs elements side-by-side, reversely placed in the center of a rectangular patch antenna and excite these two resonances with a 90° phase difference. The first resonance is generated by the two CSRRs, while the second resonance is the inherent rectangular patch resonance. Since the probe feed is in the center of the rectangular patch and wave propagation is directed towards the two diagonal lines oppositely with 45° phase delay, the 90° phase difference is automatically introduced. The principle of circularly polarized patch antenna is to use the CSRR as an asymmetric perturbation in the patch of a linearly polarized fed square patch antenna.[29–31] Etching the CSRR in a specific orientation and position on the square patch antenna, the surface current paths of the original patch antenna are modified and for a given size of the CSRR a good circularly 'polarized antenna is obtained. In that case, the non-resonant property of a single CSRR etched in a rectangular patch antenna is used. In contrast, in the present

work, the circularly polarized antenna is achieved by the propagation of an Electro-Inductive Wave (EIW)[32] at the quasi-static resonant frequency of a CSRR array, which is etched at a specific location on the rectangular patch antenna and which can be viewed as a dual element from a Magneto-Inductive Wave (MIW) propagation achieved with conductor based resonators, such as SRRs.

Generally, EIWs are supported by chains of resonators drilled on a metallic substrate. EIWs can be interpreted as the dual counterpart of the so called Magneto-Inductive Waves (MIWs),[38–45] which are due to the mutual inductance between chains of resonators. Previously, chains of CSRR elements have been studied as supporting structures for EIWs, due to inter CSRR interaction given mainly by E-field coupling. This phenomenon has been employed in the implementation of devices such as delay lines or compact filters. The proposed structures enable power flow following the path of the CSRR elements. If unit CSRR elements are geometrically modified, in terms of their relative dimensions or of their position (e.g., relative resonator rotation), potential modification of wave polarization can be achieved. This concept has already been employed in order to implement low-loss waveguiding structures, by supporting so called "spoof plasmon polaritons," which can be viewed as complex surface waves within the microwave and millimeter wave regime,[36] providing alternative paths to device integration.

In this work, the EIW phenomenon is employed to define and characterize new and simple structures based on CSRR configurations for generating circular polarization in a rectangular patch antenna. Depending on the configuration of the resonant particles printed on the patch, Right or Left handed circularly polarized antennas are obtained. The proposed design is applied to a conventional patch antenna configuration. When compared to other routes employed in order to achieve polarization rotation (such as the use of metasurfaces coupled to a radiating source), the approach followed in this work directly embeds chains of CSRR elements which support EIW propagation, providing a more compact structure and reducing to certain extent inaccuracies given by misalignment or by non-uniform air gap spacing between the radiating elements and other structures.

The outline of this paper is as follows. In Section II, antenna designs are presented, EIW propagation phenomenon and polarization rotation is explained and demonstrated. Section III describes the experimental work carried out in which simple demonstration structures have been constructed and tested. Moreover, CSRRs design parameters have been tuned in order to compensate reflection coefficient shift in fabricated prototypes. The paper ends with a discussion and conclusions on the advantages and limitations of the realization and performance of these structures.

II. DESIGN

As previously stated, CSRR resonators etched within a conductor layer can support EIWs and can modify polarization states, as a function of geometrical configuration of the embedded resonators, which can be successfully applied in order to implement low-loss wave guiding structures or delay lines, owing to inherently dispersive frequency response.[32,36] In order to induce the propagation of EIW and coupling to radiation sources, several antenna configurations that generate circular polarization by EIW propagation phenomenon have been designed and are schematically depicted in Fig. 1. This geometry is composed of a chain of three rectangular CSRRs printed in the patch of a rectangular patch antenna. The difference between both configurations presented in Fig. 1 is the sequential rotation of the CSRRs, in order to modify induced currents within the CSRR elements, and hence, the phase variation which can be effectively be accomplished by each chain of CSRRs. Antenna configuration #1 and #2 exhibit Left handed and Right handed polarizations, respectively. Fig. 2 shows the geometries of antenna configurations #3 and #4. These configurations present linear polarization and they have been defined for comparison purposes in order to explain EIW phenomenon in antenna configurations #1 and #2. In addition, a rectangular patch antenna of the same patch dimensions and no CSRRs (antenna configuration #5) has been used as a reference antenna for comparison purposes. Antenna configurations #3 and #4 have been defined from antenna configurations #1 and #2, respectively, displacing the

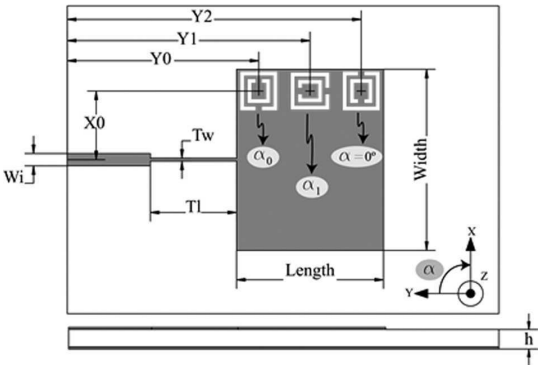

FIG. 1. Structure configurations with Circular Polarization: Configuration #1 is generated by setting $\alpha_0 = 180°$ and $\alpha_1 = 90°$ (as illustrated in the drawing). Configuration #2 is generated by setting $\alpha_0 = 0°$ and $\alpha_1 = 0°$ (the rotation scheme of the CSRR is illustrated in Fig. 3).

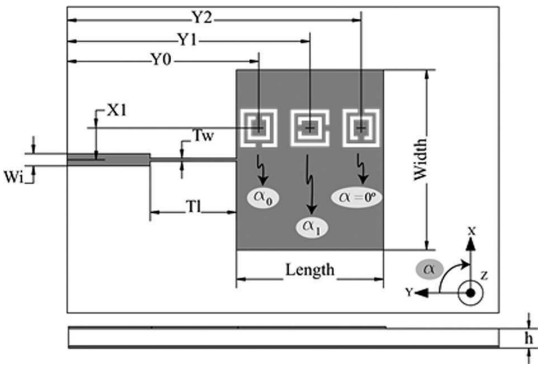

FIG. 2. Structure configurations with Linear Polarization: Configuration #3 is generated by setting $\alpha_0 = 180°$ and $\alpha_1 = 90°$ (as illustrated in the drawing). Configuration #4 is generated by setting $\alpha_0 = 0°$ and $\alpha_1 = 0°$ (the rotation scheme of the CSRR is illustrated in Fig. 3).

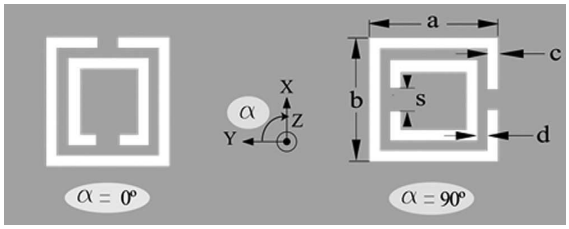

FIG. 3. Geometry, design parameters and particle rotation definition (α angle) of the rectangular CSRR part of the resonant chain.

resonant particle chain from the X0 position to the X1 position in the antenna patch. Fig. 3 shows the geometry and the relevant dimensions of the CSRR used as part of the CSRR chain printed in the rectangular patch. In the designs, rectangular CSRRs have been used instead of the well-known circular CSRR. In this way, the coupling between adjacent resonant particles in the CSRR chain is enhanced, boosting EIW phenomenon.

Table I shows the design parameters values for the different antenna configurations employed. In the design cases, CSRR particles dimensions in every antenna configuration are the same. The geometrical differences among antenna configurations are the X0, X1, and α parameters. Antenna configurations have been designed using Arlon Cuclad 250 LX with a thickness (h) of 0.49 mm and relative dielectric constant (ε_r) of 2.43, providing a good compromise in terms of radiation efficiency, loss reduction, and inhibition of propagation of higher order substrate modes within the device. The width of the microstrip line (W_i) corresponds to a characteristic impedance of 50Ω, in order to adequately match the antenna to the source generator.

Simulated reflection coefficient and the axial ratio for the different antenna configurations have been depicted in Fig. 4. Circularly polarized antenna configurations (#1 and #2) resonate at two frequencies, represented in Fig. 4(a) as R1 and R2, corresponding to the first and second resonant frequencies, respectively. R1 is the inherent resonant of the rectangular patch, while R2 is produced by the resonant chain composed by the complementary split ring resonators. Circular and linear polarizations are achieved at R2 and R1 resonant frequencies, respectively.

TABLE I. Antenna configurations and CSRR parameters dimensions.

Parameter	Dimensions (mm)	Parameter description
Length	17.0	See Figs. 1 and 2
Width	20.8	
Wi	1.4	
Tl	9.93	
Tw	0.34	
X0	7.8	
X1	2.5	
Y0	21.9	
Y1	28.0	
Y2	34.1	
a	4.6	See Fig. 3
b	4.2	
c	0.2	
d	0.2	
s	0.3	
α	Depending on antenna configuration	See Figs. 1 and 2

Observed field enhancement can be obtained by optimizing the initial radiating element design, in order to optimize device matching. For antenna configuration 1, the input impedance at R1 is characterised with a real part of 40 Ω and an imaginary part of 7 Ω, while at R2 it is characterised as a lower real part compared to R1 of 29 Ω and an imaginary part of 0 Ω. For antenna configuration #2, the input impedance at R1 is characterized with a real part of 46 Ω and an imaginary part of −15 Ω, while at R2 it is characterised as a lower real part compared to R1 of 13 Ω and an imaginary part of −12 Ω. Hence, in antenna configurations #1 and #2 at R2, at the minimum value of axial ratio (approximately 1.2 dB, see Fig. 4(b)), the real part of input impedance is much lower than the value of 50 Ω, which is the designed value of the characteristic impedance of the microstrip line. At simulation level for antenna configuration #2, an input matching network has been implemented in order to improve

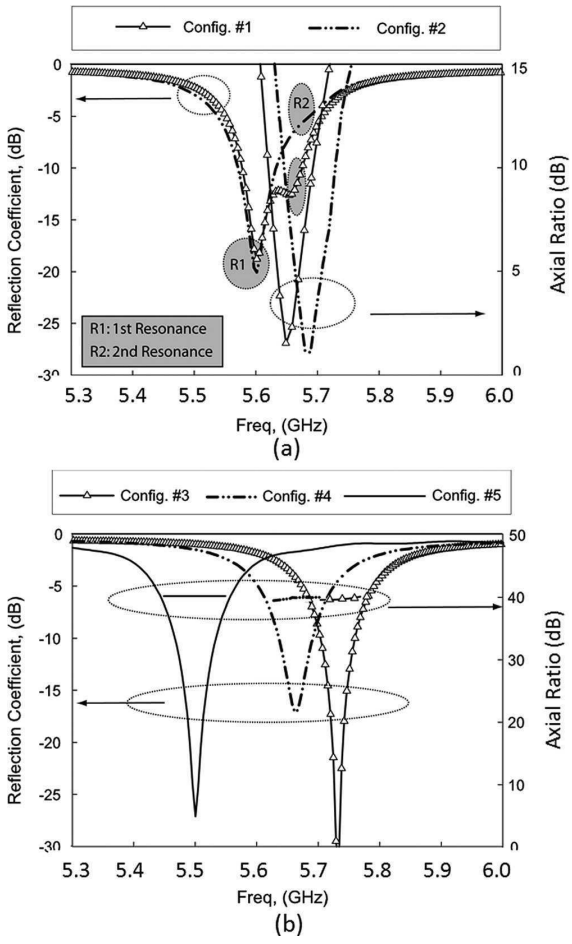

FIG. 4. (a) Simulated reflection coefficient and axial ratio for circular polarized antenna configurations: #1, #2; (b) Simulated reflection coefficient and axial ratio for linear polarized antenna configurations: #3, #4, and #5.

TABLE II. Designed configurations: Resonant frequency summary.

Antenna configurations	1st resonance, (GHz) linear polarization	2nd resonance, (GHz) circular polarization
#1	5.60	5.65
#2	5.60	5.68
#3	5.73	…
#4	5.66	…
#5	5.50	…

the reflection coefficient at R2 resonance. Simulated results show that a reflection coefficient lower than −20 dB at R2 for antenna configuration #2 is obtained with a $\lambda/4$ transformer and a short stub in parallel. Simulated results also show comparable axial ratio result to the one depicted in Fig. 4(a). In contrast to the two resonances exhibited in the reflection coefficient in antenna configurations #1 and #2, configurations #3 and #4 present a single resonance. The real part of the input impedance in these configurations is close to 50 Ω, while the imaginary part is nearby 0 Ω. It is worth noting that the R2 resonant frequency for configuration #1 lies in 5.65 GHz and #2 in 5.68 GHz, in close vicinity but exhibiting different resonant frequency values.

Comparing the resonant frequencies of antenna configurations #3 and #4 and R1 in antenna configurations #1 and #2 to the resonant frequency of a reference antenna (configuration #5), the resonant frequencies have been shifted towards higher frequencies (see Figs. 4(a) and 4(b)). This effect is produced by the loading of the rectangular patch with the CSRRs, as the CSRRs etched in the patch reduce

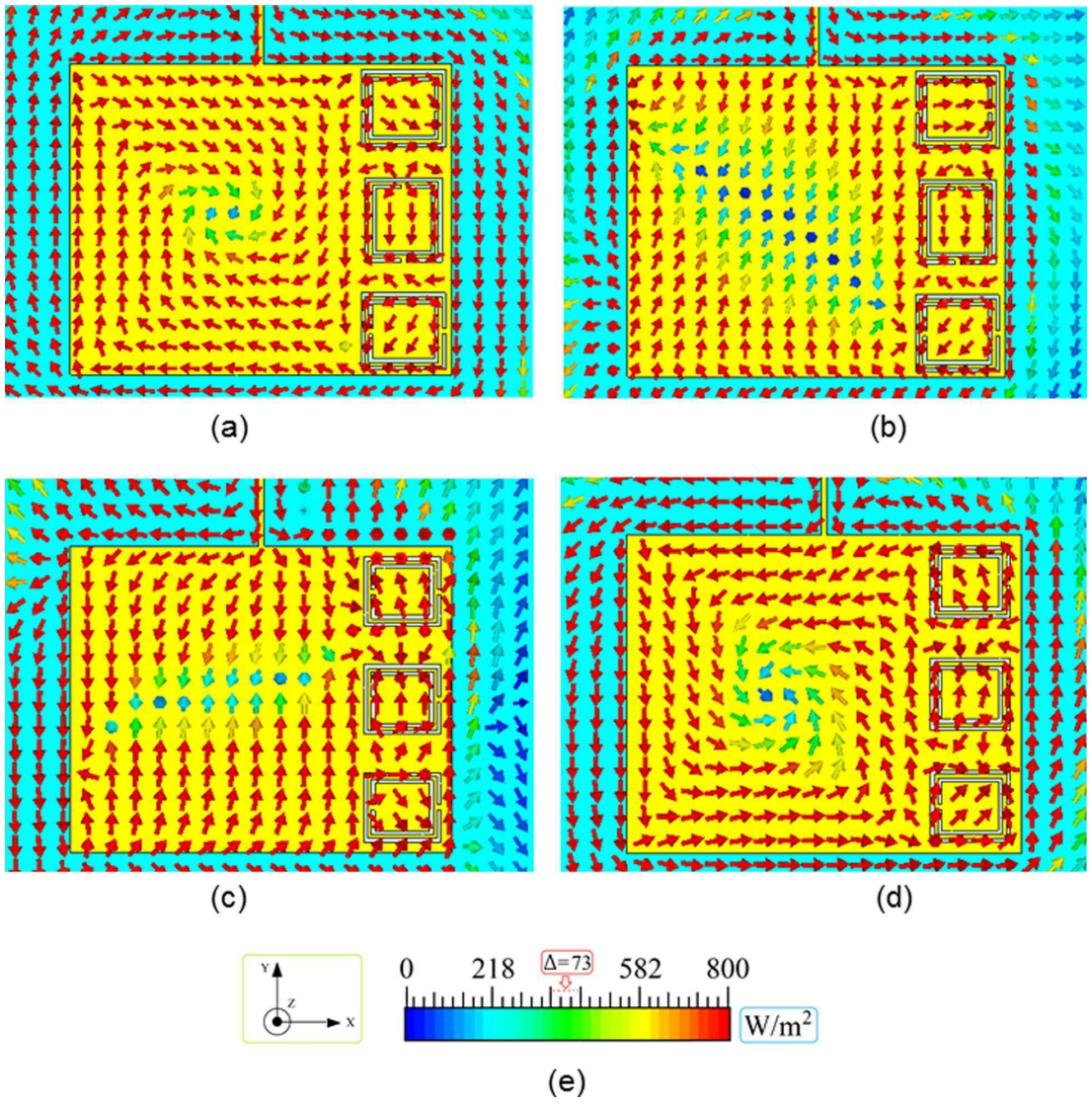

FIG. 5. Power flow (W/m^2—Linear scale) in XY plane at z = h (0.49 mm) for: (a) Configuration #1 at 1st resonance: 5.6 GHz, (b) Configuration #1 at 2nd resonance: 5.65 GHz, (c) Configuration #2 at 1st resonance: 5.6 GHz, (d) Configuration #2 at 2nd resonance: 5.68 GHz, (e) Reference coordinate system and common colour bar scale.

the electrical length of the rectangular patch. Table II summarizes the resonant frequencies corresponding to the cases depicted in Fig. 4.

A. Circular polarization demonstration

In order to demonstrate circular polarization generation, Poynting vector on every antenna configuration has been simulated with the aid of *CST microwave studio*™, providing a clear physical picture of the power flowing along the rectangular patch for all configurations under analysis. Figs. 5 and 6 show the simulated results of the directional energy flux in 2D plane at frequencies specified in Table II. Energy flux represents the Poynting vector.

Figs. 5(b) and 5(d) show how power flows in y-axis direction and it is transferred along the resonant chain, and how it is guided and rotated when the chain is placed close to one of the non-resonant slots of our reference antenna; hence, right or left handed circular polarization is generated; respectively, at the second resonance of antenna configurations #1 and #2. In contrast, in Figs. 5(a) and 5(c) at first resonance in antenna configurations #1 and #2, power is not transferred along the resonant chain in the same direction, and circular polarization is not generated. This last performance is also presented in linear polarized antenna configurations (#3, #4 and #5) shown in Fig. 6.

In order to gain insight on the effect of the inclusion of the CSRR chains within the radiating elements, Figs. 7(a) and 7(b) show electric field distribution at first and second resonant frequencies for antenna configuration #1; respectively. Fig. 7(a) shows a linear electric field distribution polarized in $\varphi = 135°$, which is along the diagonal line of the rectangular patch originated by the first CSRR in the resonant chain and the opposite side edge of the rectangular patch. Hence, in Fig. 7(a) the CSRRs are not sequentially excited. In contrast, Fig. 7(b) shows electric field propagation over phase along the CSRR

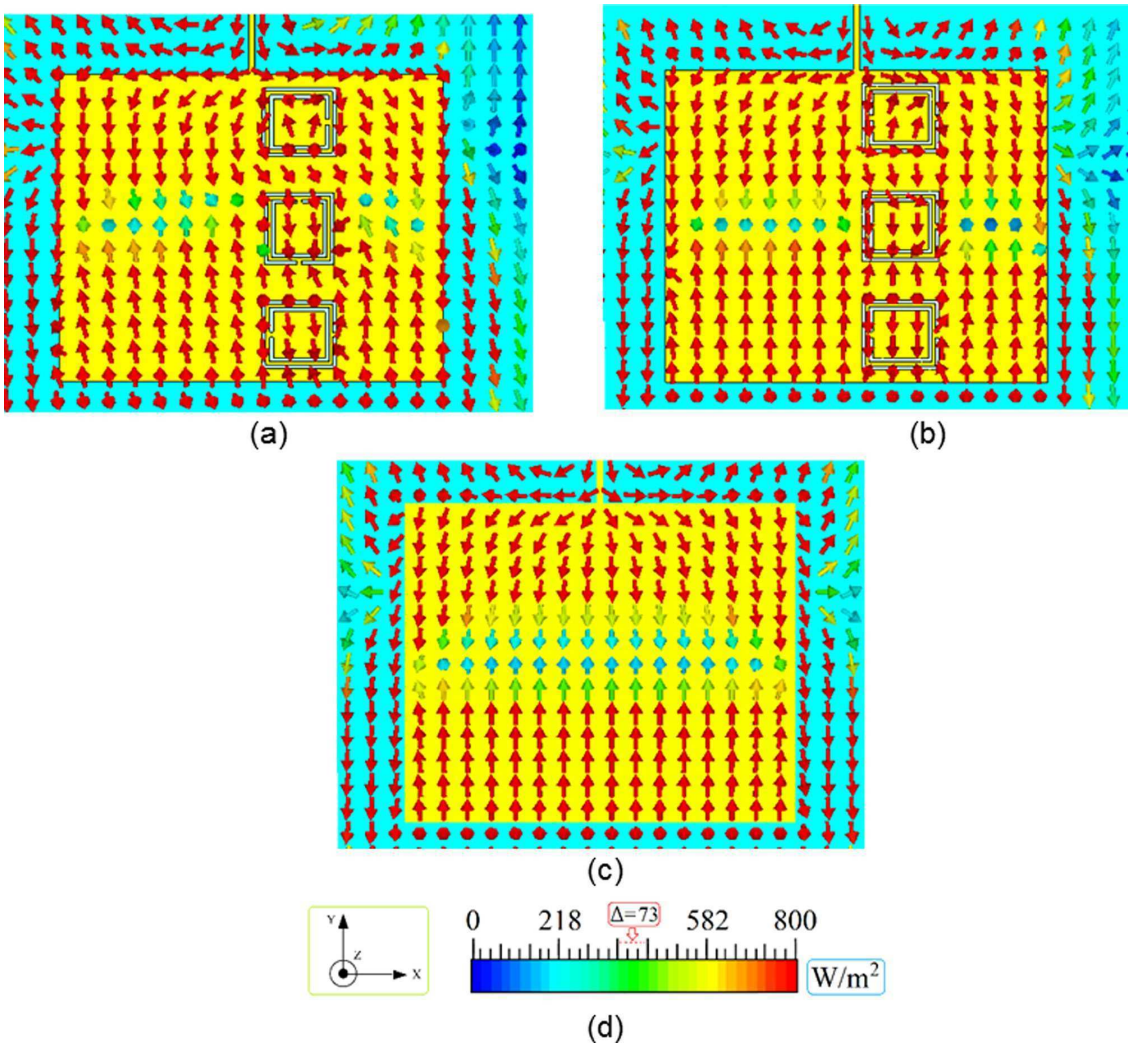

FIG. 6. Power flow (V·A/m^2–Linear scale) in XY plane at z = h (0.49 mm) for: (a) Configuration #3 at resonance frequency: 5.73 GHz, (b) Configuration #4 at resonance frequency 5.66 GHz, (c) Configuration #5 at resonance frequency: 5.5 GHz, (d) Reference coordinate system and common colour bar scale.

resonant chain. So, CSRRs are sequentially excited by an electro-inductive wave. As seen in Fig. 5, the difference between configuration #1 and #2 is the circular polarization orientation. Antenna configuration #1 shows clockwise orientation; while polarization orientation in configuration #2 is counterclockwise.

Figs. 8(a) and 8(b) show electric field distribution for antenna configurations #3 and #4. Both antenna configurations exhibit linear electric field distribution polarized in $\varphi = 0°$. As in Figs. 7(a), 8(a) and 8(b) show no energy transfer between adjacent resonant particles, and no electromagnetic wave propagation along the CSRR resonant chain.

In this section, polarization rotation has been demonstrated at the second resonance of antenna configurations #1 and #2. In these cases, power is guided by means of electro-inductive wave propagation along the CSRR resonant chain, due to inter-resonator coupling mainly given by E-field excitation (CSRR elements are bi-anisotropic, and hence, can also by excited by H-field components exhibiting lower frequency selective responses).

B. Circular polarization generation explanation

Circular polarization generation capability is explained by means of EIW propagation along the CSRR resonant chain, which can provide phase modifications as a function of induced current distribution, given by relative CSRR slot rotation. EIWs supported by chains of planar resonators as CSRRs were first theoretically and experimentally introduced in Ref. 37, where EIW phenomenon was employed to design a transducer delay line. In the case of the circular polarization generation, EIW wave introduces a phase delay of 90° in one of the polarized modes of the rectangular patch. EIW phenomenon explanation is mastered by two features. First, every CSRR shall be excited and second, energy shall be transferred from one CSRR to the other along the resonant chain. These two features are analysed here after.

1. CSRR excitation inside the resonant chain

Figs. 5 and 6 show that every CSRR that is part of the resonant chain is excited in every configuration. This fact is easily explained identifying the excitation fields that independently excite the CSRRs printed in our antenna configurations. It is noted that excitation fields of a single CSRR printed in a rectangular patch antenna have already been described.[28] In order to identify the excitation fields, let us review the equivalence between SRR and CSRR topologies shown in Fig. 9. Comparing the excitation of a SRR with a CSRR, the CSRR particle should be rotated 90° from the position of SRR particle, as it is shown in Fig. 9(a). As explained in Refs. 5 and 6, the operation of the SRR (and consequently CSRR operation) near its first resonance obeys to the effect of resonant polarizabilities. Generally, the excitation of CSRRs has been usually driven by an incident electric field normal to the particle plane, E_z^{inc}, giving an electric dipole p_z. However, due to the bianisotropy property of SRRs and CSRRs, CSRRs can also be excited by an incident magnetic field tangent by the particle plane perpendicular to

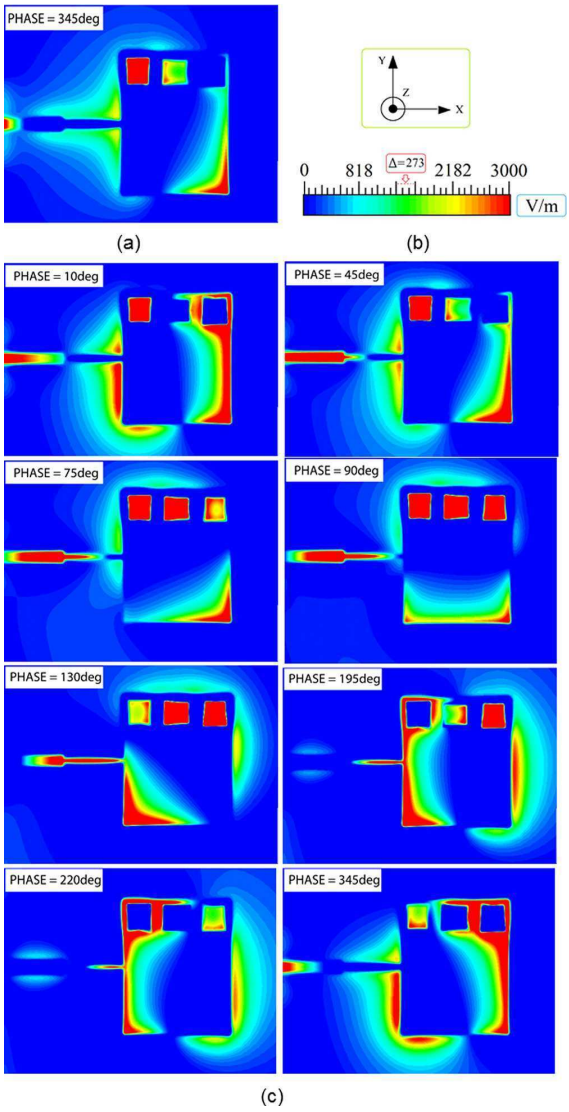

FIG. 7. Electric field distribution (V/m) in XY plane at z = h (0.49 mm) for antenna configuration #1: (a) First resonant frequency (5.60 GHz); (b) Reference coordinate system and common colour bar scale; (c) Second resonant frequency (5.65 GHz).

the slits (s parameter in Fig. 9(a)).[5,6] Following the coordinate system definition presented in Fig. 9(a), B_x is the incident magnetic field that can excite due to the bianisotropy property the CSRR particle, being able to produce the magnetic dipole, m_x.

In Fig. 9 the electric and magnetic fields presented in a conventional rectangular patch antenna and field components that can excite the CSRR particles located as in antenna configurations #1, #2, #3 and #4 are summarized. So, depending on the location and orientation of the CSRR particles in the rectangular patch antenna, each particle will be basically excited either by the electric field component normal to the particle plane E_z (for CSRRs with $\alpha = 0°$ and $\alpha = 180°$

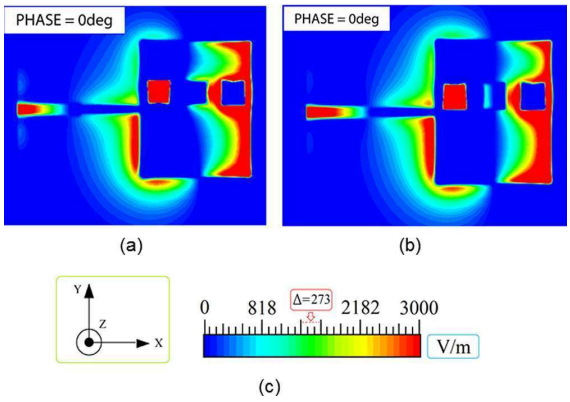

FIG. 8. Electric field distribution (V/m) in XY plane at z = h (0.49 mm) for: (a) Antenna configuration #3 at 5.73 GHz; (b) Antenna configuration #4 at 5.66 GHz; (c) Reference coordinate system and common colour bar scale.

orientations) or by the magnetic field component tangent to the particle plane B_x (for CSRR with $\alpha = 90°$ orientation).

In conclusion, every CSRR printed in our antenna configurations is independently excited, as a direct consequence of the electric and magnetic fields presented in a rectangular patch antenna and the CSRR particles position and orientation in the patch.

2. Energy transfer between CSRRs inside the resonant chain

Energy transfer between CSRRs inside the resonant chain is characteristic of EIWs. Energy is transferred due to the strong electric coupling between adjacent CSRRs in the resonant chain.

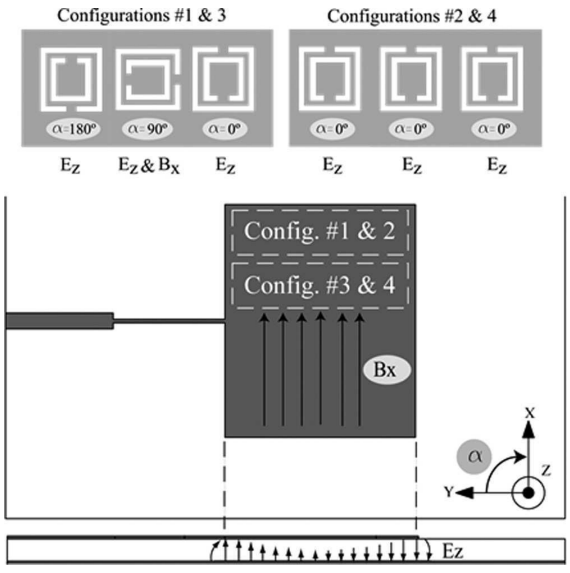

FIG. 9. Electric and magnetic fields in a rectangular patch antenna and CSRR excitation versus CSRR orientation and position in the antenna patch for antenna configurations.

The electric coupling has been already analyzed in previous work.[37] For theoretical explanation purposes of EIW, the CSRR unit cell equivalent circuit model was updated including the electric coupling between adjacent resonators in the chain.[37] This electric coupling is given by the capacitance C_M. In the same work, dispersion relation of electro-inductive waves in planar configuration was also computed including this electric coupling. In addition, several structures composed of different length of CSRRs were simulated; such as, a linear 1D array with 50 CSRR elements drilled in an infinite ground plane, where the first CSRR was excited by an electric monopole, and a transducer composed of a chain of 5 square complementary split ring resonators. The simulation results for both structures clearly showed that the electric energy was trapped in the vicinity of the resonant particles being negligible out of them. The dispersion relation of the EIWs in planar configuration without considering losses can be written as[37]

$$\frac{\omega^2}{{\omega_0}^2} \approx 1 + \frac{2C_M}{C_c}\cos(ka), \tag{1}$$

where ω is the angular frequency, k is the propagation constant, a is the CSRR centre-to-centre separation between CSRRs, C_c is the total capacitance (which includes the mutual coupling between the adjacent resonant particles and the capacitance between the CSRR and the ground plane), and ω_0^2 can be written as[36] where L_c is CSRR total inductance

$${\omega_0}^2 = \frac{1}{C_c L_c}. \tag{2}$$

As previously described,[32] in this paper, energy transfer is also explained by demonstrating the existence of electric coupling between adjacent CSRRs. In this paper, the existence of electric coupling between CSRRs is demonstrated by computing the electric field x, y, and z components amplitude at different locations in the antenna patch for antenna configurations #1 and #3 and by comparing the electric field x, y, and z components amplitude with the ones of the reference antenna (configuration #5). The computation of the electric field x, y, and z components in the patch antenna has been carried out with the aid of *CST microwave studio*™, computing the magnitude and phase of the electric field probes that have been inserted in the antenna patch of different antenna configurations. Fig. 10 shows the position of the electric field probes that have been inserted in the patch. Fig. 11 shows electric field component magnitude in dB computed from the electric field probes for antenna configurations #1 (at F1 and F2 resonant frequencies), #3 and #5.

Fig. 11 shows magnitude variation of x, y, and z electric field components in the antenna patch for antenna configurations #1 (F1 and F2 resonant frequencies) and #3 compared to the reference antenna (configuration #5). Based on the expressions (4) and (5), the electric field variation shown in Fig. 11 generates an electric coupling variation in the CSRRs and between adjacent CSRRs for x, y, and z electric field components, due to the slots geometry that compose the resonant particles printed on the patch.

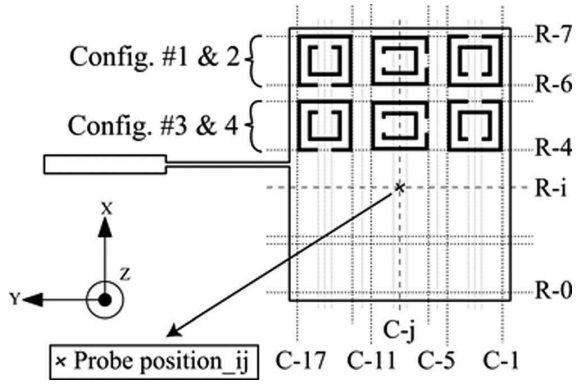

FIG. 10. Electric field probes position in antenna configurations. Field probe position in z axis corresponds to z = h/2. In total 152 probes have been set for each configuration (8 rows × 19 columns). Probes have been set at the intersection of R-i and C-j lines. In the region of the CSRRs, the probes lie on the edge of the slots of the resonant particles. Probes positions in x-axis are represented by (R7-R6) rows in antenna configuration #1 and (R5-R4) in antenna configuration #3; while (C1–C5) columns represent the probes in y-axis for the first CSRR, (C7–C11) for the second CSRR and (C13–C17) for the third CSRR.

In the case of the E_x magnitude component, the electric field magnitude increases in the area where the CSRRs are located (shadowed areas in Fig. 11), as the slots within the CSRRs are present and the distance between these slots decreases in x direction, (see c parameter in Fig. 3 and Table I dimensions). Hence, in order to keep constant the given potential difference, the electric field magnitude increases. E_x magnitude increase is comparable in the cases of first resonance of antenna configuration #1 and antenna configuration #3. In these cases, where linear polarization is obtained, electric field magnitude is maximum in the first and third CSRRs and lower in the second CSRR. In contrast, in the case of the second resonant frequency of antenna configuration #1 where circular polarization is achieved, the electric field magnitude increases progressively from the first to the third resonant particles.

In Fig. 11, the E_y magnitude component also shows electric field magnitude variations in the regions where the CSRRs are printed in the antenna patch (shadowed areas in Fig. 11) comparing to the reference antenna. The E_y Magnitude component shows a decrease in the centre of

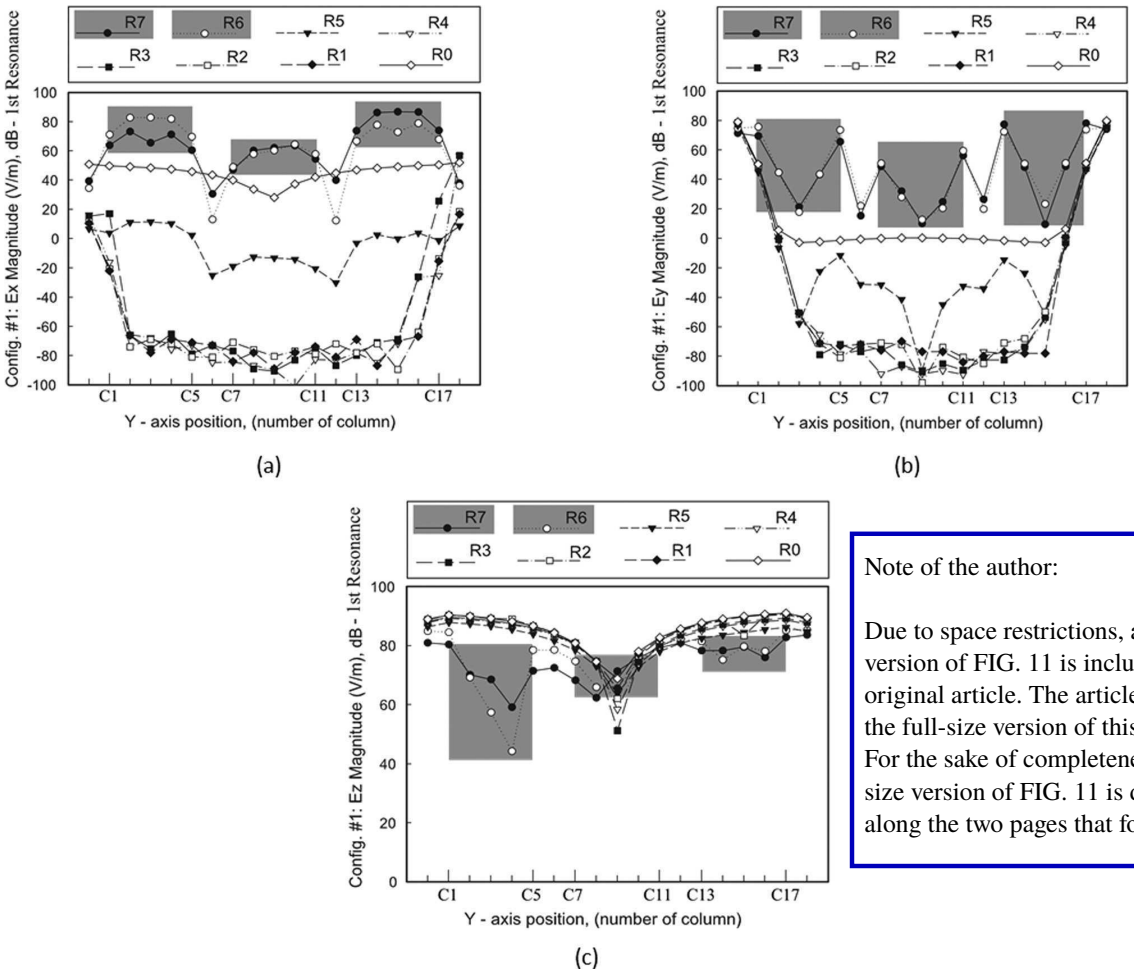

Note of the author:

Due to space restrictions, a reduced version of FIG. 11 is included in the original article. The article describes the full-size version of this figure. For the sake of completeness, the full-size version of FIG. 11 is displayed along the two pages that follow.

FIG. 11. E_x, E_y, and E_z field magnitude in dB for: Config. #1 at F1 = 5.60 GHz.

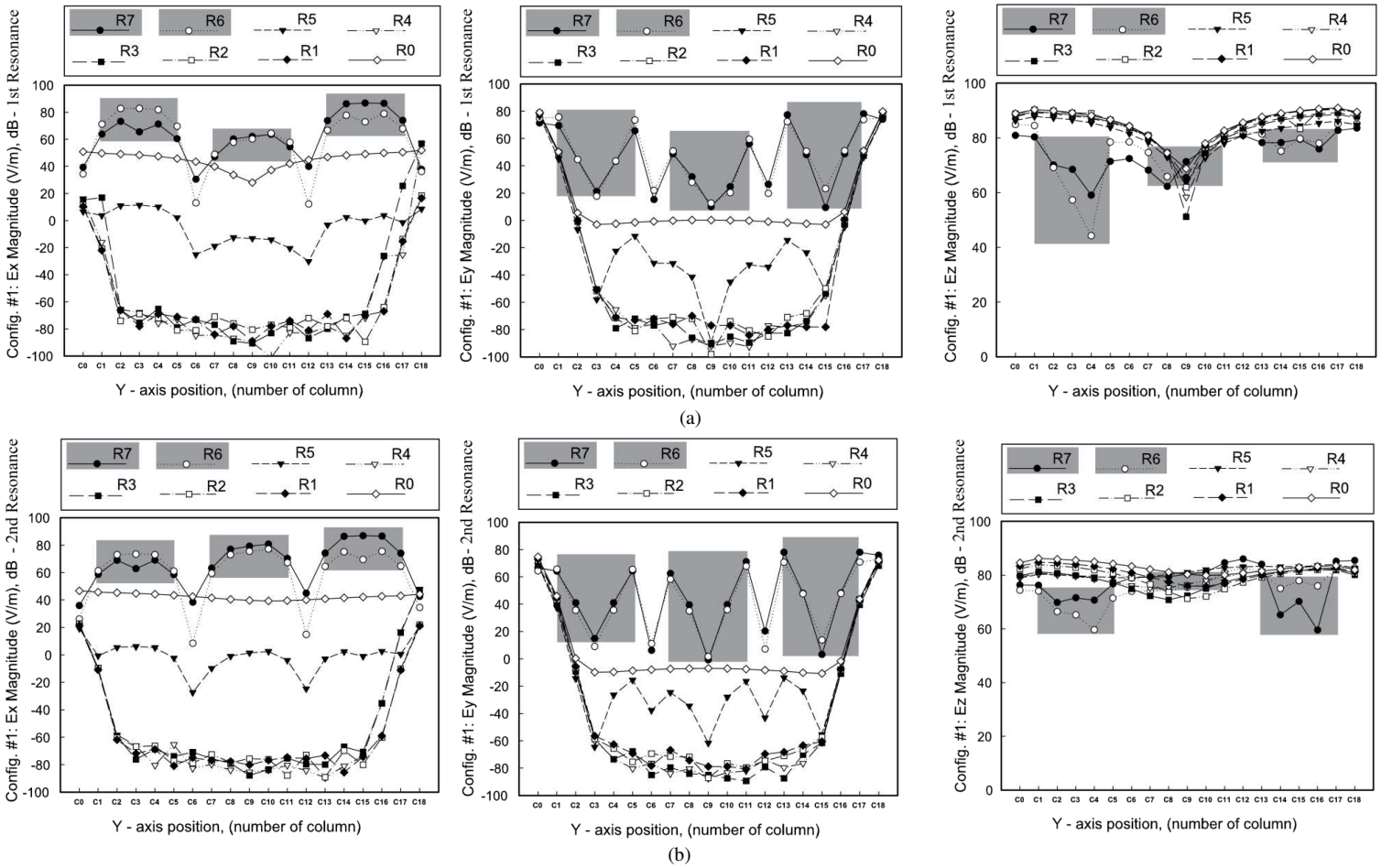

FIG. 11. Ex, Ey, and Ez field magnitude in dB for: (a) Config. #1 at F1=5.60 GHz; (b) Config.#1 at F2=5.65GHz; (CONTD.)

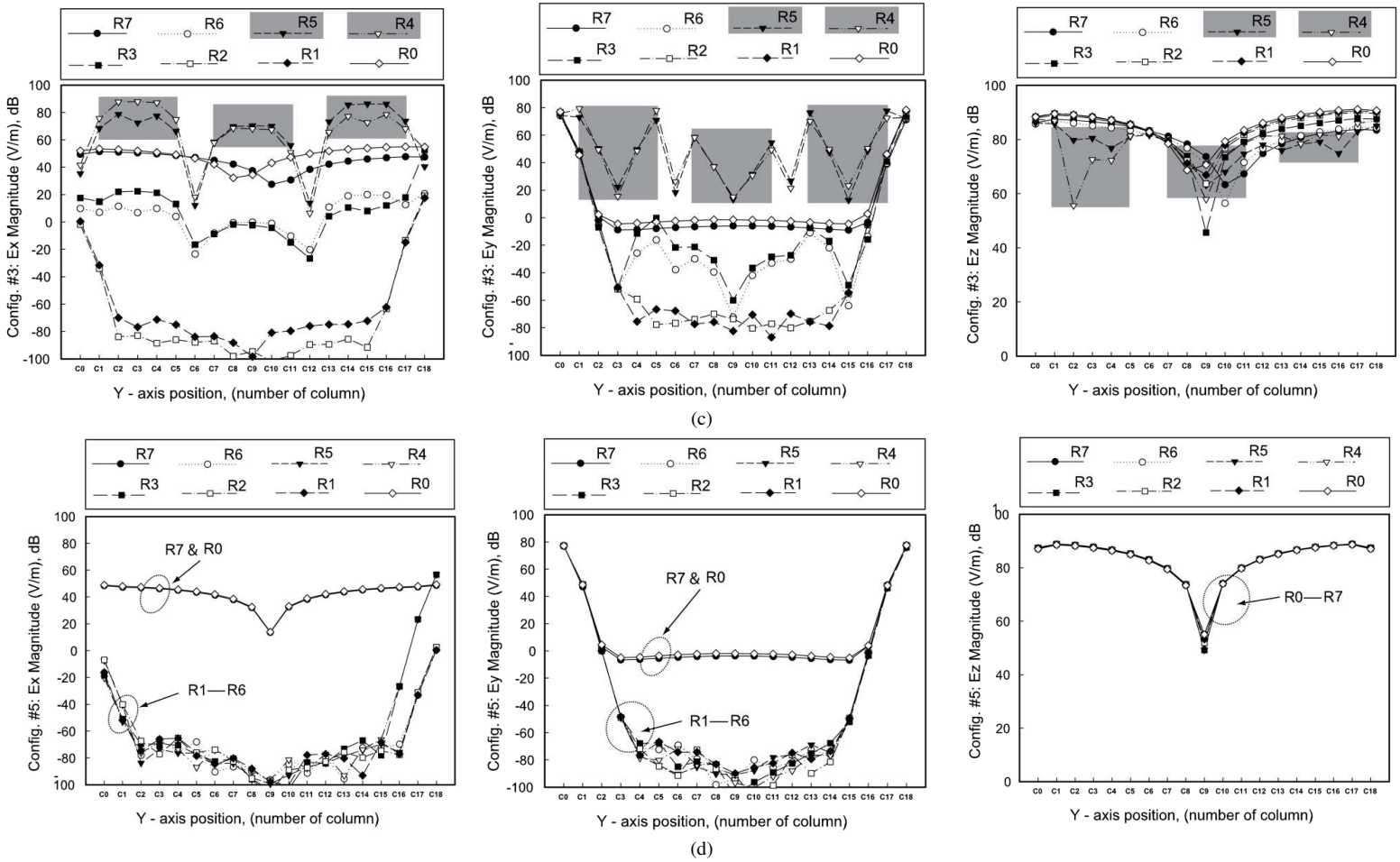

FIG. 11. Ex, Ey, and Ez field magnitude in dB for: (c) Config.#3 at 5.73GHz; (d) Config.#5 at 5.50GHz.

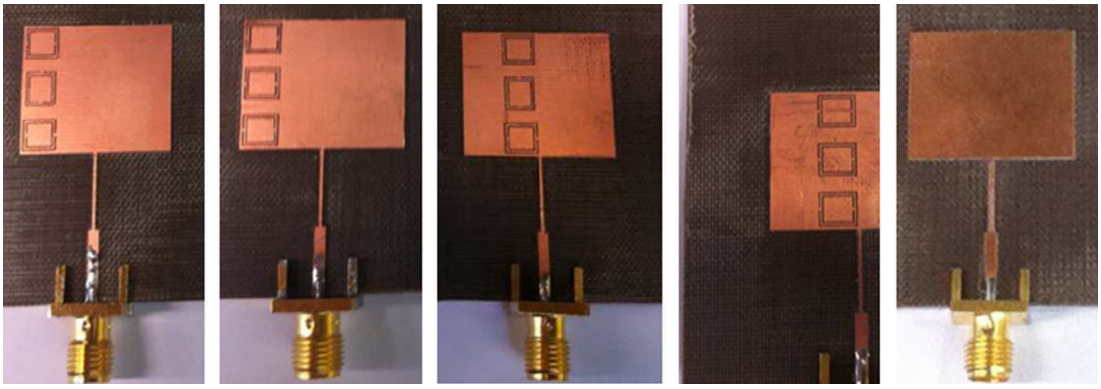

FIG. 12. Prototype pictures, from left to right Antenna configurations #1, #2, #3, #4, and #5.

each CSRR, as at this position the distance to the closest slot within the complementary split ring resonators in y direction increases, the electric field magnitude decreases for the given potential difference. In the case of circular polarization that corresponds to the second resonant frequency of antenna configuration #1, the E_y magnitude variation in the CSRRs increases progressively from the first to the third CSRR, while in the case of linear polarization (first resonance of antenna configuration #1 and antenna configuration #3), the E_y magnitude variation is minimum in the second CSRR compared to first and third CSRRs. Hence, for linear polarization a symmetrical performance of electric field magnitude from the centre of the patch in y direction is observed. In contrast, the progressive increase of the E_y magnitude variation predicts the capacitance variation, and hence, the EIW propagation and the energy transferred in y direction.

E_z magnitude component depicted in Fig. 11. shows a minimum in the electric field magnitude in the centre of the patch for the cases of linear polarizations for rows R0 to R7. This behaviour follows the theoretical value of E_z magnitude distribution of linear polarized patch antennas.[37] In contrast, in the case of circular polarization the E_z magnitude for rows Ro to R7 does not exhibit a minimum in the magnitude field distribution along the column C9 (column that defines the centre of the patch in y direction).

III. EXPERIMENTAL WORK

Polarization rotation phenomenon validation has been carried out by means of the antenna configuration prototypes presented in Figs. 1 and 2. Fig. 12 shows the pictures of fabricated antenna prototypes, which have been designed and fabricated in Arlon Cuclad 250 LX of 0.49 mm thickness.

The design parameters of fabricated prototypes are specified in Table I. Fig. 13 shows the simulated and measured reflection coefficient (for design parameters in Table I). Reflection coefficient measurements have been performed using Agilent 8722 vector network analyzer. Fig. 13 shows the frequency deviation between simulated and measured prototypes in configurations #1, #2, #3 and #4. Table III quantifies and summarizes the frequency deviation and reflection coefficient values at the resonant frequencies between the simulated and measured data from Fig. 13. For antenna configurations #1 and #2, the frequency deviation of

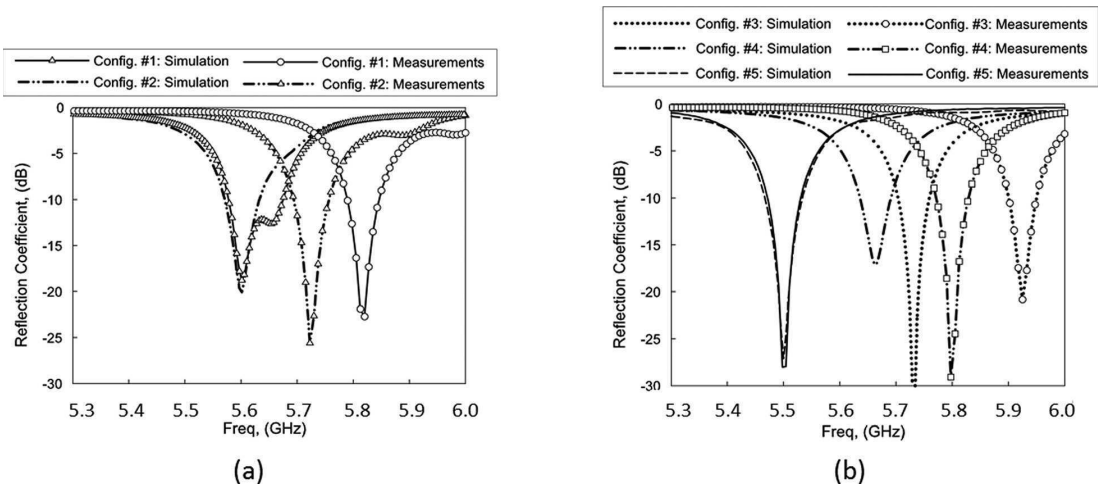

FIG. 13. Simulated and measured reflection coefficient: (a) Configurations #1 and #2; (b) Configurations #3, #4, and #5.

TABLE III. Resonant frequency/reflection coefficient frequency deviation.

Antenna conf.	1st resonance, (GHz)/(dB) Linear polarization	2nd resonance (GHz)/(dB) Circular polarization
#1	Simulated: **5.60**/−18.5	Simulated: **5.65**/−12.6
	Measured: **5.82**/−23.5	Measured: **5.98**/−3.4
	Deviation: +0.22	**Deviation: +0.33**
#2	Simulated: **5.60**/−15.7	Simulated: **5.68**/−5
	Measured: **5.72**/−25.6	Measured: **5.88**/−4.3
	Deviation: +0.12	**Deviation: +0.20**
#3	Simulated: **5.73**/−30.2	…
	Measured: **5.92**/−20.8	
	Deviation: +0.20	
#4	Simulated: **5.66**/−17.8	…
	Measured: **5.79**/−29.4	
	Deviation: +0.13	
#5	Simulated: 5.50/−28.1	…
	Measured: **5.50**/−28.4	
	No deviation	

TABLE IV. Tuned designed parameters.

Parameter	Antenna conf. #1	Antenna conf. #2	Antenna conf. #3	Antenna conf. #4
Length	16.92	16.80	16.92	16.95
Width		20.81		
Wi		1.40		
Tl		9.93		
Tw		0.34		
X0	7.9	7.7	…	…
X1	…	…	2.6	2.4
Y0	22.0	22.1	22.0	22.1
Y1	28.0	28.0	28.0	28.0
Y2	34.0	33.9	34.0	33.9
a	4.0	4.2	4.0	4.2
b	3.8	3.8	3.8	3.8
c		0.2		
d		0.2		
s		0.3		
α		See Figs. 1 and 2		

the second resonance is higher than that of first resonance. So, at second resonance the reflection coefficient exhibits mismatching (measured reflection coefficient at second resonance is around −3 dB). Frequency deviation between simulated and measured data is due to manufacturing tolerances of the milling machine. These prototypes have been fabricated using a mechanical milling machine with tolerances around +/−200microns. In particular, CSRRs are strong resonant particles, so that their frequency response is sensitive to manufacturing tolerances.

In spite of the fact that antenna configurations #1, #2, #3 and #4 resonant frequencies have been shifted towards higher frequencies, radiation characteristics of the manufactured prototypes still exhibit the predicted simulated performance: circular polarization at the second resonant frequency in configurations #1 and #2 and linear polarization in the rest of resonant frequencies for different configurations. Thus, manufactured prototypes demonstrate the aimed polarization rotation phenomenon. It is remarkable to say, that the objective of this paper is to validate polarization rotation capability based on EIW phenomenon, and not to present an optimized antenna.

A. Antenna configurations design parameters tuning

In order to provide a fair comparison between simulated and measured data for reflection coefficient and radiation characteristics, the design parameters depicted in Figs. 1 and 2 have been tuned in each antenna configuration in order to obtain comparable reflection coefficient performance to that of the measured data. Table IV shows tuned values of design parameters. Only the parameters related to the position and dimensions of CSRRs have been tuned. These parameters are: *Length, X0, X1, Y0, Y2*, *a* and *b*. Tuned values exhibit good agreement between the simulated and measured data. Fig. 14 shows the reflection coefficient for antenna configurations #1, #2, #3 and #4 (according to tuned parameters

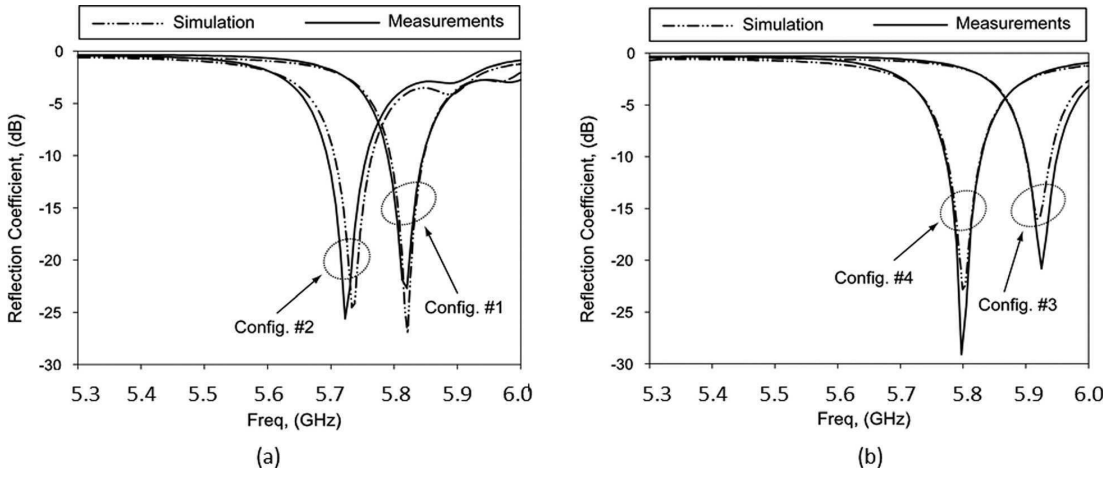

FIG. 14. Simulated and Measured Reflection coefficient: (a) Configurations #1 and #2; (b) Configurations #3 and #4.

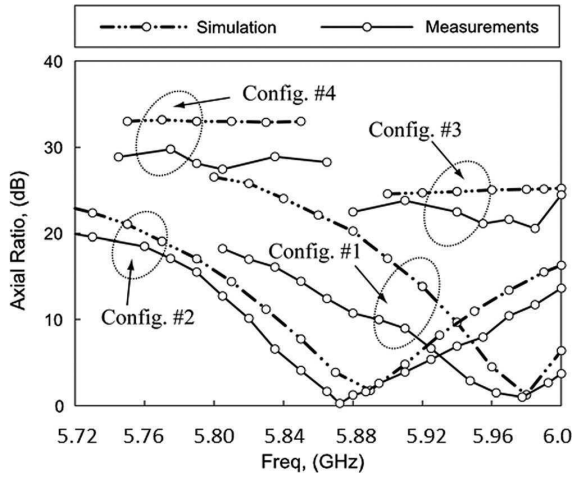

FIG. 15. Simulated (for tuned parameters in Table IV) and Measured Axial Ratio for antenna configurations #1, #2, #3, and #4.

depicted in Table IV). For summarizing and simplicity purposes, from now on, antenna configuration #5 measured data is not shown.

Antenna configurations #1, #2, #3, #4 have been measured in an anechoic chamber. Measurements have been performed using linear polarized horn antennas as reference antennas. Hence, E and H planes measurements are shown for linear and circular polarizations. For simplicity purposes, measured data of antenna configuration #5 is not shown. Fig. 15 shows simulated (data from Table IV tuned parameters simulations) and measured realized gain radiation patterns at measured frequencies depicted in Table IV. Both simulated and measured realized gain peak values and the radiation pattern performance show good agreement between the simulated and measured data. Table V shows an overview of E-plane simulated and measured realized gain and gain peak values and radiation efficiency. Gain difference between F1 and F2 in antenna configurations #1 and #2 is around 3 dB.

TABLE V. Radiation performances overview.

Antenna configuration	Gain peak, (dB): simulated measured	Realized gain peak, (dB): simulated measured	Radiation efficiency, (%): simulated measured
#1 @ F1	6.1	6.1	
(5.82 GHz)	**5.6**	**5.6**	
#1 @ F2	2.7	−0.6	
(5.98 GHz)	**2.2**	**−0.9**	
#2 @ F1	6.3	5.9	
(5.72 GHz)	**6.2**	**6.2**	
#2 @ F2	3.1	0.6	
(5.88 GHz)	**2.9**	**−0.1**	
#3 @ F1	**6.3**	**5.9**	70.9
(5.92 GHz)	**6.5**	**6.4**	**74.3**
#4 @ F1	6.3	5.9	70.6
(5.79 GHz)	**5.4**	**5.4**	**57.4**
#5 @ F1	6.4	6.4	71.8
(5.5GHz)	**6.3**	**6.3**	**70.2**

This difference is due to the fact that circular polarization has been measured with linear polarized antennas. Hence, comparable gain performances are obtained for linearly and circularly and polarized frequency bandwidths.

Fig. 15 show simulated and measured data of axial ratio over frequency for different antenna configurations. Axial ratio bandwidth values lower than 3 dB is 0.42% and 0.51% in simulation and 0.92% and 0.81% in measurements for antenna configurations #1 and #2; respectively. These results show that circular polarization radiation performance is retained in a comparable axial ratio bandwidth to that of state of the art edge truncated circular polarized microstrip patch antennas.[38]

Further improvement could be achieved by providing frequency tuning mechanisms, similar to those previously applied in individual resonators or in distributions, such as metasurfaces, in which tenability can be provided by means of inclusion of elements such as PIN or varactor diodes or the use of photoconductive materials embedded within the initial circuit. In the case of patch antennas loaded with CSRR chains, tenability could be achieved, for example, with the inclusion of varactor diodes within the CSRR gaps, in order to actively modify CSRR capacitance, and hence, resonant frequency and overall frequency response.

IV. CONCLUSION

This work demonstrates a practical application of the EIW propagation phenomenon. Thanks to EIW propagation along a chain composed of CSRRs printed on a rectangular patch of a patch antenna, circular polarization is generated. Antenna prototypes have been fabricated by means of conventional milling techniques, showing good agreement between simulation and measurement results, considering the effect of fabrication tolerances in initial frequency shifts. The proposed design, which combines coupled CSRR elements in a conventional microstrip patch provides a simple, low cost alternative in order to provide polarization modification properties for multiple antenna communication systems. The coupling of EIW in order to provide polarization rotation capabilities can be extended in order to demonstrate the phenomena in different configuration, such as in guided wave structures, or with enhanced capabilities provided by the inclusion of active elements in order to achieve certain level of tunability in the frequency selective or phase response of the implemented devices.

ACKNOWLEDGMENTS

The authors wish to acknowledge the financial support of Project No. TEC2013-45585-C2-1-R, funded by the Spanish Ministry of Economy and Competiveness.

OBITUARY: Dr. Mario Sorolla Ayza.

[1]F. Falcone, T. Lopetegi, M. A. G. Laso, J. D. Baena, J. Bonache, M. Beruete, R. Marqués, F. Martin, and M. Sorolla, "Babinet principle applied to metasurface and metamaterial design," Phys. Rev. Lett. **93**(12), 197401 (2004).

[2]J. B. Pendry, A. J. Holden, D. J. Robbins, and W. J. Stewart, "Magnetism from conductors and enhanced nonlinear phenomena," IEEE Trans. Microwave Theory Tech. **47**(11), 2075–2084 (1999).

[3]D. R. Smith, W. J. Padilla, D. C. Vier, S. C. Nemat-Nasser, and S. Schultz, "Composite medium with simultaneously negative permeability and permittivity," Phys. Rev. Lett. **84**, 4184–4187 (2000).

[4]R. Marqués, F. Martin, and M. Sorolla, *Metamaterials With Negative Parameters: Theory, Design and Microwave Applications* (John Wiley and Sons, New York, 2008).

[5]R. Marqués, F. Mesa, J. Martel, and F. Medina, "Comparative analysis of edge and broadside coupled split ring resonators for metamaterial design. Theory and Experiment," IEEE Trans. Antennas Propag. **51**, 2572–2581 (2003).

[6]R. Marqués, F. Medina, and R. Rafii-El-Idrissi, "Role of bianisotropy in negative permeability and left-handed metamaterials," Phys. Rev. B: Condens. Matter **65**, 144440 (2002).

[7]F. Martin, F. Falcone, J. Bonache, T. Lopetegi, R. Marqués, and M. Sorolla, "Miniaturized coplanar waveguide stopband filters based on multiple tuned split ring resonators," IEEE Microwave Wireless Compon. Lett. **13**(12), 511–513 (2003).

[8]J. Bonache, I. Gil, J. Garcia, and F. Martin, "Complementary split ring resonators for microstrip diplexer design," Electron. Lett. **41**(14), 810–811 (2005).

[9]J. García-García, F. Martin, E. Amat, F. Falcone, J. Bonache, A. Marcotegui, M. Sorolla, and R. Marqués, "Microwave filters with improved stop band based on sub-wavelength resonators," IEEE Trans. Microwave Theory Tech. **53**, 1997–2006 (2005).

[10]S. S. Karthikeyan and R. S. Kshetrimayum, "Harmonic suppression of parallel coupled microstrip line bandpass filter using CSRR," Prog. Electromagn. Res. Lett. **7**, 193–201 (2009).

[11]M. Keshvari and M. Tayarani, "A novel miniaturized bandpass filter based on complementary split ring resonators (CSRR) and open-loop resonators," Prog. Electromagn. Res. Let. **23**, 165–172 (2011).

[12]J. Niu and X. Zhou, "A novel dual-band branch line coupler based on strip-shaped complementary split ring resonators," Microwave Opt. Technol. Lett. **49**(11), 2859–2862 (2007).

[13]E. Jarauta, M. A. G. Laso, T. Lopetegi, F. Falcone, M. Beruete, J. D. Baena, J. Bonache, I. Gil, J. García-García, J. A. Marcotegui, F. Martin, R. Marqués, and M. Sorolla, "Novel microstrip backward coupler with metamaterial cells for fully planar fabrication techniques," Microwave Opt. Technol. Lett. **48**(7), 1205–1209 (2006).

[14]M. Beruete, R. Marqués, J. D. Baena, and M. Sorolla, "Resonance and cross-polarization effects in conventional and complementary split ring resonators periodic screens," in Proceedings of the IEEE Antennas and Propagation Society International Symposium (2005).

[15]M. Navarro-Cía, F. Falcone, M. Beruete, I. Arnedo, J. Illescas, J. A. Marcotegui, M. A. G. Laso, and T. Lopetegi, "Left-handed behaviour in a microstrip line loaded with squared split-ring resonators and an EBG pattern," Microwave Opt. Technol. Lett. **49**(11), 2689–2692 (2007).

[16]Y. Lee, S. Tse, Y. Hao, and C. G. Parini, "A compact microstrip antenna with improved bandwidth using complementary split-ring resonator (CSRR) loading," in Proceedings of the IEEE Antennas and Propagation International Symposium (2007), pp. 5431–5434.

[17]M. S. Sharawi, M. U. Khan, A. B. Numan, and D. N. Aloi, "A CSRR loaded MIMO antenna system for ISM band operation," IEEE Trans. Antennas Propag. **61**(8), 4265–4274 (2013).

[18]J. Liu, S. gong, Y. Xu, X. Zhang, C. Feng, and N. Qi, "Compact printed ultra-wideband monopole antenna with dual band-notched characteristics," Electron. Lett. **44**(12), 710–711 (2008).

[19]Y. Dong and T. Itoh, "Miniaturized patch antenna loaded with complementary split-ring resonators and reactive impedance surface," in Proceedings of the European Conference on Antennas and Propagation (EUCAP) (Rome, 2011).

[20]Y. Dong, H. Toyao, and T. Itoh, "Design and characterization of miniaturized patch antennas loaded with complementary split-ring resonators," IEEE Trans. Antennas Propag. **60**(2), 772–785 (2012).

[21]J. J. Ma, X. Y. Cao, and T. Liu, "Design the size reduction patch antenna based on complementary split ring resonators," in Proceedings of International Conference on Microwave and Millimeter Wave Technology (ICMMT), May 2010, pp. 401–402.

[22]R. T. Prashant, R. M. Vani, and P. V. Hunagund, "Design of microstrip patch antenna using complementary split ring resonator loaded ground plane for size reduction," Int. J. Adv. Res. Electr. Electron. Instrum. Eng. **3**(3), 7932–7937 (2014).

[23]N. Ortiz, F. Falcone, and M. Sorolla, "Dual band patch antenna based on complementary rectangular split-ring resonators," in Proceedings of the Asia-Pacific Microwave Conference (APMC) (Singapore, 2009), pp. 2762–2765.

[24]Y. Xie, L. Li, C. Zhu, and C. Liang, "A novel dual-band patch antenna with complementary split ring resonators embedded in the ground plane," Prog. Electromagn. Res. Lett. **25**, 117–126 (2011).

[25]D. Sarkar, K. Saurav, and K. Srivastava, "Design of a novel dual-band microstrip patch antenna for WLAN/WIMAX applications using complementary split ring resonators and partially defected ground structure," Progress in Electromagnetics Research Symposium Proceedings, Taipei, March 25–28, 2013, pp. 821–825.

[26]Y. Sidana, R. K. Chaudhary, and K. V. Srivastava, "Novel dual band hexagonal patch antenna coupled with complementary split ring resonator," in Proceedings of the Asia-Pacific Microwave Conference (APMC) (December, 2012), pp. 4–7.

[27]V. Rajeshkumar and S. Raghavan, "A compact CSRR loaded dual band microstrip patch antenna for wireless applications," in Proceedings of the IEEE International Conference on Computational Intelligence and Computing Research (ICCIC) (December, 2013), pp. 26–28.

[28]N. Ortiz, F. Falcone, and M. Sorolla, "Gain improvement of dual band antenna based on complementary split-ring resonator," ISRN Commun. Networking **2012**, 951290 (2012).

[29]H. Zhang, Y. Q. Li, X. Chen, Y. Q. Fu, and N. C. Yuan, "Design of circular polarization microstrip patch antennas with complementary split ring resonators," IET Microwave Antennas Propag. **3**(8), 1186–1190 (2009).

[30]H. Zhang, Y. Q. Li, X. Chen, Y. Q. Fu, and N. C. Yuan, "Design of circular/dual-frequency linear polarization antennas based on the, anisotropic complementary split ring resonator," IEEE Trans. Antennas Propag. **57**, 3352–3355 (2009).

[31]M. J. Lee, Y. Sung, S. H. Kim, and Y. S. Kim, "Polarization reconfigurable microstrip patch antenna with complementary split ring resonator (CSRR)," in Proceedings of the Asia Pacific Microwave Conference (APMC) (2012).

[32]F. Qin, L. Ding, L. Zhang, F. Monticone, C. C. Chum, J. Deng, S. Mei, Y. Li, J. Teng, M. Hong, S. Zhang, A. Alù, and C.-W. Qiu, "Hybrid bilayer plasmonic metasurface efficiently manipulates visible light," Sci. Adv. **2**, e1501168 (2016).

[33]J. D. Baena, J. P. del Risco, A. Slobozhanyuk, and S. B. Glybovski, "Self-complementary metasurfaces for linear-to-circular polarization conversion," Phys. Rev. B **92**, 245413 (2015).

[34]P. Kapitanova, A. P. Slobozhnanyuk, I. V. Shadrivov, and P. A. Belov, "Competing nonlinearities with metamaterials," Appl. Phys. Lett. **101**, 231904 (2012).

[35]A. D. Boardman *et al.*, "Active and tunable metamaterials," Laser Photonics Rev. **5**(2), 287–307 (2011).

[36]A. P. Slobozhanyuk *et al.*, "Nonlinear interaction of meta-atoms through optical coupling," Appl. Phys. Lett. **104**, 014104 (2014).

[37]M. Beruete, F. Falcone, M. J. Freire, R. Marqués, and J. D. Baena, "Electroinductive waves in chains of complementary metamaterial elements," Appl. Phys. Lett. **88**(8), 083503 (2006).

[38]E. Shamonina, V. A. Kalinin, K. H. Ringhofer, and L. Solymar, "Magneto-inductive waveguide," Electron. Lett. **38**, 371–372 (2002).

[39]E. Shamonina, V. A. Kalinin, K. H. Ringhofer, and L. Solymar, "Magnetoinductive waves in one, two, and three dimensions," J. Appl. Phys. **92**, 6252–6261 (2002).

[40]R. R. A. Syms, E. Shamonina, V. Kalinin, and L. Solymar, "A theory of metamaterials based on periodically loaded transmission lines: Interaction between magnetoinductive and electromagnetic waves," J. Appl. Phys. **97**, 064909 (2005).

[41]M. Navarro-Cía, M. Beruete, S. Agrafiotis, F. Falcone, M. Sorolla, and S. A. Maier, "Broadband spoof plasmons and subwavelength electromagnetic energy confinement on ultrathin metafilms," Opt. Express **17**(20), 18184–18195 (2009).

[42]J. D. Baena, J. Bonache, F. Martin, R. Marqués, F. Falcone, T. Lopetegi, M. A. G. Laso, J. García, I. Gil, M. Flores, and M. Sorolla, "Equivalent circuit models for split ring resonators and complementary split ring resonators coupled to planar transmission lines," IEEE Trans. Microwave Theory Technol. **53**(4), 1451–1461 (2005).

[43]C. A. Balanis, *Microstrip Antennas in Antenna Theory Analysis and Design*, 3rd ed. (Wiley, 2005), pp. 811–843.

[44]K. L. Wong, *Compact and Broadband Microstrip Antennas* (John Wiley and Sons, Inc., New York, 2002).

[45]S. Ramo, J. R. Whinnery, and T. Van Duzer, *Fields and Waves in Communication Electronics*, 3rd ed. (Wiley and Sons, Inc., New York, 1994).

References

[1] E. Shamonina, V. Kalinin, K. H. Ringhofer, and L. Solymar, "Magneto-inductive waveguide," *Electronics Letters*, vol. 38, no. 8, pp. 371–373, Apr 2002.

[2] E. Shamonina, V. A. Kalinin, K. H. Ringhofer, and L. Solymar, "Magnetoinductive waves in one, two, and three dimensions," *Journal of Applied Physics*, vol. 92, no. 10, pp. 6252–6261, 2002.

[3] R. R. A. Syms, E. Shamonina, V. Kalinin, and L. Solymar, "A theory of metamaterials based on periodically loaded transmission lines: Interaction between magnetoinductive and electromagnetic waves," *Journal of Applied Physics*, vol. 97, no. 6, p. 064909, 2005.

[4] M. Beruete, F. Falcone, M. J. Freire, R. Marqués, and J. D. Baena, "Electroinductive waves in chains of complementary metamaterial elements," *Applied Physics Letters*, vol. 88, no. 8, p. 083503, 2006.

[5] A. P. Slobozhanyuk, P. V. Kapitanova, D. S. Filonov, D. A. Powell, I. V. Shadrivov, M. Lapine, P. A. Belov, R. C. McPhedran, and Y. S. Kivshar, "Nonlinear interaction of meta-atoms through optical coupling," *Applied Physics Letters*, vol. 104, no. 1, p. 014104, 2014.

[6] X.-C. Zhang, Z.-Y. Yu, and J. Xu, "Novel band-pass substrate integrated waveguide (siw) filter based on complementary split ring resonators (csrrs)," *Progress In Electromagnetics Research*, vol. 72, pp. 39–46, 2007.

[7] M. J. Lee, Y. Sung, S. H. Kim, and Y. S. Kim, "Polarization reconfigurable microstrip patch antenna with complementary split ring resonator (csrr)," in *2012 Asia Pacific Microwave Conference Proceedings*, Dec 2012, pp. 619–621.

5. Leaky Wave Radiation Phenomenon in CSRRs Arrays

L'imagination est tout.
C'est un avant-gôut de ce que la vie nous réserve.
Albert Einstein

Single Complementary Split Ring Resonator particle and a reduced finite array of such particles are implemented in the rectangular patch of a patch antenna in *Chapter 3* and *Chapter 4*; respectively. In both cases, a finite structure based on CSRRs is considered.

In *Chapter 4* the EIW phenomenon is demonstrated using a reduced finite array of CSRRs. This result provided us the motivation to analyze the radiating performance of infinite arrays composed of Complementary Split Ring Resonators. As an intermediate step, and in order to validate simulated results, a finite array composed of nine Complementary Split Ring Resonators is manufactured and partially tested. Though partial, this test results show very encouraging results; which motivates a more in deep measurement campaign and it is expected to result into new publications on this topic. Partial results of this work shows the feasibility to use the presented structures as based radiation structures for the design of leaky wave antennas for wireless communication application. Throughout this chapter the current prototyping stages are presented together with the measurement results available so far.

5.1 Leaky Wave Radiation: Pioneering and recent Works

The properties of leaky waves were originally derived in the pioneering work of Oliner and Tamir in the late 1950s and early 1960s [1], [2] and [3]. This was followed by an extensive development of leaky-wave theory and applications to antennas. However, interest in the behavior and application of these antennas at millimiter-wavelengths only began several decades later. Canonical structures are presented by A. Oliner and D. Jackson in [4].

The basic working principle of LWAs is based on a wave propagating along a guiding structure and gradually leaking out a small amount of energy in form of coherent radiation. LWAs are popular in the microwave band and above, because they can achieve a high directivity with a simple structure, without the need for a complicated and costly feed network as typically used in a phased array. On the other hand, for applications that can take advantage of frequency beam scanning, LWAs are often ideally suited, as LWAs offer a frequency scanning over a large bandwidth [2].

Planar LWAs have recently attracted much attention due to their structural simplicity, easy fabrication, and integration with other planar components [5] and [6]. The level of interest and the development in the field of planar LWAs have accelerated significantly in the previous years, mainly due to the surge of interest in metamaterials and the advent of metamaterial transmission lines. Over the past years, metamaterial transmission lines have been proposed as backward, forward, or backward-forward frequency scanning LWAs [6], [7], [8], [9], [10], [**?**], [11].

So far, Split Ring Resonators (SRRs) and Complementary Split Ring Resonators (CSRRs) have been used as key particles in the design of planar left-handed metamaterial (LHM) and Composite Right and Left Handed (CRLH) transmission lines, which allow leaky wave radiation in left and composite transmission lines [10], [11] and [12].

In this chapter a simple metamaterial structure based on CSRRs etched in the ground plane of a microstrip line is proposed as a base of a Leaky Wave Structure. In the following section (see *Section 5.2*) the manufacturing prototypes and partial measurements are briefly described.

5.2 Leaky Wave Radiation CSRR: Partial Results

In this section the partial results of the proposed leaky wave Metamaterial radiation structure based on CSRRs are presented.

In *Fig. 5.1* the picture of the simulated and measured prototypes is presented. As it is seen, in order to validate the radiation characteristics of the mentioned prototype, the fabricated prototype consists in an array of nine complementary split Ring Resonators.

Figure 5.1. Simulated and Manufactured Prototype

Simulated and measured results available up to date are summarized in the table below. These results confirm the agreement between simulated and mesured data for the beam pointing and operational bandwidth.

At present the measurement campaign for this prototype is on-going. So far, the results available show good agreement between simulated and measurement data. Then, the performance of this structure is promising and it is expected to complete a new publication once all the measurement results are available.

	Simulation Results	Measurement Results
Radiation pattern pointing (degrees)	48º at 4.3GHz	50º at 4.3GHz
Operational Bandwidth (GHz) (*)	(4.3-4.5)GHz	(4.3-4.5)GHz
Radiation efficiency	50% over (*)	To be computed
Gain Value	3dB over (*)	To be computed

Figure 5.2. Simulated and partial measurement results

References

[1] T. Tamir and A. A. Oliner, "Guided complex waves. part 1: Fields as an interface," in *Proc. Inst.Electr.Eng.*, 1963, pp. 110–310.

[2] ——, "Guided complex waves. part 2: Relation to radiation patterns," in *Proc. Inst.Electr.Eng.*, 1963, pp. 110–325.

[3] L. Goldstone and A. Oliner, "Leaky-wave antennas 1: Rectangular waveguides," *IRE Trans. Antennas Propag.*, vol. 7, 1959.

[4] A. Oliner, , and D. Jackson, "Leaky-wave antennas,," *in Antenna Engineering Handbook, 4th edn., by J. Volakis (McGraw-Hill, New York)*, 1969.

[5] A. Sutinjo, M. Okoniewski, and R. H. Johnston, "Radiation from fast and slow traveling waves," *IEEE Antennas and Propagation Magazine*, vol. 50, no. 4, pp. 175–181, Aug 2008.

[6] D. R. Jackson, C. Caloz, and T. Itoh, "Leaky-wave antennas," *Proceedings of the IEEE*, vol. 100, no. 7, pp. 2194–2206, July 2012.

[7] L. Liu, C. Caloz, and T. Itoh, "Dominant mode leaky-wave antenna with backfire-to-endfire scanning capability," *Electronics Letters*, vol. 38, no. 23, pp. 1414–1416, Nov 2002.

[8] A. Grbic and G. V. Eleftheriades, "Leaky cpw-based slot antenna arrays for millimeter-wave applications," *IEEE Transactions on Antennas and Propagation*, vol. 50, no. 11, pp. 1494–1504, Nov 2002.

[9] G. Lovat, P. Burghignoli, and D. R. Jackson, "Fundamental properties and optimization of broadside radiation from uniform leaky-wave antennas," *IEEE Transactions on Antennas and Propagation*, vol. 54, no. 5, pp. 1442–1452, May 2006.

[10] I. Arnedo, J. Illescas, M. Flores, T. Lopetegi, M. A. G. Laso, F. Falcone, J. Bonache, J. García-García, F. Martín, J. A. Marcotegui, R. Marqués, and M. Sorolla, "Forward and backward leaky wave radiation in split-ring-resonator-based metamaterials," *IET Microwaves, Antennas Propagation*, vol. 1, no. 1, pp. 65–68, February 2007.

[11] S. Eggermont, R. Platteborze, and I. Huynen, "Investigation of metamaterial leaky wave antenna based on complementary split ring resonators," in *2009 European Microwave Conference (EuMC)*, Sept 2009, pp. 209–212.

[12] G. Zamora, S. Zuffanelli, F. Paredes, F. J. Herraiz-Martnez, F. Martn, and J. Bonache, "Fundamental-mode leaky-wave antenna (lwa) using slotline and split-ring-resonator (srr)-based metamaterials," *IEEE Antennas and Wireless Propagation Letters*, vol. 12, pp. 1424–1427, 2013.

6. Conclusions

This final section contains the main conclusions obtained from the work presented in this thesis. The initial assumptions have been validated through simulation as well as measurement results from fabricated prototypes. The proposed prototypes may find industrial application and several research lines remain open as future work.

6.1 Conclusions and Future lines

This work has been devoted to the design of Metamaterial Antennas based on Complementary Split Ring Resonators. The main results are summarized as follows:

- On the one hand, CSRR as stand alone radiating element exhibits low radiation efficiencies. We therefore consider that such radiating elements have a limited scope of applications.
- On the other hand, the outcome from our research work shows that CSRR can have acceptable radiation characteristics when it is integrated within larger radiating structures. Such radiating structures concern stand-alone antennas (patch antennas with CSRR embedded), as well as antenna arrays (i.e.: CSRR arrays) and leaky wave antennas. Moreover, we have shown that CSRR structures can provide polarization agility features to existing stand-alone antennas.
- With regard to guided structures, CSRR has been confirmed to be a powerful miniaturization tool for waveguide filters.

The main results of this research work have been presented and well received in several peer reviewer journals and international conferences.

As already suggested by the promising results delivered from this research work, there are several research paths that will soon be culminated as well as new research paths to explore in the field of CSRR applications.

References

List of Figures

List of Publications

Refereed Journal Papers

1. N. Ortiz, J. D. Baena, M. Beruete, F. Falcone, M. A. G. Laso, T. Lopetegi, R. Marqus, F. Martn, J. Garca-Garca, and M. Sorolla, "Complementary split-ring resonator for compact waveguide filter design," *Microwave and Optical Technology Letters*, vol. 46, no. 1, pp. 88–92, 2005.

2. I. Arnedo, J. Gil, N. Ortiz, T. Lopetegi, M. A. G. Laso, M. Sorolla, M. Thumm, D. Schmitt, and M. Guglielmi, "Ku-band high-power lowpass filter with spurious rejection," *Electronics Letters*, vol. 42, no. 25, pp. 1460–1461, December 2006.

3. N. Ortiz, F. Falcone, and M. Sorolla, "Enhanced gain dual band patch antenna based on complementary rectangular split-ring resonators," *Microwave and Optical Technology Letters*, vol. 53, no. 3, pp. 590–594, 2011.

4. ——, "Gain improvement of dual band antenna based on complementary rectangular split-ring resonator," *ISRN Communications and Networking*, vol. 2012, no. 17, 2012.

5. F. Tiezzi, C. Dominguez, J. Padilla, N. Ortiz, C. Vigan, and S. Vaccaro, "User terminal antennas for s-band mobile satellite communication systems," *International Journal of Satellite Communications and Networking*, vol. 32, no. 4, pp. 277–289, 2014.

6. N. Ortiz, J. C. Iriarte, G. Crespo, and F. Falcone, "Design and implementation of dual-band antennas based on a complementary split ring resonators," *Waves in Random and Complex Media*, vol. 25, no. 3, pp. 309–322, 2015.

7. N. Ortiz, G. Crespo, J. C. Iriarte, and F. Falcone, "Generation of circularly polarized waves based on electro inductive-wave (eiw) coupling to chains of complementary split ring resonators," *Journal of Applied Physics*, vol. 120, no. 17, p. 174905, 2016.

Refereed Conference Papers

1. N. Ortiz, J. Teniente, R. Gonzalo, and C. del Río, "Diseño de una antena dual gaussiana de doble profundidad de corrugación," in *XIIX Simposium Nacional de la URSI*, in Spanish.

2. I. Arnedo, J. Gil, N. Ortiz, T. Lopetegi, M. A. G. Laso, M. Thumm, M. Sorolla, D. Schmitt, and M. Guglielmi, "Spurious removal in satellite output multiplexer power filters," in *2007 European Microwave Conference*, Oct 2007, pp. 67–70.

3. N. Ortiz, F. Falcone, and M. Sorolla, "Dual band patch antenna based on complementary rectangular split-ring resonators," in *2009 Asia Pacific Microwave Conference*, Dec 2009, pp. 2762–2765.

4. G. E. Dominguez, A. Sánchez, N. Ortiz, and M. S. Castañer, "Antena impresa con escaneo electrónico en sistemas embarcados para comunicaciones por satélite en banda x," in *XXV Simposium Nacional de la URSI*, in Spanish.

5. N. Ortiz, F. Falcone, and M. Sorolla, "Radiation efficiency improvement of dual band patch antenna based on a complementary rectangular split ring resonator," in *Proceedings of the 5th European Conference on Antennas and Propagation (EUCAP)*, April 2011, pp. 830–834.

Patents

1. M. Sorolla, D. Schmitt, M. Guglielmi, J. Gil, and N. Ortiz, "Microwave bandstop filter for an output multiplexer," Patent US 7,468,641 B2, December 23, 2008, uS Patent 7468641.